Differentiation of Perimortem Trauma from Heat Fractures in Cranial and Irregular Bones in Cases of Cremation

by

Hanna Friedlander

A thesis submitted in partial fulfillment of the requirements for the degree of

Master of Arts

Department of Anthropology
University of Alberta

Abstract

Trauma investigations in forensic experimentation are largely done on human long bones or animal substitutes. There is limited research on how trauma impacts human cranial and irregular bones. Distinct structural differences between these bone types means long bone trauma cannot be directly applied to cranial and irregular bones. Similarities in data collection are seen in research revolving around heat alteration and bone: long bones and animal substitutes are used, but are not proper alternatives for human cranial and irregular bones. The information and data from this research work to expand what is known about trauma and heat alteration with regards to human cranial and irregular bones. Finding fresh human cranial and irregular bones for use in forensic recreations is largely unheard of, so this research also explores the ability to use embalmed human cadavers as a source for future forensic work. There is very little research on how formalin impacts the histological structure of bone. This research tests two problems: 1) can formalin fixed (embalmed) human cadavers be used instead of animal substitutes or fresh cadavers in experimental models? And 2) can perimortem trauma be differentiated from heat fractures in cranial and irregular bones in cases of cremation?

Formalin fixed human cadaver femoral shafts were subjected to partial cremation, both at 600°C and 800°C, with an additional sample left unburned as a control unit. The thin sections of this study were directly compared to those of another study using cremated femoral shafts of fresh cadavers. Results indicated the control sample was largely unaltered by formalin, as were those samples burned at 600°C; however, samples burned at 800°C showed increased structural damage when compared to their non-formalin fixed counterparts. The 800°C samples more closely resembled the non-formalin fixed samples that burned at 1000°C. Conclusions for this experiment indicate formalin

fixed human remains can be used in forensic recreations, so long as the temperature is kept under 800°C.

Five formalin fixed human calottes and five human hemipelves were donated by the Anatomical Gifts Program (AGP) at the University of Alberta. These remains were used to help determine if perimortem trauma could be differentiated from heat fractures in cases of cremation. The remains were traumatized while unburnt with blunt or sharp force trauma; two were left untouched as control units. Post-cremation, 180 mixed traumatic and heat fractures were analyzed to discern the two. Curvature analysis was done by creating 3D virtual models of various points along the 180 fracture lines, looking at fracture boundary lines, slopes, and variances in the microscopic details within the fracture walls. This analysis showed distinct differences, on a microscopic level, between types of traumatic fractures and heat fractures. Qualitative analysis of the remains proved successful; attempts at quantitative analysis have thus far failed, requiring a greater examination of the quantitative aspects of fracture patterns and slope based on fracture morphology.

Preface

This thesis is an original work by Hanna Rose Friedlander. The research project, of which this thesis is a part, received research ethics approval from the University of Alberta Research Ethics Board, Project Name "Differentiation of Perimortem Trauma Fractures from Heat Fractures in Irregular Bones", No. Pro00070625, 15 May 2017.

Some of the research conducted for this thesis forms part of an interdisciplinary research collaboration, supervised by Pamela Mayne Correia at the University of Alberta. The investigatory study in Chapter 3 was designed and carried out by me, with the assistance of Pamela Mayne Correia. The development of methods, techniques, analysis, and data collection in Chapter 4 were designed and carried out by me, with the assistance of Pamela Mayne Correia, Dr. Samer Adeeb, Devon Stone, B.Sc., and Dr. Elizabeth Brooks-Lim. The model creation and data collected in Chapter 5 were carried out by me, having been designed by Dr. Samer Adeeb. The data analyses in Chapters 3, 4 and 5 are my original work, as well as the literature review in Chapter 2.

A version of Chapter 2 will be submitted to the American Journal of Physical Anthropology, titled: "Ossification of the Cranium and Irregular Bones and the Implications for the Interpretation of Fire Damage." This paper is co-authored by Pamela Mayne Correia. I am responsible for the analysis of the literature review and manuscript composition. Pamela Mayne Correia was the supervisory author and was involved with concept formation and manuscript edits.

A version of Chapter 3 will be submitted to the Journal of Forensic Sciences, titled: "The Use of Formalin Fixed Human Remains in Experimental Procedures." This paper is co-authored by Pamela Mayne Correia. I am responsible for the literature review, project design, data collection, and manuscript composition. Pamela Mayne Correia was the supervisory author and was involved with concept formation and manuscript edits.

A version of Chapter 4 will be submitted to the Journal of Forensic Sciences, titled: "Differentiation of Perimortem Trauma from Heat Fractures in Partial Cremations of Cranial and Pelvic Bones." This paper is co-authored by Pamela Mayne Correia, Dr. Samer Adeeb, Devon Stone, B.Sc., and Dr. Elizabeth Brooks-Lim. I am responsible for the literature review, project design, data collection, and manuscript composition. Dr. Samer Adeeb and Devon Stone, B.Sc. assisted with reverse engineering

concepts. Pamela Mayne Correia was the supervisory author and was involved with concept formation and manuscript edits.

A version of Chapter 5 will be submitted to the Journal of Forensic Sciences, titled: "Technical Note: Virtual Reconstruction and Identification of Traumatic Fractures and Heat Fractures." This paper is co-authored by Pamela Mayne Correia. I am responsible for the literature review, assisted project design, data collection, and manuscript composition. Dr. Samer Adeeb and Devon Stone, B.Sc. assisted with reverse engineering concepts and project design. Pamela Mayne Correia was the supervisory author and was involved with concept formation and manuscript edits.

Acknowledgements

First and foremost, I want to thank the anonymous donors from this study – without you, this work would not have been possible.

Although I have put many hours filled with laughter and tears, my incredible supervisor, Pamela Mayne Correia is the reason this research was brought to life. Her continual support and feedback has allowed me to grow and produce work that I am proud of. Pam has helped me to be a well-rounded student, starting when I met her 5 years ago during a study abroad period. Since then, she has helped shape me into the anthropologist I am today by constantly pushing me to work harder and do better. The learning experiences and opportunities Pam has offered me has given me practical applications, as well as a large breadth of knowledge that I am hopeful to apply in future positions. She is the inspiration for my coming to graduate school to pursue a Master's degree – learning from an extraordinary woman has truly been a blessing. I would not be where I am today without Pam's supervision, help, stories, lessons, and the many, many hours of proof-reading. For that, Pam, I thank you a thousand times over.

To Dr. Sandra Garvie-Lok, thank you for being as helpful and encouraging as you have been throughout this process – I am pleased and excited to have you on my Examining Committee. Dr. Lesley Harrington, I offer you many thanks for allowing me to use the Keyence VHX-2000 and helping me troubleshoot along the way. Your enthusiasm towards this research during our informal chats have given me the extra push to succeed and work through any complications that have come my way. Thank you for being the defense committee chair. To Harvey Friebe, who deserves an enormous thank you for the time and energy he put into this thesis via significant technological assistance during the preliminary formalin study, as well as technical support learning the Keyence VHX-2000 and proof-reading some of the articles that will come out of this thesis.

During this study, I was fortunate enough to have the Interim Chair of Civil Engineering, Dr. Samer Adeeb, partner with this research. He worked with me to create virtual models of the fractures from this project to provide better analysis of the fractures. This led to pioneering new techniques of trauma and heat fracture analysis – something I hoped to accomplish and have been able to see come to life. The feedback and conversations generated from this work have truly been helpful in advancing the work done in this thesis. Alongside Dr. Adeeb, I thank his student, Devon Stone, B.Sc. for working with me and showing me how to create the models you see in this study.

Thank you to Jason Papirny, head of the Anatomical Gifts Program (AGP) at the University of Alberta for organizing the collection of samples and connecting me with his father, Ken Papirny, who gave me access to crematorium ovens and staff to burn the remains. I thank Dr. Elizabeth Brooks-Lim, Chief of the Office of the Medical Examiner, for collaborating on this work by providing a work space, X-ray technology, and Medical Examiner personnel to aid in preliminary work.

To my friends whom I have known for years, I thank you for listening to me when I needed someone to talk to and supporting me throughout this work. You guys have been there for me through the ups and downs for many years. To my friends here in Edmonton, thank you for the little pick me ups, the discussions and reassuring words that kept me going. I am so thankful to have you all in my life.

Finally, I want to thank my parents, because without them I truly would not be who I am today. Mom and Dad, you have always looked out for me and supported me as I walked down this path. Throughout all the phone calls, text messages, and emails, I have not once forgotten the support, guidance, and love that you have given me. You are my biggest role models and I hope you know that every part of me is here today because you have always been there for me. Thank you for picking me up when I stumbled and pushed me to go on when I struggled to balance everything on my "to-do" list. Thank you for letting me know how proud you are and for raising me the way you did. I couldn't do it without you. Benjamin and William, thank you for being amazing brothers who always take the time to ask how I am doing, what is going on, and offering support when I needed it. I appreciate your wisdom and value your opinions so much. Thank you for opening my eyes to new possibilities and having my back as I moved to a new country to pursue new endeavors. Grandma Lowee, thank you for all the phone calls and messages, for being inquisitive and always asking how my research is coming along, and for all the grilled cheese sandwiches that fueled me.

This project was made possible with generous support from the University of Alberta through the Graduate Travel Award to present my research at various conferences, the Graduate Teaching Assistant (GTA) Award, which allowed me to expand my knowledge and do hands on work with fellow students, and the Gerald Ferro Memorial Scholarship in Anthropology. Thank you all for supporting me and my work.

Table of Contents

List of Tables

List of Figures

Figure 4.12 Keyence VHX-2000 Microscope Image of Heat Fractures on a Calotte (T29) 53

Chapter 1: Introduction

1.1 Overview of Issues Surrounding Trauma Identification from Fire and Death

Informed decision making in the field of forensic anthropology is critical for processing, analyzing, and observing human remains during field recovery and examination. Using prior scientific descriptions of perimortem trauma and heat fracture identification the two can be differentiated, in case dependent situations (Mayne Correia 1997, Pope and Smith 2004). When analyzing skeletal elements, especially in forensic cases, it is imperative to make science-informed decisions based on macroscopic analysis, comparison to proven past scientific models, and even sometimes microscopic analysis. Using novel techniques, the aim of this research is to differentiate traumatic fractures on cranial and irregular bones from heat fractures of partially cremated human remains to help develop and advance the scientific investigations. Previous work on the differentiation of perimortem trauma fractures from heat fractures centers on long bones; there is not a lot of research on how these varying types of fractures interact on bones such as the skull, os coxa, or vertebrae (Pope and Smith 2004). Mayne (1990) worked on identifying precremation trauma in cremated animal bones. That work shows how traumatized animal long bones fracture under the pressures of heat. Baby (1954), Bohnert (1997), Dokládal (1971), Fairgrieve and Molto (1994), and Holland (1989) discuss the destruction of crania during cremation, but show no indication of how perimortem trauma is impacted. Irregular bones have thinner layers of cortical tissue than long bones, and therefore have less plasticity and will deform differently than long bones. This is forensically relevant because the cranium "is not only a frequent target of injury, it is also one of the most thermally susceptible, making critical analysis vital" (Pope and Smith 2004). This thesis research takes information from long bones analysis and separates it from information on irregular bones by understanding the embryological and biomechanical differences of the two bone types. This is further exemplified by how trauma affects irregular bones differently than long bones, as well as how heat alters fractures of irregular bones. The differentiation of pre-created trauma fractures from heat fractures will be discussed and analyzed via a new technology based methodology to distinguish the two.

1.2 Bone Structure

Bone biomechanics inform our understanding of fractures. Bone, being viscoelastic, will respond to stressors and weight bearing loads by resisting deformation through the dispersal of interstitial fluids and reform once the stressors are removed (Berryman and Haun 1996). The basic multicellular units (BMU) of bones include osteons – the rudimentary structure of cortical bone – and Haversian canals, containing nutrients and blood vessels. Osteons are cylindrical structures including osteoclasts, which resorb bone, and osteoblasts, which create new bone (van Oers *et al.*, 2008). Haversian systems (osteons) mainly consist of hydroxyapatite mineral and collagenous proteins, which are organized to provide efficient arrangement, strength, and resistance of bone to outside forces (Vaughan *et al.*, 2012). Osteons are separated by cement lines, or boundaries (White *et al.*, 2012). There are three distinct types of bone found in the human skeletal system.

Long bones primarily consist of cortical bone, otherwise known as compact bone. Compact bone is composed of lamellar layers that are arranged around the Haversian canal. In order to provide the rigid structure around the Haversian canals that is needed to support skeletal functions, osteons are formed – or micro-sections of lamellar bone that alternate direction (Vaughan *et al.*, 2012). Lamellar bone is composed of collagen fibrils which are laid down adjacently in five distinct sublayers, each rotated at approximately 30°, creating a "plywood-like organizational motif" (Weiner *et al.*, 1999). The collagen fibril bundles within the plywood structure mineralize to create the smooth structure of lamellar bone. Osteonal lamellae are oriented in a unidirectional manner to create the cylindrical shape of osteons (Faingold *et al.*, 2013). As the bone is continually remodeled through life, the primary osteons, or original osteons, are replaced by secondary osteons which in turn cause a reorientation of the lamellae, altering the stiffness of the bone (Vaughan *et al.*, 2012). The layers are woven together tightly so there are only empty spaces reserved for nutrient flow and vascularization via the Haversian canal, Volkmann's canals, lacunae, and canaliculi (Wedel and Galloway 1999). The lamellar bone and Haversian bone contains blood vessels that proliferate throughout the entire bone (Berryman and Haun 1996). The framework laid down by the lamellae allows cortical bone to tolerate heavy loads and impacts from varying directions. Cortical bone can resist mechanical loads both on the longitudinal and horizontal axes (Bajaj *et al.*, 2014, Wedel and Galloway 1999, Zimmerman and Ritchie 2015). Within this system, osteocytes, osteoblasts, and osteoclasts constantly work to maintain and repair cortical bone.

Within the inner portion of long bones, around the medullary cavity, and at the metaphyseal ends of long bones, lies cancellous or trabecular bone. The lamellae of trabecular bone are vastly different from cortical bone. Instead of being laid down in an organized pattern, trabecular lamellae are longitudinally oriented, which takes the brunt of loading and compressive forces that are applied to bone (Gupta and Zioupos 2008, Turunen *et al.*, 2013, Vaughan *et al.* 2012, Wedel and Galloway 1999). The spongy nature of trabecular bone is derived from its vast system of lacunae and canaliculi that are constantly being remodeled (Vaughan *et al.*, 2012). Cancellous bone is primarily composed of hydroxyapatite crystals and collagen fibrils which provide a fracture resistant, lightweight structure (Vaughan *et al.*, 2012); however, the strength of the cancellous bone lies in the overall health of the whole bone because of its ornate, thin structure. When bones become weaker due to disease, its ability to resist force and absorb energy decreases (Wedel and Galloway 1999). Long bones are composed of dense layers of cortical bone, with a thin inner layer of trabecular bone, except at the ends where most of the bone is cancellous. Working as one unit, cancellous and cortical bone provide a strong, flexible, and lightweight material that does not overtly yield to compression and other forces.

Cranial bones are vastly different from long bones. Cranial vault bones are known as dermal bones, or bones that formed from membrane and neural crest cell origins (White *et al.*, 2012). Cranial bones have a thin cortical bone layer that compose the inner and outer tables of bone. The interior is filled with diploic bone, a type of cancellous bone only found in the cranium. These two structures work together to provide a strong, lightweight structure (Pritchard *et al.*, 1956, Wedel and Galloway 1999) The skeletal anatomy is highly vascularized, hence the dense diploic nature of the bone. Unlike long bones, cranial bones do not have metaphyseal ends. Instead, they are joined to one another via sutural lines – interlocking articulations that fuse as the human ages (White *et al.*, 2012). Irregular bones, or those of the pelvic girdle, shoulder girdle, vertebrae, hands and feet, are composed similarly to the cranial bones; however, unlike cranial bones, irregular bones are enveloped by a thin layer of cortical bone that is filled with a thicker layer of cancellous bone (White *et al.*, 2012). These bones are lightweight and do not have the double-walled cortical bone that is seen in cranial bone.

Finally, seen during fetal growth and during fracture repair, woven bone is an intermediate bone type that can be associated with long bones, cranial bones, and irregular bones. In human development, the fine fibers that compose collagen are randomly organized along the longitudinal axis of the forming bones. As the fetus continues to develop, woven bone is replaced by lamellar bone and collagen sheets. Over time, the lamellar bone turns into Haversian bone as secondary osteons

replace primary osteons (Wedel and Galloway 1999). Woven bone is therefore the beginning stage of all bone growth. Regardless of age, when cortical or cancellous bone is fractured or needs external repair that is beyond the daily microfracture repair, woven bone is formed. Acting as a temporary tissue post-breakage, woven bone is created in an attempt to stop subsequent fractures from occurring and while the damaged bone is repaired. Composed of fibrolamellar bone and cartilaginous bone, woven bone is known to be more resistant to fractures due to its random organization of collagen, which better absorbs and diverts crack propagation (Silva and Toulhey 2007).

1.3 Long Bone Fracture Mechanics

As it is not very ductile, bone can undergo drastic changes while resisting deformation and fractures (Berryman and Haun 1996, Hart 2005, Zimmermann and Ritchie 2015). This concept is built on bone elasticity and inelasticity – collagen fibrils can remodel and disperse energy (Zimmerman and Ritchie 2015). The lamellar composition of long bones utilizes various tissue structures to deflect and protect bone from micro-cracks (Peterlik *et al.*, 2005). As lamellae thicken, they wrap around a Haversian canal making a "fracture resistant barrier" (Gupta and Zioupos 2008). Different osteon axis angles have different lamellar thicknesses (Gupta and Zioupos 2008, Peterlik *et al.*, 2005). Lamellar are held together by a bony glue composed of an organic matrix.

Fractures are a byproduct of bone failure based on a bones inability to maintain elasticity. Bone as a whole is anisotropic in nature, which alters the mechanical properties of bone based on its multicellular orientation – bone collagen provides tensile strength, blow absorbance, intrinsic and extrinsic properties (Berryman and Haun 1996, Gupta and Zioupos 2008, Zimmermann and Ritchie 2015). Bone is also hypertrophic, having the ability to regrow, which is seen in remodeling from stresses/strains that impact bone structure, as well as fracture repairs (Berryman and Haun 1996, Chamay and Tschantz 1972, Wedel and Galloway 1999). However, the atrophic nature, or ability for bone density to decrease, is present at the time of fracture propagation (Berryman and Haun 1996, Chamay and Tschantz 1972, Wedel and Galloway 1999). Fractures occur when the stress/strain yield point is reached. This is where permanent elastic damage can occur. Stress, noted as a bone distortion (Wedel and Galloway 1999) and strain, the noted change in shape (Wedel and Galloway 1999), are key components of plastic deformation of bone. Plastic deformation is defined as a "slippage between the layers of atoms and molecules" (Wedel and Galloway 1999). Plastic deformation occurs when outside

forces apply enough load to the bone to cause it to change shape or distort (Chamay and Tschantz 1972, Wedel and Galloway 1999).

Together, these defined forces make bone a viscoelastic material. This means bone is both viscous (uses fluids to resist gradual deformation) and elastic (bone can resist forces that cause plastic deformation and rebound back to normal once the force is removed). Once stress has fully impacted bone causing unalterable plastic deformation, a fail point will be reached. Fail points are when the bone is unable to maintain its flexibility and finally fracture (Hart 2005, Wedel and Galloway 1999). Failure points are dependent on a bone's ability to absorb forces, be hypertrophic, atrophic, and disperse interstitial fluids to help compress and/or increase bendability (Berryman and Haun 1996, Chamay and Tschantz 1972, Wedel and Galloway 1999). When micro-cracks do form during plastic deformation, a crack tip is formed and fractures have a greater chance of proliferating.

A crack tip initiates by weakening a section of bone; the crack then proliferates along the bone by running along cement lines (FIG. 1.1) (Gupta and Zioupos 2008, Nalla *et al.*, 2005, Peterlik *et al.*, 2005, Zimmermann and Ritchie 2015). The crack tip does not go through osteons, instead osteons are pulled to either side of the crack via osteonal bridging. The lamellar lines holding the osteon in place are broken so as to not damage the osteon (van Oers *et al.*, 2008). Lamellae and cement lines not impacted by the micro-crack are known as bridges, deflecting the crack in attempt to stop the organism from collapsing (Zimmerman and Ritchie 2015). the ability to toughen from the inside while the micro-crack is still being produced is one of the most extrinsic mechanisms of a bone. The associated intrinsic mechanism works ahead of the crack tip in attempt to stop the micro-crack from proliferating further (Nalla *et al.*, 2006, Zimmermann and Ritchie 2015).

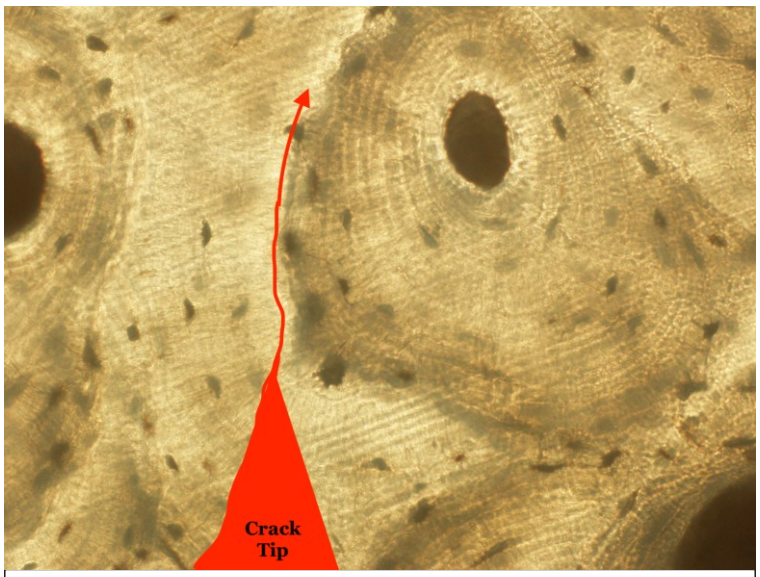

FIG. 1.1 Crack tip propagation shown on the left (in red) highlighting the path a crack would take on a histological thin section. [drawn by Friedlander (2018)].

Regulating collagen fibril deposition and organic bone matrix are important to bone structure maintenance. The energy from the micro-crack shears the inner 'glue'

layer of organic matrix, causing a need to rebuild and reinforce collagen fibrils (Peterlik *et al.*, 2005). Cross section analysis of bone shows the stiffness, flexibility, and osteonal turnover rate in any given portion of bone. The more porous the cross-section of bone, the less resistant to plastic deformation the bone is. Secondary osteons cause a weakness in the cement lines of the lamellae. Cracks therefore proliferate when the impact of outside forces is too much for the bone to handle (Nalla *et al.*, 2006, Wedel and Galloway 1999). Bones reach a critical fail point when the collagen, organic matrix, and non-collagenous proteins separate (Zimmerman and Ritchie 2015). As these bonds break, the bones tear and create micro-lesions. Coupled with reduced stability and overall stiffness of the bone, this is known as "post-yield deformation" (Gupta and Zioupus 2008). After the stressors are removed, the collagen fibrils reform and are remodeled to gain back their original strength. This occurs as bones heal themselves through daily repair and woven bone is introduced into the skeletal system at the site of the fracture. Long bones are known to "re-align themselves in the axis of force by hypertrophy in the zones under compression" (Chamay and Tschantz 1972). With long bones, plastic deformation is more likely to occur because of the thickness of the cortical bone compared to irregular bones. Continually, plastic deformation is impacted by a bone's ability to "absorb the blow, bone elasticity, plasticity, and density" (Berryman and Haun 1996).

1.4 Cranial and Irregular Bone Fracture Mechanics

Faces, recognized as the main point of identification by criminal investigators, make the cranium and face a central point of attack for perpetrators of crime (Wedel and Galloway 1999). When analyzing cranial bones, it is known that the outer table is generally thicker than the inner table due to the development of the brain in utero (Wedel and Galloway 1999). The developing brain applies pressures to the inside of the cranial vault, causing the inner table to be flatter than its outer counterpart (Wedel and Galloway 1999). The diploic layer of bone between the inner and outer tables disperses applied forces throughout the cranial bones in attempt to minimize damage. Mechanical failure often occurs when the bending strength reaches its fail point on either the outer or inner table. The outer table typically shows more damage than the inner table due to the diploic layer scattering outside forces. Fractures on the thicker tables of bone will absorb and deflect the energy to weaker portions of bone by default (Wedel and Galloway 1999).

There are five main types of cranial fractures that can occur: linear, diastatic, depressed, stellate, and comminuted (FIG. 1.1). Linear fractures, or fissure fractures, follow the path of least

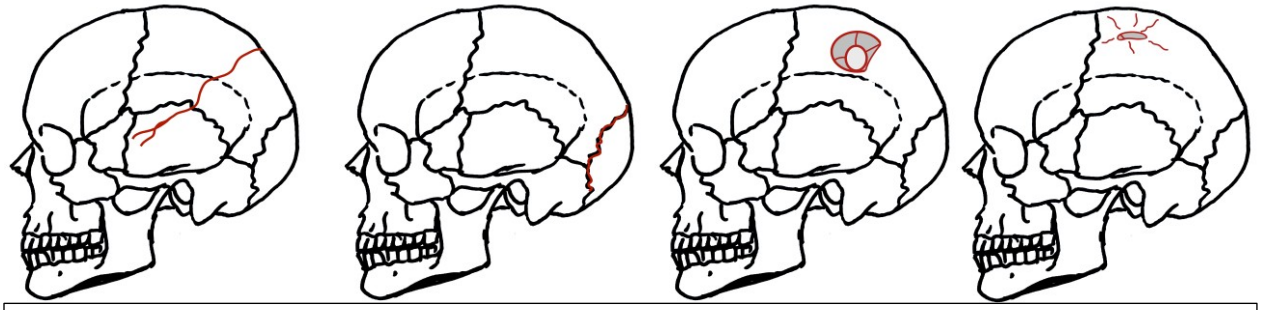

A) Linear	B) Diastatic	C) Depression	D) Stellate/Comminuted

FIG. 1.2 Skulls showing four of the five major types of fractures, outlined in red, that can impact the cranium. Note a comminuted fracture is shown in combination with stellate fractures because of their similar nature [hand sketched by Friedlander (2018), modelled from Wedel and Galloway 1999].

resistance (Wedel and Galloway 1999), separating the inner and outer tables from the diploë. The energy is dispersed from thicker to thinner portions of bone. These fractures do not form a straight line, but rupture across bone like an earthquake (Wedel and Galloway 1999). Linear fractures can form radiating or concentric fractures, where the cranial vault reacts like "a semi-elastic ball that can be bent inwards at the impact site, with out-bending occurring in all areas around this point" (Wedel and Galloway 1999). Diastatic fractures, similar to linear fractures, become diverted upon impact and are forced into suture lines as the bone structure fails. These are commonly seen in cases of low-velocity cranial trauma (Wedel and Galloway 1999). Depression fractures, on the other hand, cause structural collapse of the outer table and diploë. The inner table typically fails as well, causing radiating linear fractures around the depression site (Wedel and Galloway 1999). Stellate fractures, similarly, form a star shaped depression with radiating linear fractures that extend from the point of impact along the path of least resistance. The outer table bends inwards and fractures (Wedel and Galloway 1999). Finally, comminuted fractures are created like stellate fractures and produce heavy fragmentation and circular fractures around the point of impact (Wedel and Galloway 1999). Differentiating between the five fracture types is not always easy, but can be done based on trauma indicators. Every cranial fracture is different because of their specificity and relation of the outer table, inner table, and diploë (Wedel and Galloway 1999).

1.5 Fracture Mechanics of Burned Bone

Fracture patterns on bone derive from the existing biomechanical structure. In burned bone, the fractures propagate as they move through Haversian systems. Unlike fresh bone, the burned bone has become a brittle substance and cannot deflect the force of the fractures – they simply form rifts

in the bone. In these instances, Haversian canals can have fractures splitting right through them, as opposed to fractures going along the cement lines and path of least resistance. Unlike fresh bone, burned bone does not have osteocyte response to stressors and signal ions in the bone, or interstitial fluids and cilia, to react and form a precursory woven bone structure over the fracture site (Chen *et al.*, 2010). Though this is obvious, it is critical to be understood and said as to introduce why trauma to fresh bones will be distinguished from fractures on burned bones.

Once structural differences are understood, the distinction between perimortem fractures and heat fractures needs to be identified. Perimortem fractures occur around the time of death and show no signs of healing. It is critical to look at perimortem trauma fractures because they can be indicative of cause of death, or trauma experienced leading up to death. Bones at the time of perimortem trauma will still deflect fractures, because they have not turned into brittle structures yet; they are still 'wet.' Heat fractures, on the other hand, occur from the general dehydration of the bone. During direct exposure to heat, dehydration (water loss), decomposition (removal of organic components), inversion (loss of all carbonates), and fusion (melting of bone crystals) occur (Dzierzykray-Rogalski 1967, Herrmann 1977, Mayne Correia 1997). During fire modification, the bones start to crack and fractures can proliferate on the surface. Distinguishing heat fractures from trauma fractures is mostly studied in long bones, not irregular bones (Pope and Smith 2004). Longitudinal fractures, which occur along the axis of a bone, are the main fracture type found on thermally altered long bones. Secondary fractures are described as curved and straight transverse fractures (Baby 1954, Binford 1963).

This is different from trauma related fractures. Sharp force trauma fractures are typically identified by cut marks, saw marks, kerf marks and striation of the unburned cortical and cancellous bone (Guilbeau 1989, Symes *et al.*, 2008), and these indicators remain visible post-burning on cortical bone. These types of fractures are caused by cuts, chops, stabs, punctures, saws, or any other item that can segment tissues (Wedel and Galloway 1999). Depending on the type of bone, i.e. long, cranial, or irregular, the sharp force trauma can affect the bone differently. Bone is rigid in nature, so it holds the characteristics of the trauma that has impacted it – but a thinner bone may be more prone to splintering or fracturing entirely, versus a thicker bone that has remnants of a deep wound (Wedel and Galloway 1999). Blunt force trauma, conversely, is trauma resulting from a wide device that crushes or tears the bone (Wedel and Galloway 1999). Often these traumas leave behind circular or oval-shaped defects. In crania, for example, the inner and outer tables compress and the bone becomes beveled around the point of impact. This can lead to what is known as concentric fractures (Symes *et*

al., 2008). In fresh bone, both sharp force trauma and blunt force trauma leave distinct markers based on weapon type and class because of the bone's ability to disperse force via interstitial fluids.

Burned bone is a brittle substance, however, and will not disperse force, but can still show remnants of sharp force and blunt force trauma. Burned (brittle) bone is extremely stiff and fragile in nature and, therefore, fractures easily under force due to the lack of collagen. Without collagen, bone becomes non-elastic and susceptible to fractures (Bontrager and Nawrocki 2008). Due to the known heating process that bones undergo, it has been observed that long-bones break down in a zonal manner (Chamay and Tschantz 1972). As long bone breaks down, the cortical bone exhibits "superficial checking, fine longitudinal striae, deep longitudinal fracturing or splintering" (Binford 1963), whereas the trabecular bone decays via small longitudinal fractures until the trabeculae disintegrate altogether (Binford 1963). Due to this zonal breakdown, the metaphyseal portions of bone are rarely found and almost no trabecular bone is recovered in cases of high heat exposure over an extended period of time (Lisowski 1968). The breakdown process is determined by length of time, amount of heat exposure, musculature present, and temperature of fires reached (Binford 1963). The overall progression is fairly predictable with regards to how long bones break down due to the vast number of repetitive studies that are done on the process of long bone decomposition in heat studies.

Irregular bones, on the other hand, break down differently from long bones because their biomechanical and structural functions are unalike. The pelvis, for example, is brittle because of the thinner cortical bone. However, due to the protective nature of the thick musculature, tissues, and organs that sit within or near the pelvic girdle, the pelvis breaks down relatively slowly with regards to heat exposure. In partially cremated remains, the pelvis is often found with mild damage (Bohnert *et al.*, 1997). With regards to irregular bones, however, there is not much more information on how they break down with respect to cremation. This is why, for the purpose of this study, irregular bones and cranial bones will be lumped together in one group. In crania, "[t]he human head burns in relationship to the varied thickness and anatomic distribution of insulative skin, muscle, and fat" (Pope and Smith 2004). For example, the lateral aspects of the vault are protected from high heat due to the temporal muscles (Baby 1954). This explains why the base of the cranium survives more than other portions of the cranium. Most commonly seen on crania are delamination fractures from increasing thermal destruction and from post-fire cool downs. The other main types of heat related fractures seen in cases of partial cremation are deep linear fractures, patina breakage, and curved tissue regression that produce sharp margins and shrinkage. In cases of trauma, fractures are seen to have "eroded, blunted,

deformed, or even warped margins" (Pope and Smith 2004) that show reflective thermal exposure over a period of time, damaging the inner and outer tables.

1.6 Lack of Literature on Cranial and Irregular Burned Bone

As of yet, there is limited research on the impact of heat fractures on cranial and irregular bones. It has been outlined above how cranial and irregular bones react to sharp force and blunt force trauma based on their bone structure. This paper has discussed how cranial and irregular bones break down when impacted with heat; however, there is little to no research on how fractures of cranial and irregular bones react when heat is introduced to them. This limitation is evident by prior research, which overwhelmingly focuses on long bones and animal substitutes (Pope and Smith 2004). With little information on how heat alters the remnant marks of sharp force and blunt force trauma, this field needs to be further fleshed out. Describing mechanism, morphology, and identification of normal heat-related changes on burned cranial bone (Pope and Smith 2004) is simply not enough – these three categories need to be combined with fracture morphology and fracture identification as a whole. It is known how perimortem trauma fractures will occur in fresh bone, just as it is known how heat fractures will occur in brittle bone; however, there are no studies to date that discuss how the two intertwine and can be differentiated from one another. Differentiation of fractures based strictly on surface morphology is difficult to analyze and, as stated by Herrmann and Bennett (1999), "the reconstruction, macroscopic examination, and assessment of suspect elements […] [and[select fracture surfaces should be subjected to microscopic examination." Having little microscopic evidence to prove trauma fractures and heat fractures can be differentiated makes it imperative to create a method of differentiation for forensic cases and future research.

1.7 Animal Analogues versus Human Counterparts

Frequently in experiments involving bone, animal surrogates are used in place of human remains; however, human irregular bones are vastly different from animal irregular bones, making them non-interchangeable. Much like human bones, the basic multicelluar units that comprise animal bones are osteons, Haversian canals, Volkmann's canals, canaliculi, and lacunae; however, animal bone is classified into various groups of bone based on the vascularization patterns seen microscopically (Hillier and Bell 2007). Non-human animal cortical bone, for example, can be broken down into three subgroups of bone: primary, secondary, and avascular. From there, the bone is sorted into groups described as "longitudinal, radial, reticular, plexiform, laminar, and acellular bone" (Hillier and Bell

2007). This means the bone is more complex in its structure and in some instances more dense. Microscopically as well, there are vast differences in the bone structure between animal species. Animal bones have "bimodal distributions of Haversian canal size" (Skedros *et al.*, 2013) that are reflective of the animal's overall size. This means the larger the animal, the wider the Haversian canal diameter due to the need to distribute and supply blood and nutrients throughout the bone (Hillier and Bell 2007, Jowsey 1966, Skedros *et al.*, 2013). As animal size increases, the osteons and Haversian systems grow correspondingly. This is seen mainly in greater remodeling of bones that are distally located, which take the brunt of locomotive impact (Hillier and Bell 2007). An increase in the count and density of secondary osteons can be noted, showing significant differences from more proximally located bones (Hillier and Bell 2007). Similarly, the smaller the overall size of the animal, the smaller the osteons and the Haversian canal. It has been reported that the overall growth of an osteon is limited by the size of the animal (Jowsey 1966). This is important because it shows the biomechanical structure within non-human animals differs across all species, whereas within humans, the Haversian and osteonal systems size only varies based on individual age and possibly disease. It is more unilineal (Jowsey 1966, Skedros *et al.*, 2013). Knowing there are structural bone differences across non-human animal subgroups makes it more of a challenge to pick a proper substitute for human bone.

Structurally, there are two major types of bone present in animals – woven and plexiform. The woven bone is similar to that discussed above and will not be reexamined here. The plexiform fibrolamellar bone is synonymous with human cortical bone; however, it shows distinctive seasonal banding around the lamellae based on feeding habits, nutrition intake, and other stressors. Fibrolamellar bone is fast-growing bone, with a "more dense system, or plexus, of vascularization" (Hillier and Bell 2007). Plexiform bone is built and layered on a longitudinal basis with circumferential primary osteons laid out in a '"brick wall' appearance" (Hillier and Bell 2007). This is structurally different than the plywood model that is evident in human cortical bone; these brick-like parallel layers are more simplistic. The plexiform bone of larger animals is mostly comprised of osteonal systems built up over years of remodeling. Primary lamellar bone is rarely seen in large adult animals because it is constantly being remodeled due to location contact, micro-cracks, and stress. Remodeling in smaller animals is typically seen around ligament and tendon attachment sites due to bone alterations from mechanical stressors. Aside from the aforementioned remodeling, the lamellae of plexiform bone remain mostly untouched (De Ricqles *et al.*, 1991, Weiner *et al.*, 1999). Like the human skeletal system, animal bone also contains trabecular bone. Here, the trabecular bone is mostly seen in

epiphyseal ends of long bones and in the flat bones of the crania (Hillier and Bell 2007). In fibrolamellar, weight bearing portions of long bones, the trabeculae appear in "long lines of interior bone instead of compact and dense small circles" (Beisaw 2013), which is seen in cranial bones.

Cranial bone formation between humans and animals are vastly different as well. Animal crania have five distinctive layers: a cortical outer and inner surface with three diploic middle sections. These 'in between' strata are composed of fibers and cells connecting the periosteum of the inner surface to the periosteum of the outer surface. Human cranial bones, on the other hand are only broken down into three distinct layers: two layers of cortical bone forming the inner and outer tables, and a diploic center (Pritchard *et al.*, 1956). Aside from structural differences, Beisaw (2013) states human cranial fragments are, in general, curved and consistently smooth compared to their animal counterparts. Distinctions between human and animal inner tables, outer tables, and diploë are evident as well. Animal cranial bones have been described as "flat or otherwise irregular in shape […] in cross-section the bone may or may not have a clear sandwich like appearance" (Beisaw 2013). The variation in histology between human and animal bone leads to differences in fracture patterns (Wang *et al.*, 1998). Therefore, anatomical distinctions between human and animal cranial bones could yield potentially unreliable results in this research.

Another point of difference between human and animal bones stems from differences in locomotor behaviors. Animal bones undergo different stressors than their human counterparts. For example, the distal ends of animal bones have an increased number of Haversian canals due to their constant remodeling from micro-cracks stemming from contact with the ground (Hillier and Bell 2007). Animal bones are required to remodel, reform, and respond to stressors differently than human bones (Hillier and Bell 2007). Remodeling of animal bones occurs in longitudinal growth successions and will occur in response to mechanical stressors applied to the limbs. In doing so, much like humans, animal bodies are constantly swapping minerals between the bone and the other surrounding tissues (Jowsey 1966). The brick-wall appearance of plexiform bone changes how fractures propagate throughout the bone. The vascular system within plexiform bone is known as a plexus, or a "three-dimensional, symmetrical arranged network" (Hillier and Bell 2007) that is rectilinear in shape. The vascular arrangement found in plexiform bone allows for easier fracture proliferation, as micro-cracks tend to travel through this vascular system, increasing the speed in which the fractures travels (Wang *et al.*, 1998).

There are multiple justifications for choosing to use human remains over animal remains, most of which are summarized above. This study will utilize human remains rather than animal remains because of the distinct differences in irregular bone structure. As discussed above, bone development in humans and animals differs (Pritchard *et al.* 1956), most distinctively via the presence or absence of plexiform bone. Unlike their animal counterparts, humans do not have woven bone except in fetal development and in cases of ante-mortem injury or inflammation, i.e. periostitis (Hillier and Bell 2007). The second major difference between human and non-human animal bones lies in the Haversian canal area and diameter (Cattaneo *et al.*, 1999). The Haversian structure of humans versus animals show distinguishable differences in the collagen-bundle sizes and organization patterns when magnified. Collagen bundles, which help with deflecting fractures via energy absorption and displacement, are more closely packed in human cortical bone than animal plexiform bone (Wang *et al.*, 1998). When studied, these variances "are reflected in higher fracture properties" (Wang *et al.*, 1998) in animal plexiform bone. As well, there are distinct differences in the bone mineral density between various species, specifically human and non-human animals. This is largely due to different osteonal sizes, remodeling and bone turnover rates, and calcium hydroxyapatite formation and composition between bone types (Jowsey 1966).

1.8 Hypotheses

By understanding the basics of fracture production and the impact of heat on bone, this project hypothesizes that it is possible to differentiate perimortem trauma from heat trauma on cranial and irregular bones. Burn patterning and identification is mainly studied using long bones, where as "little has [been] focused on cranial structures" (Pope and Smith 2004). Research on long bones is extensive and includes predictable patterning based on the type of fracture and heat exposure because these bones are more accessible or can be supplemented with other animal bones more easily. However, the way cranial and irregular bones are structurally formed and thermally altered is different from long bones. Irregular bones are impacted by heat based on musculature, thickness of bone, trauma, and length of exposure. The overall loss of organic components makes cranial and irregular bones weaker, fragile, and more easily impacted by heat exposure and fire. As noted by Pope and Smith (2004), "to differentiate burn patterns of the traumatized head from purely thermal effects, it is necessary to develop an expectation of features produced by thermal damage", which is what this project entails. Given the limited knowledge of how heat fractures interact with traumatic fractures, my research question aims to analyze and differentiate trauma fractures from heat fractures in cases

of partial cremation. This research will add to the growing volume of literature on identification and differentiation of trauma from heat fractures in irregular bones.

Based on the above discussion, I anticipate seeing differences between trauma fractures and heat fractures in cranial bones and irregular bones because of the elasticity of the bone during traumatization versus the lack of collagen and flexibility during cremation. Cranial bones are expected to still exhibit their perimortem trauma fractures post-cremation. Trauma fractures and heat fractures will be differentiated based on the peeling of the top layer of cortical bone from the point of impact and the curvature created from the impact as seen on a microscopic level. In irregular bones, I expect to see similar results; however due to the thinner cortical layer and thicker trabecular layer, I anticipate the structural integrity of the bone to be overall weaker than the cranial bone. This will cause greater fracturing and skewing of trauma fractures upon burning since no musculature will be present. The traumatization will occur on fresh bone, which I hypothesize will lead to distinct differences seen on a microscopic level between perimortem trauma fractures and heat fractures.

Chapter 2: Ossification of the Cranium and Irregular Bones and the Implications for the Interpretation of Fire Damage[1]

2.1 Introduction

Differentiation of heat and trauma fractures in forensic investigations is crucial to understanding cause of death; however, based on bone structure, different types of fractures can form. Though our understanding is limited in this topic, a prime example lies in long bones, which are cylindrical and thick, causing them to incur longitudinal, transverse, buckling, greenstick fractures and more (Wedel and Galloway 1999). On the other hand, the large flat bones of the cranium are thin and curved, causing concentric fractures, linear fractures, depression fractures, and more (Hart 2005, Kimmerle & Baraybar 2008, Klepinger 2006). With regards to crania, there is limited knowledge of how the ossification of cranial bones impacts the types of trauma seen, and furthermore how the introduction of heat alters those fracture lines. This topic is highly relevant to forensic anthropology because the cranium is a major target of injury in forensic cases, and is highly susceptible to heat alteration (Pope and Smith 2004).

In developing bone, ossification begins the scaffolding for the base of the architectural strength of the bone. There are two main types of ossification, intramembranous and endochondral, which are found in different parts of the skeleton. There is little to no research on how these types of ossification impact the strength and integrity of the bone. However, it is critical to understand how and where these types of ossification occur on the skeleton to understand how they impact strength of each type of bone respectively. By recognizing the origin and growth processes each type of bone undergoes, the mechanical aspects of how each bone behaves can be better understood. This is particularly important with regards to cranial bones, as they are the only collective group of bones formed from both intramembranous and endochondral ossification.

Based on the structural and mechanical properties of cranial and irregular bones, there needs to be an understanding of how these bones fracture, what causes the perpetuation of fractures, and how these fractures can be differentiated from one another? Furthermore, when heat is introduced, what happens? There is very little research on how trauma seen on cranial and irregular bones is

[1] A version of this chapter is ready for submission for publication to the American Journal of Physical Anthropology.

impacted with regards to heat alteration. Being able to distinguish traumatic fractures from heat fractures on cranial and irregular bone is crucial when completing skeletal analysis of cremated remains. This review of the literature attempts to look at the roots of ossification, as well as ossification types and how the large flat cranial bones and irregular bones are formed, with the intent to inform and provide a predictive model for what will happen structurally in traumatized, burned bone. This chapter will look at effects of trauma on cranial and irregular bones, in addition to heat alteration of cranial and irregular bones. To address this aim, the intent of this review is twofold. Firstly, to detail the background of ossification and its origins by succinctly documenting embryological development of bones. Secondly, to explore the complexities and limitations of research that encompasses cranial bone and irregular bone trauma and heat exposure in attempt to direct future research and improve current understandings of how ossification in utero molds how trauma and heat will impact large flat cranial bones.

2.1.1 Mesenchyme versus Cartilaginous Origins

Bone formation occurs in one of two ways – either through intramembranous ossification or endochondral ossification. Intramembranous ossification arises from mesenchymal origins, except for dermal bones which use neural crest cells. Endochondral ossification on the other hand stems from cartilaginous precursors (Cunningham *et al.*, 2016, Kawasaki and Richtsmeier 2017). Mesenchyme is a type of embryonic connective tissue that is laid down at the start of osteogenic sites (Cunningham *et al.*, 2016, Freemont 1993). Once mesenchyme is laid down, osteogenic cells arise and interact with one another to spawn bone growth. Fibrous condensation begins and intramembranous ossification continues to generate new bone. On the surface of the forming bone, mesenchymal cells condense and vascularize the periosteal, or outer most, layer of bone (Cunningham *et al.*, 2016).

Cartilaginous origins begin with chondrocytes. A chondrocyte secretes a cartilaginous matrix and moves along the developing bone to proliferate cartilaginous growth. The cells begin to enlarge and secret type X collagen, which is used in the chondroid matrix during calcification (Freemont 1993). After, the chondrocytes die and become embedded in the forming cartilage, blood vessels vascularize the area leaving calcified cartilage. Remodeling then takes place turning the cartilage into bone (Freemont 1993). Cartilaginous bone occurs within the perichondral region of developing bone matter and will either ossify via endochondral, periosteal, or endosteal ossification (Kawasaki and Richtsmeier 2017).

2.1.2 Collagen Synthesis

Collagen is one of the main building blocks for creating strong, yet flexible bones. Bone is composed of four main components, of which three are organic and one is inorganic. Together, the organic matter forms osteoid, a non-mineralized bony matrix. Hydroxyapatite crystals, composed of calcium and phosphorus, help aid in bone structure and mechanics (Freemont 1993). As collagen bundles are bound together to form the basis of bone, some osteoblasts become embedded in the tissues, becoming osteocytes. The osteocytes are then surrounded with interstitial fluids, nested in the lacunae of bone (Cunningham *et al.*, 2016, Freemont 1993). It is theorized that osteocytes are responsible for the overall maintenance of bone matrix, able to "[sense] microdistortions of the matrix and [translate] them into signals that influence the activity of bone surface cells (osteoblasts, osteoclasts and resting surface cells)" (Freemont 1993).

Secreting osteoid to help bones develop, osteoblasts and osteoclasts are introduced to the growing bone. Osteoblasts continually build the bone and shape according to bodily needs. Osteoclastic cells, on the other hand, are multinucleated and adhere to the bone's surface. Osteoclasts remove bone, allowing the tissue to be formed and remodeled as needed. This particular cell allows calcium to be absorbed into the extracellular matrix, circulate hormones, and react to daily mechanical loads (Freemont 1993). Once collagen is synthesized, osteogenic cells work together to mold the collagen into bone and constantly maintain it throughout the life of the individual.

2.1.3 Woven and Lamellar Bone

During bone formation, two types of bone classifications are seen: woven and lamellar bone. Woven bone is a precursor, seen during fetal growth in the flat bones of the cranium, and in bone repair (Cunningham *et al.*, 2016, Currey 2003, Freemont 1993). The process in which this bone type is formed is called *de novo* – central growth occurring around osteoblasts in a random, disorganized manner (Currey 2003, Freemont 1993). Classified under intramembranous ossification, woven bone starts from mesenchymal cells without a cartilaginous precursor (Gorski 1998). The fine fibers that compose collagen are randomly organized along the longitudinal axis of the forming bones (Cunningham *et al.*, 2016, Wedel & Galloway 1999). The rapidly laid down fibers are highly mineralized; the structure is composed of a loose scaffolding that is "mechanically inferior to lamellar bone" (Currey 2003). During formation, woven bone is laid down and continually remodeling until lamellar bone is formed (Cunningham *et al.*, 2016, Wedel & Galloway 1999). As the fetus ages, woven bone is replaced by primary lamellar bone and collagen sheets (Wedel & Galloway 1999). Woven bone

is only seen again during fracture repair, acting as a temporary tissue in attempt to stop fracture proliferation until bone repair can be completed (Silva and Toulhey 2007).

Unlike woven bone, lamellar bone is highly organized in nature and laid down in parallel layers (Cunningham *et al.*, 2016, Currey 2003). Comprised of collagen sheets, lamellar bone forms from a collagenous precursor. The collagen precursor creates bundles of fibrils that are laid down adjacently to one another (Currey 2003, Gupta and Zioupos 2008, Weiner *et al.*, 1999). This forms the basic scaffolding unit of bone, which is remodeled constantly throughout life (see Chapter 1.2 for a more detailed description). Between the collagen fibril bundles is excess space, filled with randomly organized collagen fibrils, many of which run perpendicular to the lamellae. Canaliculi are present here (Reznikov *et al.*, 2014). In lamellar bone, there are primary and secondary osteons. Primary osteons are known as Haversian systems, which develop canals to supply nutrients throughout the bone. These are connected to the periosteal surface via blood vessels interspersed in the lamellar bone (Cunningham *et al.*, 2016). As the primary osteons get reworked, secondary osteons form in their place, causing a reorientation of lamellae (Reznikov *et al.*, 2014, Vaughan *et al.*, 2012).

This modelling takes place over six steps: activation, resorption, reversal, formation, mineralization, and quiescence. Activation requires the basic multicellular unit (BMU) to form precursor cells. During resorption, the BMU osteoclasts begin to resorb the primary osteonal bone, demineralizing it. Osteoclasts then tunnel through the axis of the bone. Reversal occurs when the leading osteoclast stops working and osteoblasts begin rebuilding the bone. The osteoblasts line the tunnel and lay down new, circumferential lamellae around a nutrient artery in a process known as formation. Mineralization follows, as minerals grow between the collagen fibril layers. Finally, during quiescence, osteoclasts are eliminated, osteoblasts turn into osteocytes, and metabolic processes continue (Cunningham *et al.*, 2016). The overall look of this bone as it is remodeled through life is akin to "grain in wood round a knot" (Currey 2003). This stable material is what comprises adult bone.

2.2 Ossification Types

2.2.1 Intramembranous Ossification

Developmental embryology of bone shows various types of ossification. The two main categories are endochondral ossification, beginning with a cartilaginous precursor, and intramembranous ossification, that arises directly from mesenchymal tissues (Cunningham *et al.*, 2016, Kawasaki and Richtsmeier 2017). Endochondral ossification creates cancellous or trabecular bone

formation. Intramembranous bones, however, can be either perichondral, cortical, or dermal, i.e. the center of flat cranial bones. The order of formation in utero is as follows: dermal (diploic) intramembranous ossification, perichondral (cortical) intramembranous ossification, then endochondral ossification (Cunningham *et al.*, 2016). This type of ossification occurs via an osteoblast filled matrix and connective tissue membrane base. In long bones, the mineralization occurs in the periosteal surface (outer surface), perichondral layer, and endosteal surface (inner surface facing the medullary cavity) (Kawasaki and Richtsmeier 2017). In doing so, intramembranous ossification is directly responsible for the organized lamellar bone that is laid down in a systematic manner (Cunningham *et al.*, 2016).

Perichondral ossification is the basis for cortical bone development. In order for these bones to develop though, the perichondral ossification works in unison with endochondral ossification to create a trabecular network inside the cortical bone structures (Cunningham *et al.*, 2016). This type of ossification begins with perichondral osteoblasts and a network of arteries and vessels via mesenchymal origin. The tissue structures around the perichondral cells have an abundance of fibroblasts, mesenchymal cells, and macrophages that help to develop the support structures of the developing bone. There are unmyelinated nerve fibers and lymphatic vessels that infiltrate the forming structure to allow for metabolic processes to penetrate the bone (Cunningham *et al.*, 2016). The entire forming bud is highly vascularized, allowing for chrondrogenesis to occur via interactions of extracellular matrix and basal lamina or ectodermal-mesenchymal exchanges (Cunningham *et al.*, 2016). As the mesenchyme develops a scaffold for the rest of the bone, osteogenic cells begin to infiltrate the structure. A collagen matrix is introduced to the structure, beginning the process of bone growth. Lamellar bone is laid down via osteogenic cells, forming and remodeling the bone structure

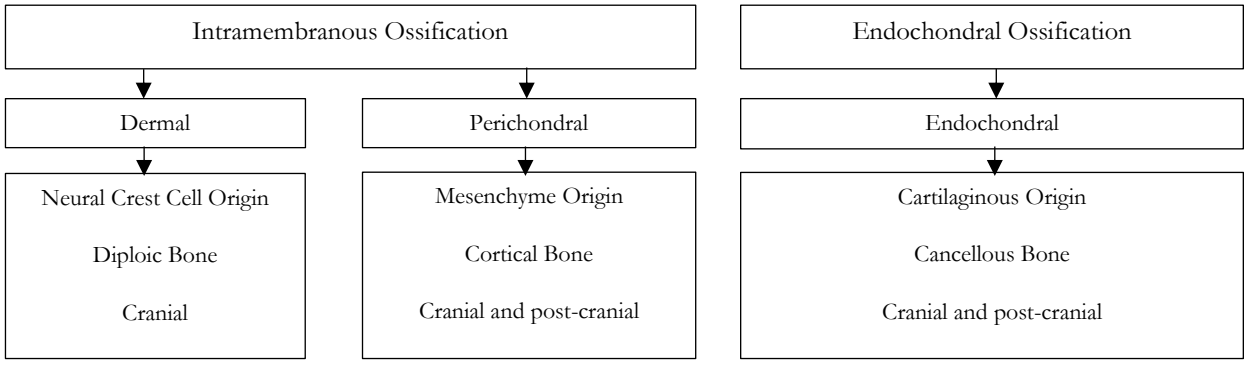

FIG. 2.1 Adapted from Cunningham *et al.*, 2016 showing origin, bone type association, and location of intramembranous and endochondral ossification.

until it is complete. This bone is constantly remodeled throughout life to account for daily micro-damages (Hart 2005).

Crania are special with regards to ossification. Unlike the rest of the body, the large flat cranial bones ossify from both intramembranous and endochondral ossification. The cranium is divided into the neurocranium and splanchnocranium (Kawasaki and Richtsmeier 2017). From there, the neurocranium is broken down into cranial base, or chondrocanium, and the cranial vault. The base of the cranium ossifies endochondrally, whereas the cranial vault is intramembranous in origin (Cunningham *et al.*, 2016, Kawasaki and Richtsmeier 2017, Tubbs and Bosmia 2012). As the large flat bones develop, the "calvarial bones are drawn downward […] the outer layer of which is osteogenic and responsible for the production of the inner table of each flat bone" (Tubbs and Bosmia 2012). These cranial bones are seen as a sandwich-like structure, where a spongy, diploic center sits between the forming inner and outer tables (McElhaney, *et al.*, 1970, Motherway *et al.*, 2009, Skrzat *et al.*, 2004). Diploë acts like the cancellous portion of long bones. This development had been hypothesized to occur from neural crest cells, as opposed to mesenchymal cells, due to the embryological need to form a protective covering for the exoskeleton during development (Cunningham *et al.*, 2016, Kawasaki and Richtsmeier 2017). Being naturally porous and highly vascularized (Tang *et al.*, 2008), diploic bone acts as a transport center for nutrients of cranial bones. Much like cortical and trabecular bone, diploic bone remodels daily to account for microdamages of the skeletal system (Corega *et al.*, 2013). In younger individuals, diploë is "filled homogeneously, the texture being smooth or slightly folded" (Skrzat *et al.*, 2004). Older individuals, however, have diploë that is "scattered, irregular and rough in texture with numerous small granular clumps which might be counterparts of random agglomerations of bony masses" (Skrzat *et al.*, 2004). The elderly individuals tend to show a thinning of the inner table with an increased build-up of diploic bone (Skrzat *et al.*, 2004).

2.2.2 Endochondral Ossification

Unlike intramembranous ossification, endochondral ossification makes up the cancellous, or trabecular bone that is seen in long bones and irregular bones. Irregular bones are classified as the short bones of hands and feet, carpals, tarsals, vertebrae, and the pelvis. While intramembranous ossification is precise and organized, endochondral ossification is more haphazard (Cunningham *et al.*, 2016). Endochondral ossification, starting in a mesenchyme cloud that produces chondrocytes, occurs over already existing cartilaginous precursors via "mineralization of the cartilage model, partial resorption of the cartilage by chondroclasts, and secretion of bone matrix onto the resorbed cartilage

surfaces by osteoblasts" (Kawasaki and Richtsmeier 2017). As osteoblasts build around the cartilaginous model, capillaries and arterial networks develop around the model. This in turn is called the periosteum, or outermost layer of bone (Cunningham *et al.*, 2016). An "irruption canal" (Cunningham *et al.*, 2016) is a canal that invades the cartilage model for the initial ossification. This acts as a pathway for cell types, like osteoblasts and osteoclasts, to enter the model, as well as connective tissues and other cells (Cunningham *et al.,* 2016). Within the medullary cavity, osteoprogenitor cells rework the woven bone into cancellous bone (Cunningham *et al.*, 2016). It should be noted that the periosteal layer is formed from mesenchymal cells, as is the cortical bone, making them intramembranous in origin; however, the internal trabeculae formation becomes endochondral.

Trabecular bone is highly porous in nature composed from hydroxyapatite crystalline structure embedded with lacunae and canaliculi (Vaughan *et al.*, 2012). The bony spicules that form are thickened by osteoid generation. Off the main trabeculae are secondary trabeculae that form at "right angles to the primary struts helping to enclose vascular spaces" (Cunningham *et al.*, 2016), and allow for the formation of the complete osteonal system. As the cancellous bone is remodeled, secondary osteons are formed much like cortical, lamellar bone (Currey 2003). This network creates a scaffold support system that allows bones to be fracture resistant and lightweight in nature (Vaughan *et al.*, 2012).

2.3 Cranial Bones

2.3.1 Effects of Trauma on Cranial Bone

2.3.1.1 Blunt Force Trauma

The large flat bones of the cranium are formed in what is known as a sandwich structure. There are two layers of thin cortical bone, creating the inner and outer tables. In between these, is a porous, spongy layer of bone known as diploë (Hubbard 1971, Pritchard *et al.*, 1956). The flat bones are formed through intramembranous ossification. When impacted with blunt force trauma, local deformations occur, typically producing linear fractures across the cranium due to bone elasticity. The trauma is typically localized, resembling a "thumbprint dent in clay" (Klepinger 2006), causing the inner and outer tables of the flat bones to crack together. These compressive forces that ultimately damage the outer and inner tables of cranial bones also create tension lines across the surrounding bone. This is due to the bone reaching its failure point, or point where the elasticity of the bone is over stretched and permanent damage is done (Klepinger 2006). Fractures emanating from the main

site(s) of impact are known as concentric fractures (Hart 2005, Kimmerle & Baraybar 2008). In the cranium, this process begins in the outer table and expands to the inner table, causing directional changes in the fractures, creating circular lines emanating from the main point of impact (Berryman & Haun 1996).

Linear fractures, diastatic fractures, depression fractures, stellate fractures, and comminuted fractures (see Chapter 1.4 for more detailed information) can be seen in cranial bones. Linear fractures, a main cause of concentric fractures (Gurjian *et al.*, 1949, Wedel and Galloway 1999) occur along the weakest spots of cranial bones, making the secondary fracture(s) that take place the second weakest portions of the cranium. Secondary stress levels continue to disperse energy from the main site of impact, and can cause stellate fractures (Gurjian *et al.* 1949). Depression fractures, similar to stellate fractures, cause the bone to immediately fail at the site of impact, piercing cranial bone and causing residual micro-fractures (Gurjian *et al.*, 1949). With respect to the point of impact, when more energy is applied, a greater amount of out-bending is noted (Gurjian *et al.*, 1949). Conversely, the less energy used, the greater chance there is of the bone directly absorbing the energy and producing a depression. In these cases, the inner and outer tables typically separate via curvilinear fractures that tear away the external surface of the large, flat cranial bones (Gurjian *et al.*, 1949). To summarize, the compressive forces on the outer table of cranial bones cause tension forces on the inner table of the cranial bones. Due to these forces, fracture lines emanate on both the outer and inner tables. As force is continually applied, the "fracture plates of the bone are bent inward by the blunt object" (Berryman & Haun 1996). Under blunt force trauma, portions of the cranium can be impacted or the entirety of the cranium can be consumed with micro-fracture lines depending on the forces applied, the size of the object, and the age of the person being affected.

2.3.1.2 Sharp Force Trauma

Sharp force trauma is classified like blunt force trauma via the fracture patterning, the number of impact sites, the type of trauma seen (i.e. narrow, wide), and the distribution pattern denoted from the main site of impact. It has been noted in many cases of sharp force trauma that the impact site(s) are localized, so in cases of multiple wounds they tend to be clustered together. Perimortem sharp force trauma is known to cause an edge of incision – a curled or raised edge – where the object was inserted. In fresh bones, the implement causes compression on both sides of entry, but when the object is removed, the raised edge is formed (Klepinger 2006). Post-mortem sharp force trauma can be confused with perimortem sharp force trauma, but is typically caused by excavation tools or

carnivore puncture wounds (Kimmerle and Baraybar 2008). These do not leave a curl or raised edge unless the incident occurs very soon after death. Trauma from sharp force objects is similar in both regular and irregular bones, except in irregular bones there is a greater chance of the sharp object penetrating through the entirety of the bone.

2.3.1.3 Trauma Alteration

As a whole, the cranium is designed to resist traumatic stresses well, however, the thickness of cranial bone overall impacts the craniumss ability to resist fractures (Hardy 1973). Deformation of the cranium in cases of trauma can be identified as one of four major categories: membrane deformation, bending deformation, shear deformation, and "local core compression and puncture of the skull" (Hubbard 1971). Membrane deformation occurs when the "sandwich" cranial bone structure is stretched or compressed to the point of failure. The stresses are evenly distributed across the panels of bone. Bending deformation on the other hand is based on the compressive and tensile resistance to force as the bone becomes stressed. Shearing deformation is caused by a stress that directly impacts the "low-stiffness core material" (Hubbard 1971). Finally, core compression and puncture deformation is when the "sandwich" structure of cranial bone is penetrated fully. The deformation of the cranium, regardless of the cause, frequently leads to linear fractures, and the overall cause of failure in large, flat cranial bones (Hubbard 1971).

Alteration in the thickness of the inner and outer tables directly impacts cranial bone susceptibility to fractures. Whether the inner table is thicker than the outer or vice versa, deformation patterns can change (Gurjian *et al.* 1949). In adults, it should be noted that the outer table is typically thicker than the inner table (Tubbs and Bosmia 2012). Cortical table bone, regardless of thickness, is still able to resist fractures relatively easily depending on force. The changes in table thickness directly leads to variation in diplöe thickness and fracture failure rates (Tang *et al.*, 2008). Knowing cranial bones are not the same thickness is important to understand the differences in diploic structure (Tang *et al.* 2008). In cortical bone impacted with blunt or sharp force trauma, the interstitial fluids disperse the force through cement lines and around osteonal systems, as collagen diverts the crack tip (Gupta and Zioupos 2008, Nalla *et al.*, 2005, Peterlik *et al.*, 2005, Zimmermann and Ritchie 2015). Mature diploë acts as a mechanism to "increase the energy absorbing capabilities of bone" (Motherway *et al.*, 2009) and as a protective material to the cranium's internal soft tissues (Motherway *et al.*, 2009). Much of the mechanical responses of cranial bones to trauma lie in the strength and structural arrangement of the diplöe; however, age and individual variation can impact the distribution of diploë in cranial flat

bones, impacting the structural integrity of the bones. Meaning, "energy absorption, gross stiffness and damping characteristics which are strongly dependent on structure – will vary greatly" (McElhaney *et al.*, 1970). Due to non-uniformity in diploic bone density across the cranium, resistance to fractures differs in varying parts of the cranium (Hubbard 1971), therefore, the weakest point of cranial flat bones, and most likely portion to fail during impact, is the diploë.

Sutures are a major component in fracture proliferation and resistance on cranial bones. By definition, sutures are "unossified and filled with cartilage, chondroid, and vascular tissue, which contain more abundant fluid content of low resistivity than surrounding bone tissue" (Tang *et al.* 2008). Though cortical bone surrounds the sutures to provide support and reinforcement, the thickness of the cortical bone and strength of underlying diploë impact sutural ability to resist fracture deformation (McElhaney *et al.*, 1970). Therefore, structural differences in sutures can significantly impact the stability of the cranium. For example, the presence or openness of suture lines makes the cranium as a whole more susceptible to fracture proliferation. The sutures themselves act as a path of lowered resistance for fractures to travel across (Tang *et al.*, 2008). The main fracture seen around sutures, as previously mentioned, are diastatic fractures. Based on the aforementioned information, once the inner and outer tables fail, diploic variation and suture lines become the major pathways for the spread of fractures and the ultimate amount of damage done to the cranium.

2.3.1.4 Heat Alteration of Cranial Bone

Heat causes fractures as the bone becomes demineralized. Flat bones of the cranium are initially formed via a mixture of cellular and extracellular components, primarily calcium, phosphate, in the hydroxylapatite (Marella *et al.*, 2012). As heat increases, bone dehydrates as water is removed (100°C to 600°C), followed by general decomposition of organic materials (300°C to 800°C). As temperatures rise, the process of inversion occurs, where the carbonate structures degrade and crystal size increases (500°C to 1100°C). Finally, the interior crystalline structures melt and break down, causes collapse of the bone structure (700°C and up) (Mayne Correia 1997, Thompson 2004). Throughout the collagen degradation process, the elastic nature of bone is compromised. There is no osteonal pullout; interstitial fluid dissipates, stopping the ability to alter where the forces go. Heat fractures, therefore, are not diverted around cement lines and osteonal systems, but pass directly through them, rupturing them entirely (Gupta and Zioupos 2008, Nalla *et* al., 2005, Peterlik *et al.*, 2005, Zimmerman and Ritchie 2015). This alters the failure rate of the bone, causing the bone to warp, shrink, and fracture (Marella *et al.*, 2012).

As the cranium breaks down mechanically, the intense fractures that form on the cranium as heat is introduced are hard to identify (Marella *et al.* 2012), as the cranium is known to "[burn] in relationship to the varied thickness and anatomical distribution of insulative skin, muscle, and fat" (Pope and Smith 2004). An example of this is seen by the temporal muscle protection of the lateral vaults of crania in high heat (Baby 1954). The relationship of skin, muscle, and fat to bone explains why the base of the cranium survives more so than other portions of the cranium. Of what remains, there can be multiple types of fractures present: potential trauma and heat. Trauma fractures can be those created at the impact site, or residual fractures that extend from the site of impact as forces are dispersed across the cranial vault. Heat fractures, on the other hand, are strictly created when bone is exposed to high temperatures, causing a degradation of the bone histology. Trauma fractures need to be studied more in relation to cremation and cranial bones. There is insufficient research on the identification and differentiation of traumatic fractures and heat fractures on cranial bones. What is known is noted by Pope and Smith (2004), who state traumatic fractures are typically seen as "eroded, blunted, deformed, or even [having] warped margins" that reflect thermal exposure over time. On the other hand, heat fractures are more predictable. One of the most clear cut methods to identifying heat fractures lies in their "clean, sharp and easily matching borders" (Marella *et al.*, 2012). On cranial flat bones, "eggshell fractures […] are very common" (Marella *et al.*, 2012), in addition to delamination fractures from increasing thermal destruction and post-fire cool downs. Deep linear fractures, patina breakage, and curved tissue regression are noted on the large flat bones of the cranium in cases of cremation (Pope and Smith 2004).

2.4 Conclusion

The basic differences of bone types emerge in utero when bone are developing. Based on their origin, intramembranous or endochondral, the structures become distinct in formation patterns. Intramembranous bone of perichondral origin begins from mesenchymal cells that slowly form in surrounding tissues. The collagenous proteins form bundles that are pulled and laid down in a specific and organized manner to create woven bone, and eventually lamellar bone. Intramembranous dermal bone, on the other hand, arise from neural crest cells as a way to create an exoskeleton to the rest of the forming embryo. These bones are largely formed from both intramembranous and endochondral ossification. Unlike traditional long bones, the dermal formation creates diploë, not trabeculae. Diploic bone is a highly porous bone that sits between the two sandwiched inner and outer tables of the large

cranial bones. Trabeculae, formed from endochondral ossification, starts from cartilaginous anlages that are infiltrated by osteogenic cells.

This is important to understand because it creates vast differences in how the bones react to trauma and heat exposure. Large, flat cranial bones are thin, sandwiched structures with a highly porous center. Unlike long bones, they do not have thick cortical bone with a thin trabecular layer that is highly resistant to fractures. The vault bones are resistant to frontal loading, but other forces cause extensive damage to the bones. Blunt force trauma compresses the two tables of bone together, leaving depressions and various fractures on the bone. The fractures are further dispersed by the thickness of the bones and strength of the sutures. This is important to understand because there is little to no research on how heat further impacts these structures. As Marella, *et al.* (2012) states, "[t]he most important task during the assessment phrase is to distinguish vital and perimortal wounds from postmortem ones, due to high temperature exposure." There needs to be a strong foundation in the knowledge of how cranial bones are different from other bones, starting from ossification. In doing so, the properties of the bone and the predictability of how they will react to fractures becomes more clear. This will allow for a further distinction of traumatic fractures from heat fractures in cranial bones.

Chapter 3: The Use of Formalin Fixed Human Remains in Experimental Procedures[2]

3.1 Introduction

Formalin, derived from formaldehyde, is a common chemical compound used to embalm human remains (Mason and O'Leary 1991). This practice is widely used for embalming medical cadavers and by morticians to prepare the body for family viewings. Formalin's impact on bone histology is not widely known, but there is speculation that the chemical alters bone structures by altering the hydroxyapatite mineral (Małgorzata and Jarosław 2006, Mason and O'Leary 1991). This modification to the bone mineral can be detrimental to forensic research when human remains are used as the research material. When using formalin-fixed human remains in cremation research, it is necessary to understand the role formalin may play in affecting the bone and temperature.

Cremation can be broken down into four stages. The first stage is known as charring, or direct exposure to a fire where the body and internal organs remain intact. The second stage is partial cremation, where modification of extremities occurs, but soft tissues remain. The third stage is incomplete cremation. This entails significant discoloration, shrinking, and fragmentation of the skeletal elements. The fourth stage is a complete cremation, where some bony masses are present, but mostly ashes remain (Mayne Correia 1997, Symes *et al.*, 2012, Ubelaker 2009). In research involving cremation, it is important to understand how the microstructure of bone is impacted by heat. With non-formalin fixed partially cremated human remains, the flash point, or maximum temperature reached, at a 600ºC burn is approximately 60ºC to 80ºC above the initial heat temperature (Pointer 2014). This could vary based on the type of fire or oven used. Hypothetically though, this means if a controlled oven is set to 600ºC, the flash point will be between 660ºC and 680ºC (Pointer 2014). For an 800ºC burn, Pointer (2014) noted a flash point between 20ºC and 45ºC above the 800ºC mark. Currently, it is unknown to what extent formalin will increase the flash point of burning bone. This needs to be understood to assess whether formalin fixed human cadavers can be used as substitutes in forensic recreations of burning and cremation.

[2] A version of this chapter is ready for submission for publication to the Journal of Forensic Sciences.

3.2 Non-Formalin Fixed Compact Bone Structure

Human bone is composed of multiple layers of tissue that are woven together to create a structurally durable, yet flexible material. Microscopically, a bone is composed of osteons, osteonal canals (Haversian canals), collagen fibers and fluid filled interstitial space. Continual remodeling takes place in the "periosteum, endosteum, and intracortical lacunae" (Chamay and Tschantz 1972). Composing these elements, and other skeletal tissues, are calcium hydroxyapatite, water, amorphous polysaccharides, and blood vessels (Wedel and Galloway 1999). In utero, the aforementioned components form the first noticeable structures of bone – crystals, collagen, and other non-collagenous proteins. Hydroxyapatite crystals and collagen fibrils develop hand-in-hand. The crystals, noted to be "thin, elongated, but irregularly shaped platelets" (Weiner and Traub 1986). Collagen fibrils, as they are laid out, create grooves between fibrils where the crystals nest. This means the hydroxyapatite crystals are directly aligned and arranged along collagen fibrils (Weiner and Traub 1986). The collagen and non-collagenous proteins simultaneously work to generate bone structures. While the non-collagenous proteins dictate the size and orientation of the crystals, the "osteoblast is […] responsible for a synthesis of collagen" (Freemont 1993). The collagen is pulled into long fibrils that bundle together longitudinally (Gupta and Zioupos 2008) and pulled into the plywood model, creating a smooth structure that is constantly remodeled (see Chapter 1.2).

The lamellar bone forms rings around osteonal canals, creating an osteon. The entire osteonal structure, otherwise known as a Haversian system, has longitudinal and transverse fibrils oriented parallel and perpendicular to the central osteon. This provides immense stability to the whole bone (Gupta and Zioupos 2008). The Haversian canal systems' integrity determines the overall mechanical behavior of the bone with regards to strength, energy absorption, and energy dispersal (Vaughan *et al.*, 2012). Within the Haversian system, excess space is filled with an interstitial fluid. This fluid acts as an energy absorber and helps prevent bone deformation and breakage (Chen *et al.*, 2010, Wedel and Galloway 1999). During the remodeling process in mature bone, the canaliculi, or network channels that transport the interstitial fluid, help to evenly distribute the pressures applied to bone (Chen *et al.*, 2010). The microstructure of bone is adapted to respond to stress induced conditions while supporting the metabolic demands of the body. As bones age and secondary osteons arise, the integrity of bone is weakened. Daily loading and remodeling of bone causes the lamellar system to be minutely tweaked to respond to and accommodate any force applied to the skeletal system (Wedel and Galloway 1999).

The outmost portion of the bone, or the periosteum, envelopes cortical, or compact, bone. The basic multicellular unit (BMU) of cortical bone is known as an osteon (Haversian system). Osteons are cylindrical structures including osteocytes, which maintain bony materials, and osteoclasts, which destroy bone tissue structures (vans Oers *et al.*, 2008). Osteoblasts help to repair and build new osteonal structures (vans Oers *et al.*, 2008). Cortical bone is composed of lamellar layers that are arranged around the Haversian canal. Each micro-section of lamellar bone alternates direction to provide a rigid structure, creating an osteonal system (Vaughan *et al.*, 2012). Bone microstructure is layered so the only empty spaces are reserved for nutrient flow and vascularization via the Haversian canal, Volkmann's canals, lacunae, and canaliculi (Wedel and Galloway 1999). The lamellar bone is interlaced with Haversian bone, which contains blood vessels that proliferate the bone (Berryman and Haun 1996). Because of the framework laid down by the lamellae, cortical bone can tolerate heavy loads and impacts. Cortical bone is stronger longitudinally than horizontally, it can repel mechanical loads from varying directions, even when they impact the horizontal axis (Bajaj *et al.*, 2014, Wedel and Galloway 1999, Zimmerman and Ritchie 2015). Within this system, osteocytes, osteoblasts, and osteoclasts constantly work to maintain and repair cortical bone.

3.3 Histological Changes in Bones from Heat Alteration

When introduced to heat, bone histology alters drastically. Microscopically, bones deteriorate in a systematic way as the organic and non-organic materials break down. Between 100°C and 600°C, bones dehydrate via water removal, physiorbtion, and chemisorbtion. As temperature increases, decomposition of organic materials occurs and the histology of the bone begins to change. This includes color change, weight loss, strength, and porosity changes, occurring between 300°C to 800°C. When bones are exposed to heat between 500°C and 1100°C, inversion, or a general increase in crystalline structure sizes, occurs. Finally, at 700°C and up, the interior crystalline structures begin to melt and break down (Thompson 2004). Variation in temperature depends on the type of fire and length of exposure to heat. The range overlap in histological breakdown based on temperature is due to differences in tissue thickness and temperature variations *in situ* (Thompson 2004). In compact bone, the lamellar structure begins to deteriorate as heat impacts the canaliculi. The histological appearance of the internal structures start to become increasingly granular and the lacunae become obscured (Forbes 1941). The debris from other portions of the bone starts to fill the Haversian canals, Volkmann's canals, and the canaliculi. The size of the Haversian systems decreases, as cracks travel along the Haversian systems, between the lamellae, eventually joining other forming cracks (Mayne Correia 1997). This process

continues until there is no way to differentiate the structures from one another and few lacunae are visible (Forbes 1941).

The crystalline mineral of compact bone slowly alters with increased heat over time. Within 15 minutes of heating at 500°C, 700°C, and 900°C, Hiller *et al.*, (2003) show crystal shapes begin to change. By 45 minutes, the differences become more noticeable until crystals have reached their maximum size (Hillier *et al.*, 2003). This difference in crystal size can be directly noticed between "the bone heated to the higher temperatures […] and that heated to lower temperatures" (Shipman *et al.*, 1984). This pattern of increasing crystal size can help differentiate approximately how long and what temperature range the bone is heated to. The crystal growth is bound by the continual heating of the bone. Exposure to constant temperatures, without accelerated heating rates, prolong the phases of biomechanical breakdown, stopping the noted changes in crystal structure (Ellingham *et al.*, 2015). Hydroxyapatite breakdown, recrystallization, and successive melting of the crystal structures are affected by continual heating (Shipman *et al.*, 1984). This is not suggestive of a one-to-one relationship between temperature and crystal size, but a more general analysis that with increased heat, there are notable differences in crystal size, linked to temperature increase.

Another key component to thermal alteration is the effect of heat on bone collagen. Since bone is constantly remodeled throughout life, the amount of bone collagen increases due to constant synthesis (Zioupos *et al.*, 1998). But, with the increased, rapid production in collagen comes a decrease in collagen strength, making it less stable (Zioupos *et al.*, 1998). In remodeled bone, there are layers created by the regions where original collagen fibrils and hydroxyapatite crystals were formed and where new collagen synthesis is occurring. In many regions, an overlap of the two occurs (Kronick and Cooke 1996). When heat is applied to bone, the collagen becomes stressed, breaking down by destruction of the helical structure into a randomly organized, shrunken coil (Zioupos *et al.*, 1998). In the previously stated overlap areas, demineralization occurs last because these areas are "less accessible to external solutions used to mineralize and demineralize" (Kronick and Cooke 1996). Upon reaching its melting point at 150°C, bone collagen continues to combust, "spiking at around 500°C" (Ellingham *et al.*, 2015). Collagen itself is constrained in bone, and when it undergoes thermal alteration under 500°C, the bone maintains a copy of the collagen fibrils and how they associate with the minerals present in bone (Kronick and Cooke 1996). These copies are kept until bone is completely broken down in later stages of thermal alteration.

3.4 Formalin and Bone Structure

The chemical compound for formaldehyde is CH2O, of which formalin is derived (French and Edsall 1945). When formaldehyde is diluted to 37% and mixed with different levels of methanol and water, formalin is created (French and Edsall 1945). This product is known to react to ε-amino groups of lysine, a stabilizing component of collagen, via a methylene bridge. The formalin itself links to the end nitrogen atom on the lysine chain. Cross-linking across other amino groups then occurs, creating an iminium ion intermediate. This reacts with the phenol groups, creating covalent bonds within bone tissues, altering the reactivity of bone tissues. Overall, the formalin does not interfere with the peptide links of collagen, nor does it impact the rigidity of the collagen itself (Gustavson 1947, Mason and O'Leary 1991, Thavarajah *et al.*, 2012).

Formalin directly alters the basic components of collagen, which could make the study of formalin fixed cadavers in forensic reconstructions problematic. How formalin directly alters the stability and nature of the basic molecular components of bone is not widely understood. Bone hydroxyapatite is a crystalline structure composed mainly of calcium and phosphorus (Vaughan *et al.*, 2012). Formalin tends to bind to these chemical elements (dissolves them), causing mineral changes, because of its naturally reactive nature with collagens ε-amino groups. However, with an increased amount of formalin, hydroxyapatite's Ca/P ratios decrease in bone and bone's naturally occurring amino groups due to mineral dissolution (Małgorzata and Jarosław 2006). If the formalin was buffered to a more neutral pH, a balance of excess phosphate absorption would "[suppress] mineral dissolution by shifting the equilibrium between hydroxyapatite mineral and calcium and phosphate ions to the left, leaving the composition unchanged" (Boskey *et al.*, 1982). With respect to collagen, formalin enlarges collagen fibrils, making them more condensed, while not altering the bone's lipid content (Boskey *et al.*, 1982). Formalin highly saturates the osseous tissue layers, causing the lamellar layers to become "thin and irregular" (Małgorzata and Jarosław 2006). This disrupts the normal bone patterning, making it appear dehydrated. Formalin's alteration of compact bone is further exhibited via hollowed Haversian and Volkmann canals and an enlargement of the canaliculi (Małgorzata and Jarosław 2006). Biomechanically, these structures can be seen in histological thin sections of bone both before and after heat alteration.

As there is limited knowledge about the impact of formalin on burned bone, research needs to be done to determine how formalin alters bone structure and the burning process of bone tissue. Compared to burned, non-formalin fixed compact bone, it is hypothesized that histological thin sections

of formalin fixed femoral compact bone will not show high rates of microstructural changes when burned. Formalin fixed samples will be burned to draw a direct comparison between formalin and non-formalin fixed cortical bone. In doing so, heat alteration of the microstructure with and without additional chemical elements will be studied. The goal of this research is to determine the suitability of using formalin fixed human remains in place of fresh animal remains in forensic research. Additionally, this research works towards understanding how formalin impacts the microstructure of human bone and the affects extreme heat has on formalin fixed bone.

3.5 Materials and Methods

The University of Alberta's Division of Anatomy Anatomical Gifts Program (AGP) provided two human femoral plug samples for this research. The bone plugs came from one individual – an 86-year-old male, whose remains had been embalmed, in a typical manner, with formalin. No other information on this individual is known. Once the samples were harvested, they were transported to the University of Alberta's Department of Anthropology Biosafety Laboratory. Here, one sample was cut in half with an autopsy saw.

These halves were labeled 'A' and 'B.' The other sample was kept whole and used as an unburned control sample, labeled 'C.' Once A and B were cut, they were placed into individual ceramic dishes and burned separately for 15 minutes in a Fisher Isotemp Muffle Furnace Model 184; A at 600ºC and B at 800ºC. The temperature gauge was watched to record the time and temperature of the flash over point. The specimens were removed from the oven and left to cool overnight before being embedded in resin and thin sectioned.

Following the burning, samples A and B were embedded in Buehlers Epo-Thin Resin to stabilize them for thin sectioning. The resin pucks were left to cure and harden overnight. The control sample was not encased in resin, as it did not require stabilization. Thin sections of samples A, B, and C were made using a Leica SP 1600. These sections were visually analyzed with an Olympus BX63 microscope with a DP73 camera. *Cellsens* software was used to capture images of these specimens for comparison.

The non-formalin fixed samples had been prepared for Pointer's (2014) thesis that addressed histological changes between burned and unburned bone, to quantitatively and qualitatively understand the similarities and differences in cremated and non-cremated human cortical bone. Pointer used five human femoral shafts obtained from the Comprehensive Tissue Center (CTC), a part of Alberta

Health Sciences (AHS) that were not treated with formalin. Her samples were burned at 600ºC, 800ºC, and 1000ºC for 15 minutes in a Fisher Isotemp Muffle Furnace. After being cremated, they were embedded in epoxy resin and thin sectioned like the samples for this study (Pointer 2014). Pointer measured the diameter of the Haversian systems, canals, and number of osteons using a statistical *t*-test.

Out of Pointer's samples, three were male, ages 50, 60, and 62 (Pointer 2014). These were the samples chosen for comparison to the femoral samples of the current study because they were all male. In Pointer's study individual B did not produce viable slides for temperatures burned at 600ºC and 800ºC; therefore, only Pointer's original slides for individuals A and D were assessed for this study. Pointer (2014) noted that the osteons and Haversian canals shrunk in response to increased heat; this ratio varied based on the temperature. Pointer was able to analyze the histological elements of bone – the Haversian system (osteon), Haversian canal, lacunae, lamellae, and canaliculi – at the control level, 600ºC and 800ºC. Metric analysis of osteonal diameters and Haversian canal diameters were taken from sample A and B of this study, as well as samples A and D from Pointer's study. The results varied as temperature increased, as carbon residue clouded some of the sections. Using the *Cellsens* software, images of Pointer's slides and of the new samples were taken and compared both visually and through metric analysis.

3.6 Results

Figures 3.1 and 3.2 show similarities in the control samples' histology from Pointer's samples and this study. The micro-cracking between lamellar layers – originally thought to be an anomaly caused by formalin – was found to be identical to the control histology slides produced by Pointer and its origin may be an artifact of the thin section production. Figures 3.3 and 3.4 give a direct comparison on how formalin fixed and non-fixed cortical bones burn at 600ºC. There are similarities in the carbon production with minimal alteration from heat. The histological features can be identified easily and there is little variation between the two samples. The

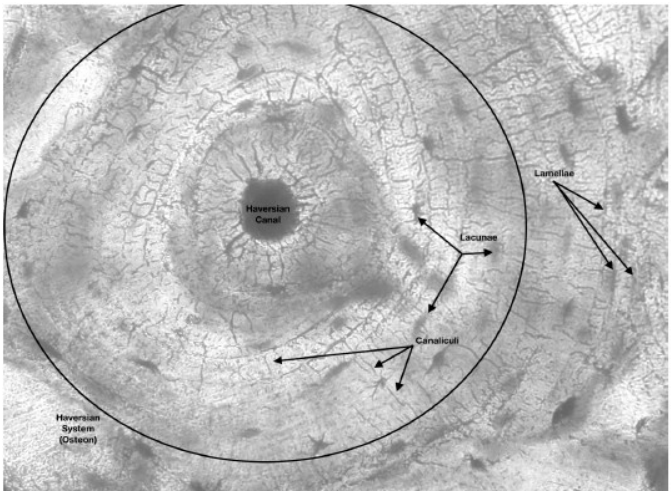

FIG. 3.1 – A close up of formalin fixed, unburned cortical bone at 400x (this study).

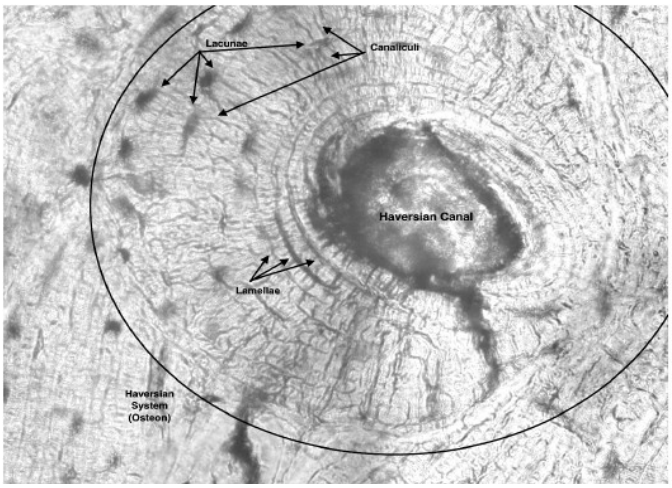

FIG. 3.2 – A close up of non-formalin fixed, unburned cortical bone at 400x, from sample D (Pointer 2014).

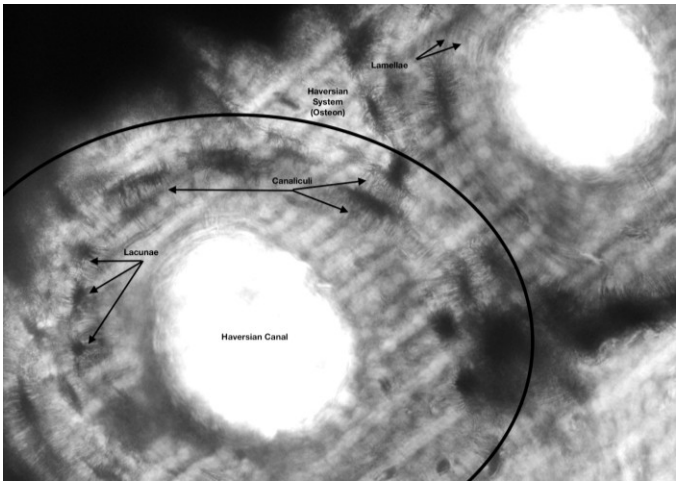

FIG. 3.3 – A close-up of formalin fixed bone, burned at 600°C from sample A (this study), 400x.

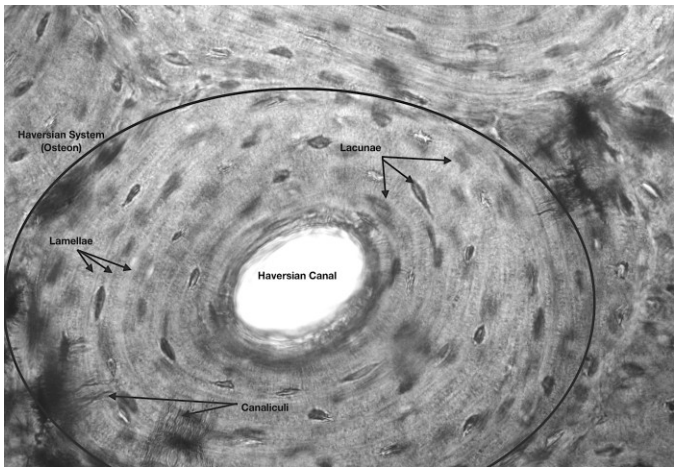

FIG. 3.4 – A close-up of non-formalin fixed bone, burned at 600°C from sample D (Pointer 2014), 400x.

flash point reached from sample A in this study took 5 minutes and 53 seconds, hitting a maximum temperature of 675ºC. Pointer (2014) noted the high temperature for her specimen A to be 680ºC, and 660ºC for specimen D. The time this took to occur was not noted in her study.

Samples by Pointer show less micro-cracking at 800ºC (FIG. 3.6). In this study's sample B, there are noted spider-web patterns (FIG. 3.5). These appear to go through the lamellar layers of bone and connect via lacunae. There is no definitive pattern, just a lattice-work structure near the Haversian systems. At this temperature, the flash point occurred at 2 minutes and 39 seconds, reaching a temperature of 860ºC. Pointer (2014) noted a flash point of 840ºC for specimen A, and 845ºC for specimen D. The time this took to occur was not noted in her study. Figure 3.7 is as a direct comparison to Figure 3.5. Even at 1000ºC, Pointer's sample D does not appear to be damaged as extensively as the formalin fixed sample B that was burned at 800ºC.

3.7 Discussion

This study focuses on incomplete cremation, where the bone is brittle, discolored, and fractured (Mayne Correia 1997, Symes *et al.*, 2012, Ubelaker 2009). According

to Thompson (2004), the samples from this study have undergone physiorbtion, chemisorbtion, and decomposition. This makes sense given the remains from this study were burned at 600°C and 800°C. Pointer (2014) burned samples at 1000°C, which may have undergone inversion (Thompson 2004).

For the control samples and samples burned at 600ºC, formalin was a negligible factor for analysis; however, as temperatures rose, the formalin appeared to cause the bone to breakdown faster, creating a spider-web pattern on the lamellar layers. As stated earlier, Małgorzata & Jarosław (2006) observed formalin to hollow Haversian and Volkmanns canals and enlarge canaliculi in unburned samples. Upon viewing histological thin sections of burned, formalin fixed bone, our samples did not show the same patterning. The thin sections taken from this study closely match those done by Pointer (2014).

As well, metric analysis supports this conclusion. Osteons and Haversian canals were chosen based on their nature, i.e. uninterrupted circles or ovals that were not overlapped by other osteons. Entire slides were scanned for these osteon types, in order to look at a subset of data. Table 3.1 shows the numbers of osteons and Haversian canals analyzed by study and temperature. As illustrated in Table 3.2, the Haversian canal diameters between these two studies are comparable, with the formalin samples having a slightly lower mean than the non-formalin fixed samples. The average for this study's control samples was 57.28 μm, versus a 60.04 μm seen in the Pointer

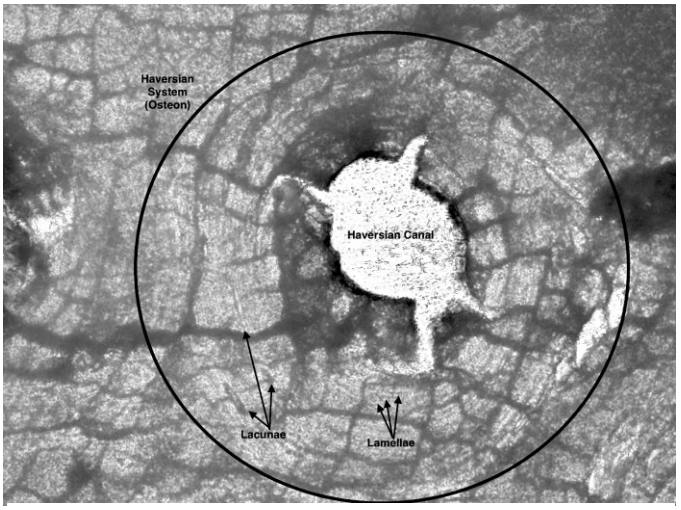

FIG. 3.5 – A close-up of formalin fixed bone, burned at 800°C from sample B (this study), 400x.

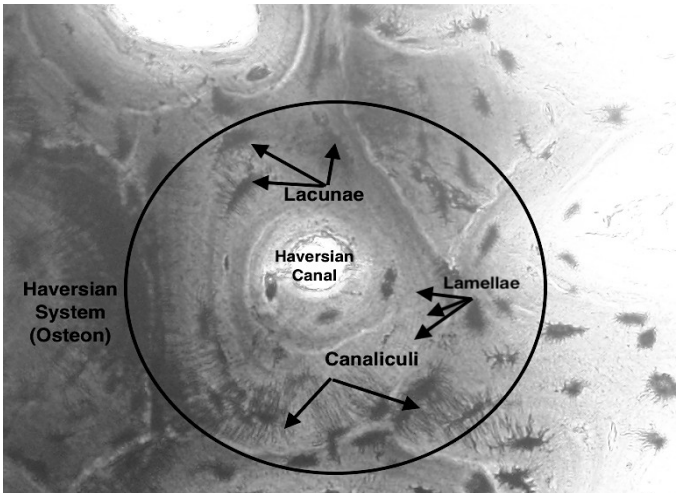

FIG. 3.6 – A close-up of non-formalin fixed bone, burned at 800°C from sample A (Pointer 2014), 200x.

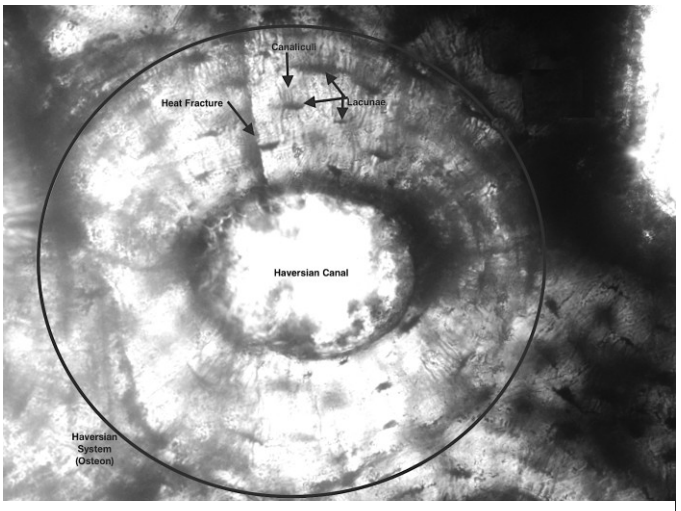

FIG. 3.7 – A close-up of formalin fixed bone, burned at 1000°C from sample D (Pointer 2014), 400x.

	Control (This Study)	600ºC (This Study)	800ºC (This Study)	Total (This Study)	Control (Pointer)	600ºC (Pointer)	800ºC (Pointer)	1000ºC (Pointer)	Total (Pointer)
Osteons	29	19	28	76	26	22	19	10	77
Haversian Canals	35	21	30	86	26	22	19	10	77

Table 3.1 – Number of osteons and Haversian canals studied, as well as a recording of what temperature the samples came from.

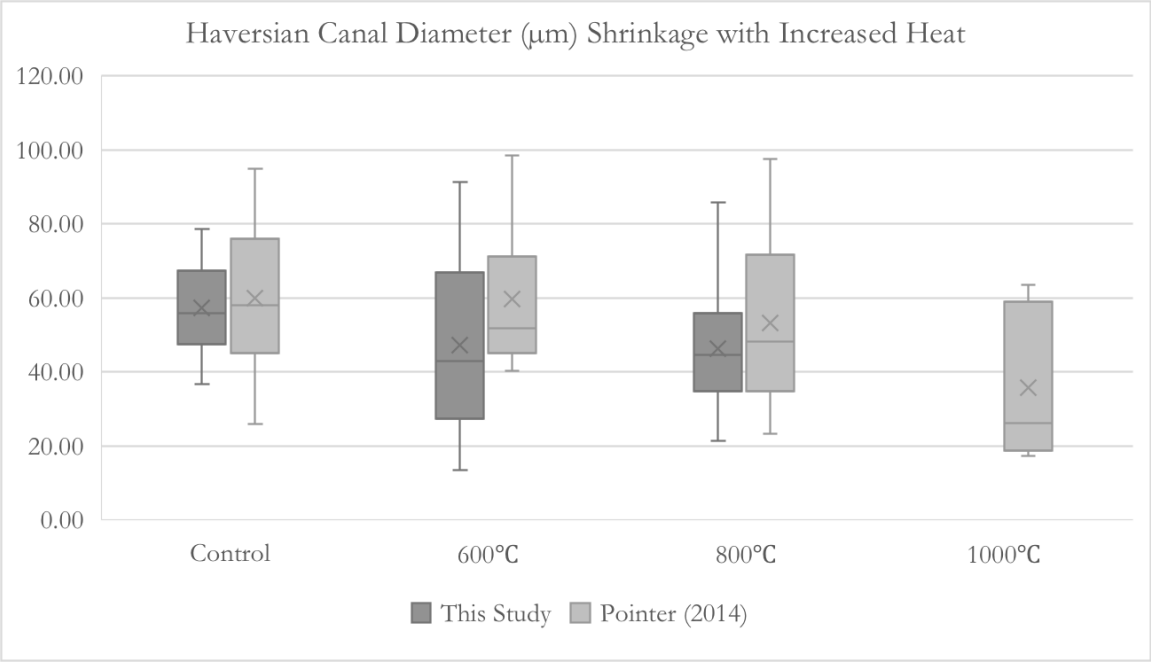

Table 3.2 – Metric analysis of Haversian canal diameter (μm) across formalin fixed and non-formalin fixed samples in comparison to increased temperatures. The darker portion represents data from this study, the lighter portion represents Pointer's samples.

(2014) samples. The 600ºC samples showed the greatest differences between this study and Pointer (2014). This study has an average of 47.30 μm, 12.54 μm less than Pointer (2014), which were 59.84 μm. At 800ºC, this study saw diameters averaging 46.26 μm, slightly lower than Pointer (2014), which averaged 53.28 μm. The results for Pointer (2014) 1000ºC samples averaged 35.88 μm, which is substantially lower than the other temperatures averages. The similarity across the control, 600ºC, and 800ºC shows the limited impact of formalin on the samples, especially when compared to the lowest average of the 1000ºC samples.

To further show the limited impact on the bone histology, osteonal area was measured across the samples. Table 3.3 shows the formalin fixed samples' osteon area are analogous to Pointer's non-

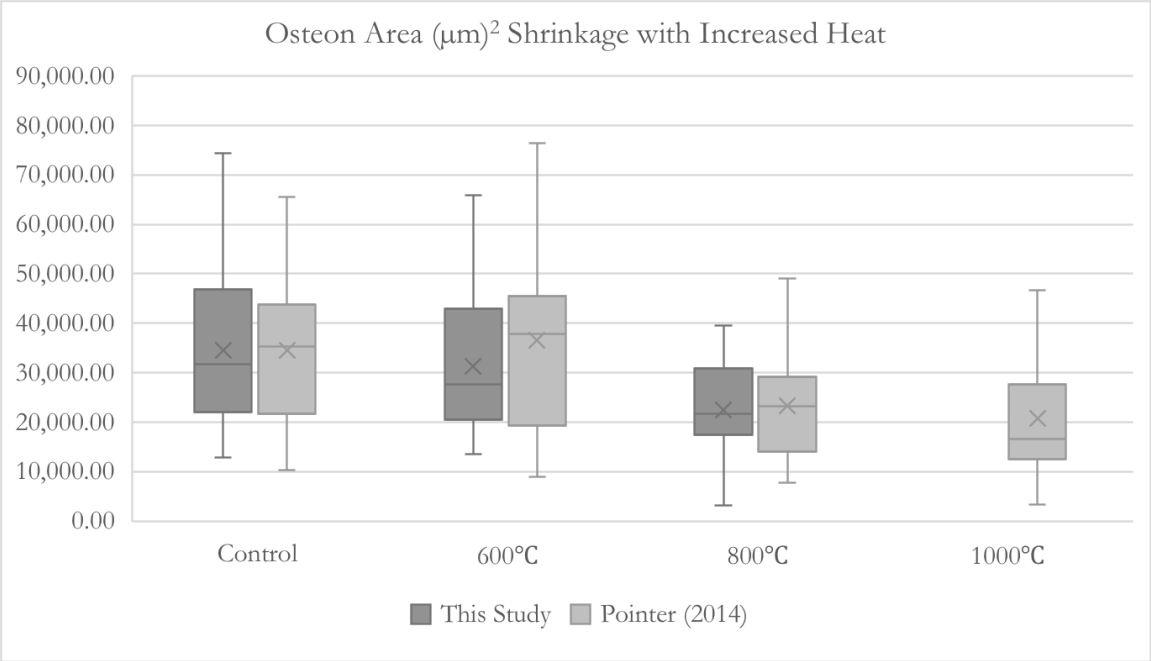

Table 3.3 – Metric analysis of osteon area (μm)² across formalin fixed and non-formalin fixed samples in comparison to increased temperatures. The darker portion represents data from this study, the lighter portion represents Pointer's samples.

formalin fixed samples. This study's control samples averaged 34,491.91 μm^2, almost identical to Pointer (2014) averaging 34,481.95 μm^2. At 600ºC, this study showed an average of 31,263.07 μm^2. This was slightly lower than Pointer (2014), whose area at 600ºC was 36,592.92 μm^2. This was again the biggest difference noted between the samples. At 800ºC the samples had closer averages, much like the Haversian canal diameters. This study sat at 22,373.03 μm^2, and Pointer (2014) was 23,230.13 μm^2. Unlike the Haversian canal diameters, the osteonal area of the 1000ºC samples from Pointer (2014) averaged 20,809.12 μm^2, which was similar to the 800ºC averages. These findings are more closely aligned with those of Mason and O'Leary (1991) showing formalin to minimally alter burned bone structure.

Microscopically, the metric analysis of the Haversian canal diameters and osteonal areas show the minimal alteration of formalin in human bone. Based on numerical analysis, it is shown that the formalin does not drastically constrict or expand the Haversian systems of cortical bone. This aligns nicely with the previously discussed research provided by Gustavson (1947) and Thavarajah *et al.* (2012) who claim formalin does not impact the overall collagen structure of bone, but embeds itself in the peptide links of the collagen. The large ranges that are seen in both Figures 2.2 and 2.3 are from various sizes of osteons and Haversian canals, which is based on remodelling and osteonal overlap as

secondary osteons arise.

This study is designed to discern if formalin impacts the histological structure of partially cremated human cortical bone. Basic units of the original bone structure are still evident in the control sample and the two burned specimens. This organizational pattern mimics that of non-formalin fixed human bone found in research done by Pointer (2014). In both cases, when the bone samples were heated, the lamellar layers became clouded by carbon, and heat-induced fractures occurred splintering the bone samples. There are no visual structural differences between the non-formalin fixed bone samples and those treated with formalin. Based on these observations, formalin fixed bone can be used in forensic experiments involving cremation at temperatures, up to 600ºC. This study suggests caution when the experimental design uses formalin fixed bone in combination with temperatures above 800ºC.

At 800ºC, the formalin fixed bone altered drastically and showed an increase in the amount of heat fractures present. One plausible explanation for these increased changes between the samples presented by Pointer (2014) and this study is the introduction of formalin. There are limited differences within the bone samples besides this study's introduction of formalin. The other possibility for increased breakdown in the specimen from this study would be the age. Individual B from this sample study was 86 years old. The comparison individuals from Pointer (2014) were aged between 50 and 62 years old. There is no known information on pathology of either specimen, but increased age could be associated with a brittle osteoporotic nature, making sample B more prone to heat damage.

Microscopically, formalin is directly altering the collagen fibrils and the new bonds that are being formed are impacted directly with heat. The grooves where hydroxyapatite crystals originally nested have been condensed by the swollen collagen fibrils. As formalin dehydrates the bone and heat is added, the bone becomes dehydrated by two sources: formalin and heat. Up until about 600°C, thermal degradation of water (i.e. water vaporization) occurs in the bone. For the 600°C samples, there is limited change noticed between this study and Pointer (2014) because dehydration is occurring simultaneously by heat and formalin. However, this study's sample that was heated at 800°C shows increased damage resembling the 1000°C cremation by Pointer (2014) theoretically because the hydroxyl bonds were prematurely broken due to the increased heat in combination with the formalin. Much like Ellingham (2015) states, the greater the increase of heat, the quicker the phases of thermal degradation occur. At 800°C, the disruption formalin caused to the bony microstructure initiated a

quicker breakdown of the basic molecular components of bone. The entire thermal alteration process was sped up because there was less water removal and therefore a quicker carbonization of the bone. Formalin, while rapidly bonding with the crystals, is breaking the hydroxyapatite crystal-collagen fibril bonds. This causes the basic molecular structure of bone to become more fragile, dehydrated, and disorganized.

One limitation of this study is the inability to compare the length of time to the flashover point in both studies. However, the maximum temperature reached in both studies can be equated. In both this study and the one done by Pointer (2014), the 600ºC burns rose to relatively the same temperatures. The 800ºC burns noted a 15ºC difference between Pointer (2014) and this study; this is attributed to the formalin. The known flashpoint for formalin is 85ºC (Anon. Formaldehyde n.d.), meaning the formalin itself is not directly altering the flash point. The exact reason why the 800ºC sample reaches a higher flash point is unknown. It could be theorized that the dehydration properties of the formalin in combination with thermal dehydration caused the later stages of thermal alteration to occur sooner. However, there needs to be more research done specifically focused at 800ºC samples to better determine the impact noted here.

There are other factors such as the weight of the individual, the size and density of the sample, and length of exposure to formalin, that could be a cause for the flash point increase. But, these implications cannot be looked into because there is no comparable data from Pointer (2014). Overall, the increased flash point is a potential problem and foreseeable implication of burning formalin fixed bones at temperatures above 800ºC.

3.8 Conclusion

The histological analysis of burned and unburned bone has been the subject of significant research (Forbes 1941, Pointer 2014, Shipman *et al.*, 1984, van Oers *et al.*, 2008). This study has provided information on the usefulness of formalin fixed cadavers in forensic experimentation. By comparing formalin fixed and non-formalin fixed partially cremated human cortical bone, it has been demonstrated that formalin produces a minimal effect on bone histology. Though this work was done on compact bone from long bones, it can be applied to cranial and irregular bones because it is looking at the impact of formalin on the bones themselves, not the microstructural differences between long bones, cranial, and irregular bones. There is no expected differences between long bone formalin alterations and those that would occur in cranial or irregular bones since the formalin is altering the collagen itself, which is the same in long bones, cranial bones, and irregular bones. This means the burning process of formalin

fixed cranial and irregular bones would burn like their non-formalin fixed counterparts. This is based off of the comparison of formalin fixed long bones and non-formalin fixed long bones. This is important to note for future research.

The goal of this research was to determine if formalin treated human bone could be used for forensic anthropological investigations on bone affected by heat. The ability to use formalin fixed human cadavers, that have been donated to science, opens new avenues of research within forensic anthropology. This paper has explored the effects of formalin on human bone and the use of formalin fixed remains involved in cases of partial cremation. Based on the results of this study, it is concluded that formalin treated bone can be used in forensic investigations that reach 600ºC, but with caution thereafter.

With regards to the control samples from this study, using formalin fixed remains for non-burned research is a new avenue of study. Knowing that the structural integrity of bone is not overtly changed with the addition of formalin, medical cadavers could prove useful in forensic experiments where animal substitutes or fresh cadavers are not viable options. The metric analysis of the control samples in this study versus Pointer (2014) once again highlight the minimal alterations formalin has on bone histology. The Haversian canal diameters of this study had an average of 2.76 μm less than Pointer (2014). As for the osteonal area, the difference was 9.96 μm^2, with this study having the larger area. It can be hypothesized that since the bone histology was not overtly altered by formalin, the reactivity of formalin fixed remains in other circumstances, i.e. trauma, will not show major differences to their non-formalin embedded counterparts. This research expands the breadth of knowledge on formalin fixed remains and allows for research growth within the field of forensic sciences.

This study provides evidence that prior to heat introduction, and at temperatures spanning between 600ºC and 800ºC, formalin fixed bone is noted to have similar histological traits as non-formalin fixed bone. Based on these direct visual comparisons of the histological slides, it is evident that the formalin has no lasting effect on the microstructure of the bone during cremation. In each instance, the samples tested by Pointer (2014) show the same histological elements as the formalin samples tested in this study. Formalin fixed bone does show a higher rate of microstructural changes then non-formalin fixed bone when burned. Due to the limited microstructural changes found between burned formalin fixed bone and burned non-formalin fixed bone, it can be concluded that formalin fixed human cadavers can be used in place of fresh animal remains in forensic research.

Chapter 4: Differentiation of Perimortem Trauma from Heat Fractures in Partial Cremations of Cranial and Pelvic Bones[3]

4.1 Introduction

Using human remains in forensic recreations is a highly debated subject. Commonly, animal substitutes are used due to their histological similarity. Chapter 3 discussed testing the suitability of using formalin embedded human remains in place of animal surrogates, or fresh cadavers, as a way to advance research methods in the field of forensic anthropology. It was found that the formalin minimally altered the histology of fresh bone and cremated bone. Previous studies discuss the biomechanical break down of crania throughout cremation, but no indication of how trauma is altered (Baby 1954, Bohnert *et al.*, 1997, Dokládal 1971, Fairgrieve and Molto 1994, Holland 1989). This study opens new avenues of research, allowing for the use of human remains, including medically embalmed ones, in forensic experimentation.

This chapter focuses on the implications of heat on irregular bones that have been subjected to trauma. As discussed in Chapter 1.6, there are limited studies on how trauma impacts cranial and irregular bones, let alone what occurs with the introduction of intense heat. This chapter will therefore discuss the differences in bone type, as well as why bone breakdown in intense heat will differ between long bone, cranial bone, and irregular bone. This experimental study tests the reactivity of crania and hemipelves when exposed to blunt and sharp force trauma, in addition to cremation. It is anticipated that differences between the traumatic fractures and heat fractures will be discernable on a microscopic level.

4.1.1 Blunt Force Trauma

Blunt force trauma (BFT) leaves a depression of sorts at the impact site, and includes "mechanizing forces such as direct impact, crushing, acceleration-deceleration, or sharp-blunt impact" (Kimmerle and Baraybar 2008). BFT can leave various marks on bone, "dependent on the amount of energy transferred from the impacting object and the size of the impacted area" (Wedel and Galloway 1999). BFT analysis is divided into distinct categories (1) biomechanical responses to loading, (2) the nature of loading forces, (3) classification of fracture morphology, (4) fractures associated with direct

[3] A version of this chapter is ready for submission for publication to the Journal of Forensic Sciences.

and indirect trauma fractures, and (5) appearance of fractures on individual elements and how to interact with direct and indirect trauma (Wedel and Galloway 1999). The minimum number of injuries, determined by cataloguing the wound(s), can show patterns reflective of the object used to create them (Kimmerle and Baraybar 2008). BFT in cranial bones typically results from a direct impact site with additional emanating fractures (see Chapter 2.3.1.1, Berryman and Haun 1996, Hart 2005, Klepinger 2006, Kimmerle and Baraybar 2008). Blunt force trauma, consistent with internal beveling and concentric fractures, may or may not be seen after cremation occurs (Symes *et al.*, 2008). BFT can radiate throughout the entire cranium with micro-fractures depending on the forces applied, size of object used, and age of the person traumatized.

The pelvis, also comprised of flat bones, acts similar to cranial bones under BFT. Most commonly seen are depressed fractures due to the thin cortical bone and its biomechanical properties. The soft tissues around the pelvis provide a cushion to the trauma, but secondary fractures can form from ligaments pulling and tearing away from the bone (Kimmerle and Baraybar 2008). This is important to note because of the limited documentation on BFT of irregular bones.

4.1.2 Sharp Force Trauma

Sharp force trauma (SFT) is defined by the class of weapon used, caused by a "pointed or edged" (Kimmerle and Baraybar 2008) object. Weapon type, not morphology, is used to classify weapons (Crowder *et al.*, 2013). SFT is frequently noted in clusters, which is helpful in identifying the minimum number of lesions and reconstructing weapon type used (Kimmerle and Baraybar 2008). Further classifications are determined by size, weight, girth, and thickness of the weapon (Crowder *et al.*, 2013, Kimmerle and Baraybar 2008). Depending on the weapon, SFT can "incise, cut, chop, dent, or crush" (Kimmerle and Baraybar 2008) bone. SFT to perimortem and postmortem remains differ. Compression of bone causes a curled or raised edge as the tool causing trauma enters the bone and is removed (Klepinger 2006), something not seen in postmortem trauma. Postmortem trauma markers are usually made from excavation tools, taphonomic processes, or carnivore puncture wounds (Kimmerle and Baraybar 2008). They do not leave a curled or raised edge unless occurring shortly after death. SFT can leave similar markers in long bones and irregular bones, except in irregular bones, the SFT object has a greater chance of penetrating through the cortical and trabecular portions of bone entirely.

4.1.3 Heat Alteration of Cranial and Irregular Bone

Heat causes bone to break down in a predictable pattern based on temperature, exposure length and time, and whether the remains are fleshed or skeletonized. Thermal alteration to bone and tissue causes "shrinkage, fragmentation, and shape alterations" (Ubelaker 2009), which can affect skeletal analysis. There are three phases of heat alteration seen: (1) non-incinerated bone, showing minor fragmentation, (2) incomplete incineration, where some organic compounds are present, but fragments are black in color and cracked, and (3) complete incineration, where bone is calcined and appears grey with transverse fractures and warping (Baby 1954).

Heat produces both macroscopic and microscopic changes. Wet bone is prone to warping based on tissue structure combustion (Symes *et al.*, 2008). Fresh bone shows curved tissue-regression (thumbnail) fractures which occur as soft tissues are pulled off the bone. Concentric semi-circular arcs are formed as tissue regresses from bone (Gonçalves *et al.*, 2014, Pope and Smith 2004, Symes *et al.*, 2008). Dry bones, on the other hand, show "superficial cracking, fine longitudinal striae, deep longitudinal fracturing, or splintering, and no warping" (Baby 1954). The bones become deformed and crack, becoming more brittle as heat rises (Grévin *et al.*, 1998). As temperatures increase, alterations are classified as being "mostly bent and cracked, and often it has a bluish coloration" (Dzierzykray-Rogalski 1967). The differences between wet and dry bones are crucial to understanding the circumstances around the initiation of burning.

Macroscopically, as the inorganic materials break down, fractures expand and digress into non-traumatized areas. The bone flakes in a non-specific pattern. In areas of extensive trauma, heat alteration is more intensive than in areas of less trauma. When flesh is involved, the heat causes fractures to occur slower due to the protective layer of tissues. Where there is less tissue, there are more fractures forming quicker because the tissues disintegrate more readily (see Chapter 2.3.1.4, Pope and Smith 2004). Delamination fractures occur as heat alteration impacts crania, and as the bones cool. Deep linear fractures, patina breakage, and curved tissue regression can be seen post-cremation, resulting in bone shrinkage and sharp, bony margins. From high heat exposure over time, trauma fractures, on the other hand become more worn, warped and rounded (Pope and Smith 2004). Irregular bones, on the other hand, are biomechanically, structurally, and functionally different. The pelvis, for example, is brittle because the cortical bone is much thinner in relation to the trabecular center. Thick muscles, tissues, and organs surrounding the pelvic girdle slow down heat exposure and

bone breakdown. In partially cremated remains, the pelvis is often found with mild damage (Bohnert *et al.*, 1997); however, studies where the musculature is limited have not been done until now.

4.1.4 Biomechanical Differences of Long and Irregular Bones

Long bones, derived from both intramembranous (perichondral) and endochondral ossification, begin mineralization in vesicles oFMarn the periosteal surface, perichondral layer, and endosteal surface (Kawasaki and Richtsmeier 2017). Intramembranous ossification develops the distinct lamellar pattern that is laid down systematically within long bones (Cunningham *et al.*, 2016). Endochondral ossification forms the cancellous, or trabecular bone, in a haphazard structure from pre-existing cartilaginous models. These are infiltrated by osteoblasts, which build around the cartilaginous precursors forming the periosteal layer (Cunningham *et al.*, 2016, Kawasaki and Richtsmeier 2017). Woven bone is remodeled into cancellous bone via osteogenic cells (Cunningham *et al.*, 2016). Lacunae and canaliculi are formed and spawn the growth of trabecular bone (Vaughan *et al.*, 2012). As the spicules form, secondary growth centers form on the ends of each spicule, creating an intricate network of spongy bone (Cunningham *et al.*, 2016). This is continually remodeled throughout life (Currey 2003).

Cranial bones also derive from mixed ossification. The large, flat bones of the vault are formed via intramembranous ossification, whereas the base of the cranium is endochondral in origin (Cunningham *et al.*, 2016, Kawasaki and Richtsmeier 2017, Tubbs and Bosmia 2012). As the inner and outer tables are formed, diplöe forms between the two via intramembranous (dermal) ossification or neural crest cells, acting like the cancellous portion of long bones (see Chapter 2.2.1, Cunningham *et al.*, 2016, Kawasaki and Richtsmeier 2017). The timing of bone formation, plus structural differences, help create a supportive system for the developing brain and spinal column. Embryologically, the cranium is built to resist fractures, especially as diplöe matures, acting as a cushion against trauma (Motherway *et al.*, 2009).

Long bone and cranial bone cortical thickness alters the way fractures are diverted. The formation and function of the trabecular bone versus the diplöe is crucial to understand, as the diplöe is the first area of failure in cranial vault bones (Motherway *et al.*, 2009). To better study fracture proliferation, the cancellous portion of irregular bones needs to be scrutinized, as it is less dense, unorganized, and makes up majority of the bone. The cortical layer of irregular bones is extremely thin. It is necessary to examine cranial bones and irregular bones aside from long bones for these

reasons. Based off of embryological differences of the various bone structures, long bones, cranial bones, and irregular bones will react differently to stressors (see Chapter 2 for more details).

Due to the embryological and structural differences of cranial and irregular bones, my research focuses on how heat impacts cranial and irregular bones when impacted with fractures. The lack of research with regards to identification and differentiation of perimortem trauma from heat fractures on cranial and irregular bones makes this research critical to further enlighten the anthropological and forensic communities about these topics. It is already known that trauma fractures will have eroded, blunted edges where the point of impact occurred when introduced to heat (Pope and Smith 2004). Heat fractures, on the other hand, show distinct sharp, clean edges due to burned bone being a brittle structure (Marella *et al.*, 2012). As of yet, the little research in this area focuses on macroscopic qualitative analysis. This work aims to distinguish qualitative analysis on a microscopic level to discern perimortem trauma fractures from heat fractures in cases of cremation on cranial and irregular bones.

4.2 Materials and Methods

Five embalmed human calottes and five embalmed human hemipelves were selected for experimental trauma and cremation. Tri-council approval through the University of Alberta Research Ethics Board, under the project Name "Differentiation of Perimortem Trauma Fractures from Heat Fractures in Irregular Bones", No. Pro00070625 was given on 15 May 2017. All remains have been anonymized and no information beyond age, sex, and bone health were collected. The calottes and hemipelves were taken from the same individuals. The ages and sex of the cadavers are: a 77 year old male, two 84 year old males, an 86 year old female, and an 87 year old male. These individuals were selected as they were the youngest individuals in the group of cadavers that were available for use. This lowers the already high rates of osteoporosis, general bone porosity, or thinning of the cortical bone from age degradation. Age, being a non-negotiable factor, meant having an inspection of the exposed bones from medical student dissections to ensure limited alteration to bone health prior to harvesting. Men were preferred choices for this research since women, especially post-menopause, "age faster than males in terms of […] trabecular bone status" (Keaveny and Yeh 2002). Women's bones are more likely to show pathological conditions such as osteoporosis, weakening the integrity of the bone structure (Keaveny and Yeh 2002). To limit the impact of osteoporosis in this study, males were predominately selected – the one female outlier was chosen because all other males were in their mid to late nineties, which was not ideal for this study. This research was designed to work around

structural context and biomechanical functions of bones that may be compromised with osteoporotic conditions. This was taken into account when looking at fracture patterning from trauma and heat, especially as the os coxa has a high predominance of osteoporosis in older individuals (Keaveny and Yeh 2002).

Chapter 3 once again highlights evidence showing that embalmed human remains can be used in place of fresh remains in forensic recreations. Calottes and hemipelves were chosen because of their unique histological structure and due to the lack of data on how these bones are impacted by trauma and cremation (Marella *et al.*, 2012, Pope and Smith 2004). See Chapter 1.6 for more information. Remains were provided by the University of Alberta's Anatomical Gifts Program. All musculature and tissues were already removed from the calottes, as they were previously used for anatomy dissections. Approximately 1 cm of musculature was left on the hemipelves after scalpels and medical scissors removed excess flesh, musculature, and ligaments. This was done to limit cutting or scraping the bone with dissection equipment.. Once mostly defleshed, a band saw was used to cut the hemipelves from the rest of the pelvic girdle. The musculature left on the hemipelves was useful in stabilizing the bone during the traumatization. Besides autopsy tool marks and saw marks on the hemipelves, no other trauma markers were noted on the calottes and hemipelves. A lack of tension fractures amidst the trauma and heat fractures will be expected, since the full musculature will not be present to snap and pull on the skeletal system during cremation.

Prior to burning, one of each bone type was left undamaged and marked as a control specimen. Two calottes and two hemipelves were bludgeoned with a standard tire iron. The other two calottes and two hemipelves were stabbed and slashed with a 10 inch chef's knife. The blows were randomly inflicted with approximately the same strength and force to produce similar markings on each bone. This was done for comparative purposes so trauma fractures could be distinguished from heat fractures post-cremation. Photos were taken, as well as x-rays[4], to ensure all trauma markers and extending fractures were recorded. These were compared to post-cremation photos, which can be seen in Figures 4.1, 4.2, 4.3, and 4.4.

To allow for full recovery of bone fragments and temperature control, a local crematorium was used to burn the remains. The cremation oven was set to mimic the temperature witnessed in common house fires. Temperatures were kept between 350°C and 550°C; house fires are noted to hit

[4] Courtesy of the Office of the Chief Medical Examiner, Edmonton, AB

a high temperature of approximately 650°C (Devlin and Herrmann 2013). Since the remains were only partially cremated, the temperatures noted allow for the initial stages of a common house fire to be simulated. Calottes were burned separately from hemipelves; the oven simulated a partial cremation. Calottes burned for 6 minutes and 32 seconds, whereas the hemipelves burned for 6 minutes and 23 seconds. The times varied because formalin, noted in embalming fluids, is highly flammable. The musculature noted on the hemipelves increased the amount of formalin in those samples, slightly altering the burn time. The cremation oven door was opened three times for the calottes and four times for hemipelves for less than fifteen seconds to check the temperature of the remains throughout the experiment. This was done to ensure even burning amongst the specimens. The remains were left to cool overnight. All fragments

FIG. 4.1 shows the blunt force trauma keyhole depression of both calottes prior to cremation and post-cremation side by side for inspection of visual changes (T13 top; T26 bottom).

FIG. 4.2 shows an example of some of the sharp force trauma markers seen on the calottes prior to cremation and post-cremation side by side for inspection of visual changes (T20 top; T21 bottom).

from the cremation process were collected and kept with their respective individual once cooled from the cremation oven.

When necessary, the remains were glued together using a common, dissolvable white glue. Once transported back to the University of Alberta, Henry Tory Marshall Building, the remains were individually scanned under a Keyence VHX-2000 microscope. In depth images of the 180 accounted fractures were scanned using a depth analysis function on the microscope. This produced colored images that show variation in the slopes and angles in which the trauma and heat fractures are cutting through the bone. Point clouds (.csv files) were extracted from the Keyence VHX-2000 for each fracture and imported into a reverse engineering software called Geomagic. With the assistance of Devon Stone, B.Sc., the point clouds were rendered into 3D models in Geomagic Studio 2014 (Geomagic®, Morrisville, North Carolina; USA) and smoothed to create polygon models, which were manipulated in Geomagic Design X 2016 (Geomagic®, Morrisville, North Carolina; USA). Once imported to Geomagic Design X, the models underwent

FIG. 4.3 shows an example of blunt force trauma on both hemipelvis samples. These images highlight the extensive damage that heat alterations have on blunt force trauma of hemipelvis samples (T13 top, T26 bottom).

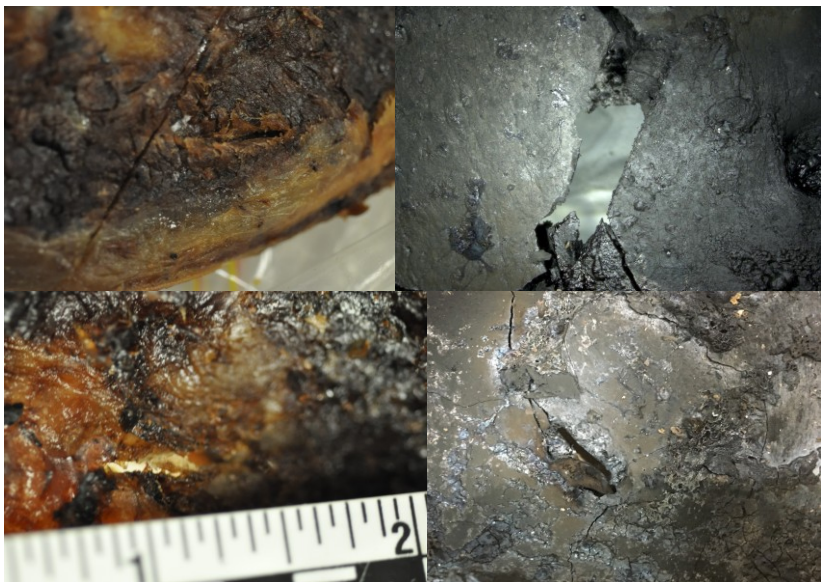

FIG. 4.4 shows an example of some of the sharp force trauma markers seen on the hemipelvis samples prior to cremation and post-cremation. These are stab wounds, which show almost complete to compete penetration of the bone (T20 top; T21 bottom).

curvature analysis, via converting each polygon model into a NURBS (non-uniform rational basis spline) surface. Geomagic Design X 2016 (Geomagic®, Morrisville, North Carolina; USA) places contour lines in areas of high curvature. The Accuracy Analyzer™ tool was then used to obtain curvature color maps (CCM's) over the areas of high curvature, showing the maximum curvature of areas on the surface. These CCM's provided a visual guide to show which types of fracture had a "sharper," or higher magnitude of curvature, as the model transitions from normal bone into fracture wall, and which fractures had a more gradual transition, or lower magnitude of curvature. It was suspected that the trauma fractures could be differentiated from the heat fractures based on these magnitudes. The CCM's were used to differentiate the fracture type by observing a reverse of curvature with regards to direction, denoted by a change between the red and blue color ranges on the map key, between the fracture walls. This allows for an in depth qualitative analysis of the fractures via color coordinated models. I am using this novel method that is not currently found in the literature.

4.3 Results

Upon removing the skeletal elements from the cremation oven, it was observed that the calottes had been charred and were in various stages of decomposition and inversion (see Chapter 2.3.1.4 for more details). The trauma markers were largely visible, in addition to the new heat fractures. Interactions between the two were counted. From the calottes, there were 12 BFT traumatic fractures, 19 SFT traumatic fractures, and 42 heat fractures observed. The definitive trauma fractures were identified by visual analysis of the calottes, as well as comparison to pre-cremation photos. The hemipelves, when removed from the oven, were more severely damaged than anticipated. The remains were largely charred, but the middle of the iliac blades on the hemipelves, inflicted with BFT, had collapsed. The data for these trauma markers was largely lost. As for those with SFT markers, the majority of fractures were seen post-cremation. There were a total of 12 observable BFT traumatic fractures and 31 SFT traumatic fractures on the hemipelves, and 64 heat fractures. The definitive trauma markers were once again identified by visual analysis of the hemipelves, as well as comparison to the pre-cremation photos. A total of 180 BFT, SFT, and heat fractures were analyzed between the calottes and hemipelves. Note the large number of combined heat fractures is due to the two control samples – one calotte and one hemipelvis. Small bone fragments that flaked off the cortical and trabecular portions of the calottes and hemipelves around trauma markers and charred musculature from the hemipelves was not analyzed as they were too small to place into context. Some ash remnants were not recovered.

From the qualitative analysis via Geomagic software, discernable differences between traumatic and heat fracture were noted. The way the Accuracy Analyzer™ created the CCM's led to stark differences in the way traumatic fractures and heat fractures were identified. Since the blunt force trauma sites of impact compressed the cortical and diploic or trabecular layers of bone together, the models were easy to identify, as they were only fracture walls with no bottom (FIG. 4.5). Sharp force trauma, on the other hand, left distinct ridging patterns in the CCM's (FIG. 4.6), which we called a double reverse of curvature. This means there is a wave of color where the CCM goes from red, orange, yellow, light blue, blue, light blue, yellow, orange, red, orange, yellow, light blue, blue and so forth until the fracture ends. This is seen predominantly in slash wounds. In stab wounds, the double reverse curvature is more notable and takes on a bubbled, or rapid wave (FIG. 4.7); however, BFT and SFT fracture lines extending from the point of impact were relatively indifferentiable. These fractures can show an 'island' of double reverse curvature (FIG. 4.8) where a section of the base of the fracture bubbles into a reverse curvature and the rest of the walls look normal. Extending traumatic fractures show a wide variation in the CCM color gradient, meaning there is a gradual shift from red

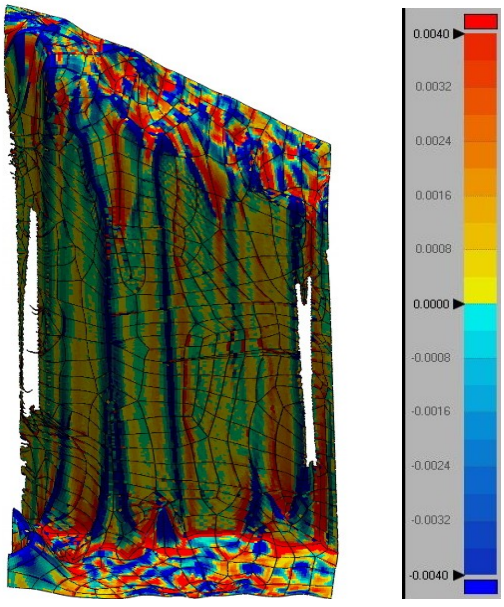

FIG. 4.5 shows an example of a BFT impact site from a hemipelvis, where the fracture base is non-existent and only the depth of the fracture wall is present.

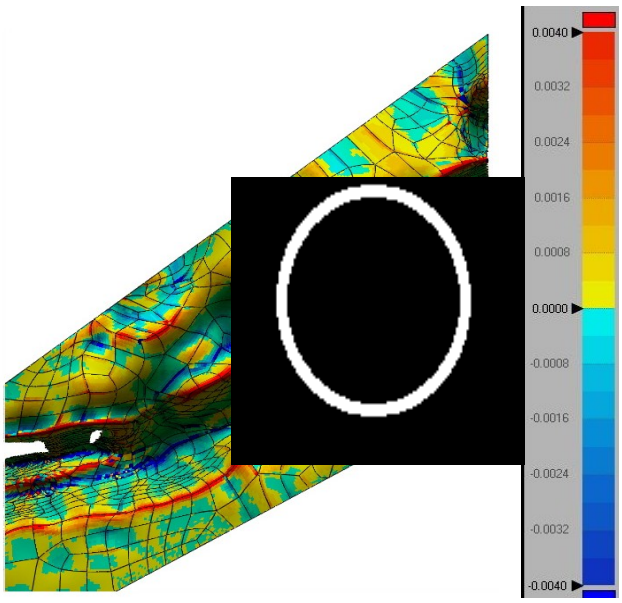

FIG. 4.6 shows a clear example of the reverse double curvature noted in the trauma impact sites of SFT (inside the white circle).

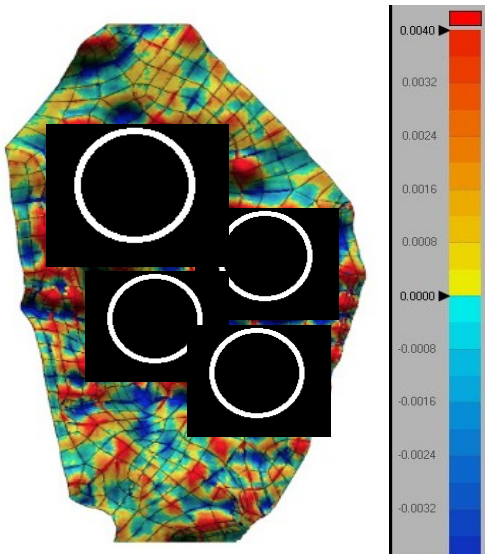

FIG. 4.7 shows an example of the bubbled, rapid double reverse curvature that looks like ripped or scabbed tissue (evident in the white circles).

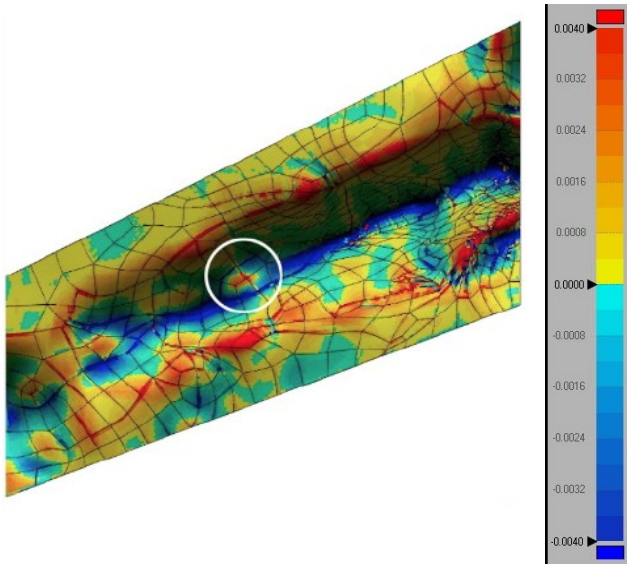

FIG. 4.8 shows an example of the 'island' (inside of the white circle) of double reverse curvature noted in approximately half of the extending trauma fractures from the main site of impact.

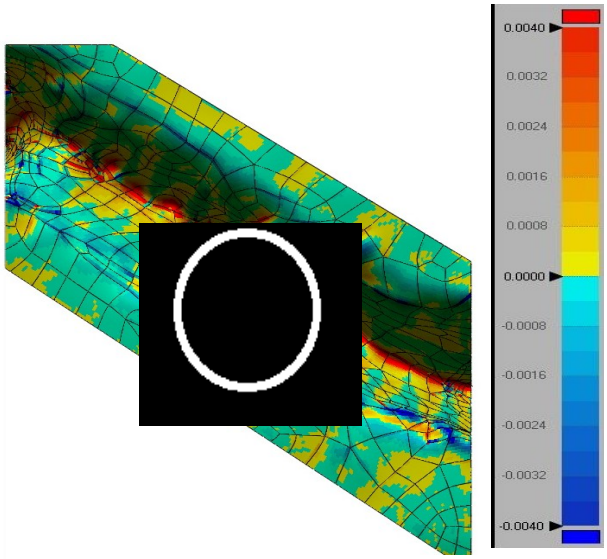

FIG. 4.9 shows the gradual color change from red to blue within a trauma fracture (inside the white circle), indicative of a more sloped entry from the flat portion of cortical bone into the fracture wall.

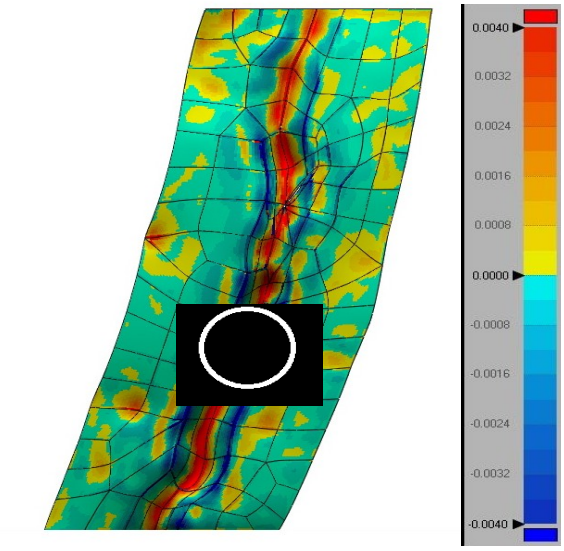

FIG. 4.10 shows the drastic change from dark red to dark blue (inside the white circle), with little gradient change between the two colors, indicative of a typical heat fracture.

to orange, yellow, light blue, and blue (FIG. 4.9). These can be seen individually or combined, but they do indicate traumatic fractures. Heat fractures, however, are noted to express two different qualities. The first shows heat fractures changing drastically from dark red to dark blue with little color variation in between (FIG. 4.10). The second visible difference are heat fractures that exhibit a bit more color differentiation, similar to traumatic fractures, but have a distinct pinching pattern along

the base where the fracture walls meet (FIG. 4.11). This is seen as color bridges between the fracture walls themselves, almost mirroring stitches.

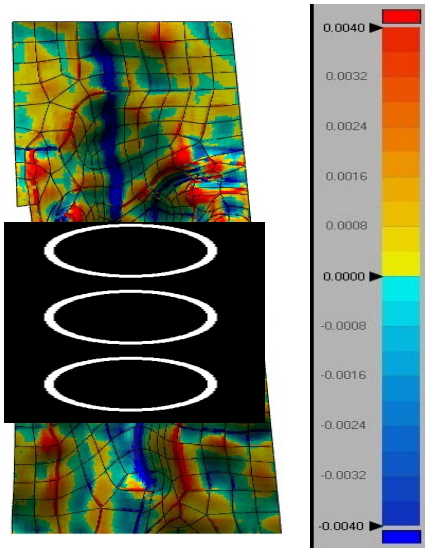

FIG. 4.11 highlights the pinching or bridged pattern (inside the white ovals)that appear at the base of a large portion of the heat fractures from this study.

4.3.1 Keyence VHX-2000

Colored images from the Keyence VHX-2000 show various depths of the fractures, illuminating elevation changes caused by fractures. The control calotte had a high survival rate, losing minimal flakes and ashes during the heating process. Heat fractures were easily recognized under the Keyence VHX-2000, as they were they only fracture types present on this sample. They matched their known description of being "clean, sharp, and [having] easily matching borders" (Marella *et al.*, 2012). These images showed distinct sharp edges at the tops of the fracture walls (FIG. 4.12, 4.13). Calotte T13, BFT, was largely complete, but upon impact from the tire iron prior to cremation the frontal bone fractured away from the rest of the calotte. Post-cremation, most of the bone was intact, minus minimal flakes and ashes from the cremation process. Under the Keyence VHX-2000, the traumatic fractures showed one sloped fracture wall and one straight fracture wall in most instances (FIG. 4.14). The heat fractures, were relatively straight and sharp as seen in the control sample (FIG. 4.15). Calotte T26 was the other sample bludgeoned with a tire ion. The calotte was again largely recovered post cremation, minus small flakes and ashes. The BFT markers survived, including residual fractures (FIG. 4.16). The concentric fractures around the site of impact are shown. Heat fractures were identifiable in this sample, and hard to pick up on the Keyence, as they were so small and shallow the microscope could not focus on their depth.

Sharp force trauma samples were readily identifiable post-cremation. Calotte T21 survived the cremation process completely intact, with the inability to recover minor ashes. The SFT left brilliant marks on the calotte (FIG. 4.17, FIG. 4.18, FIG. 4.19). The slash wound in Figure 4.17 and Figure 4.19 highlight the various depths at which the knife sliced through the cortical and diploic bone. Figure 4.19 also shows a radiating fracture from the time of impact. Stab wounds, shown in Figure 4.18 are given a stunning radiance of color, from the slopping walls at the site of impact, to the bubbled portion of exposed diplöe. Heat fractures on calotte T21 were easily identified as well, as there was a

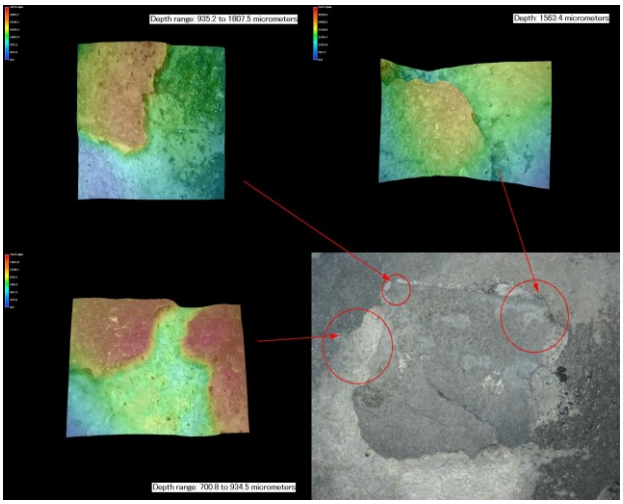

FIG. 4.12 is of a series of heat fractures showing the cracking and peeling of the outer lamina of a calotte (T29).

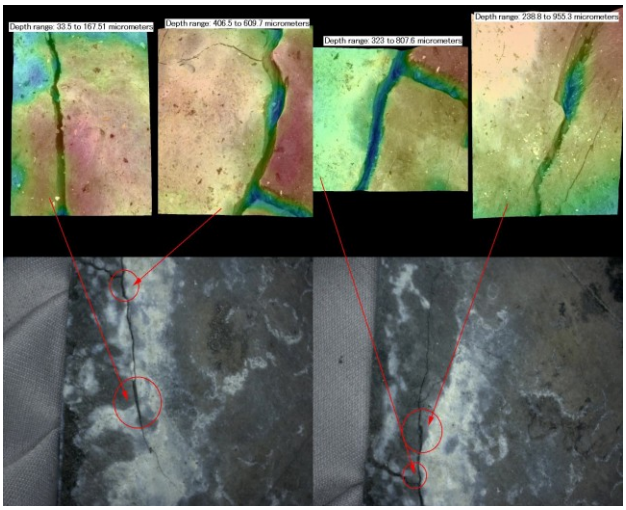

FIG. 4.13 is a series of heat fractures from a calotte stemming off an autopsy line (T29).

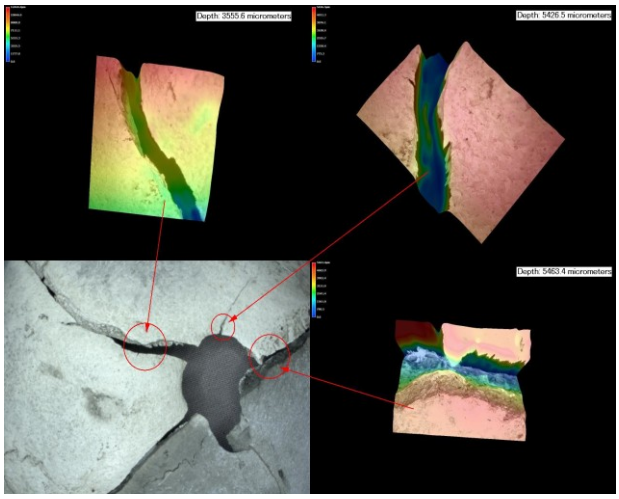

FIG. 4.14 is a series of residual fractures stemming from the main site of BFT impact on a calotte (T13).

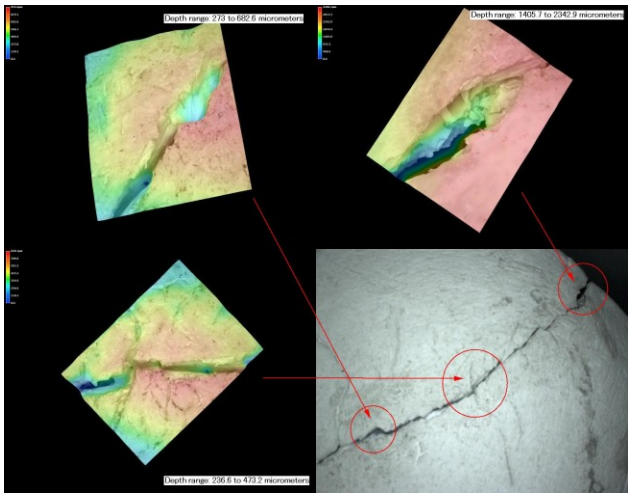

FIG. 4.15 is a series of heat fractures stemming from the base of the calotte along the autopsy saw line (T13).

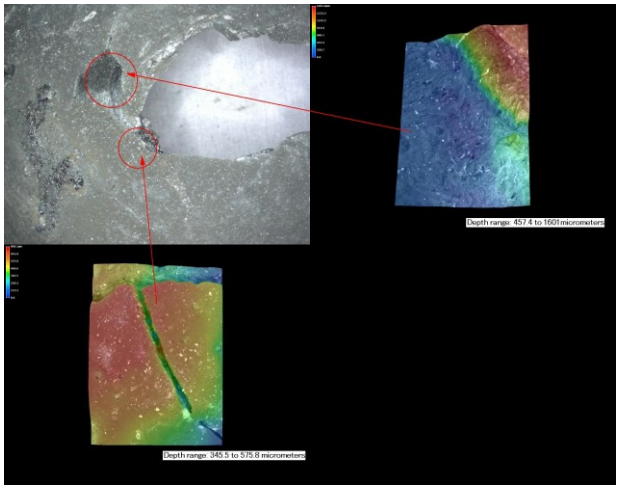

FIG. 4.16 shows two images highlighting the depth of lamina breakaway post-BFT impact, as well as a concentric fracture from the BFT (T26).

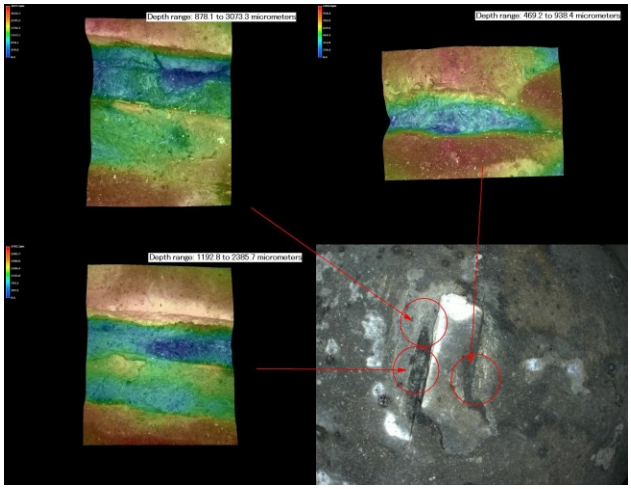

FIG. 4.17 shows various parts of one SFT slash wound on the occipital portion of a calotte (T21).

lot of lamina peeling on this sample (FIG. 4.20). Calotte T20 survived completely intact, losing only minor ashes and flakes. The slash and stab wounds seen in Figure 4.21 once again show the sloped walls created from the knife on unburned bone. Heat fractures on this calotte were easily identified, and largely ran between sutural lines (FIG. 4.22), but maintained the rigid nature seen in the control sample (T29).

The hemipelves did not survive as well as the calottes. It is possible this is due to the formalin soaked 1 cm of musculature that resided on the bones prior to burning, since it is known that formalin will cause a quicker flash over point (see Chapter 3.4). Hemipelvis T29 had the highest survival rate, presumable because it was the control sample, and was largely recovered sans a few bone chips and ashes. The heat fractures in this model (FIG. 4.23, FIG. 4.24) show the same sharp, upright fracture walls noticed in the calottes. All the heat fractures were easily identified as they were the only fractures on this sample, besides the saw band line at the distal end of the sample. Hemipelvis T13 was not fully recovered post-cremation. The center of the iliac blade that had been smashed with the tire iron completely collapsed when the soft tissue structures burned away. Figure 4.25 shows the remnants of the BFT markers as captured by the Keyence VHX-2000. The depth is shown by the

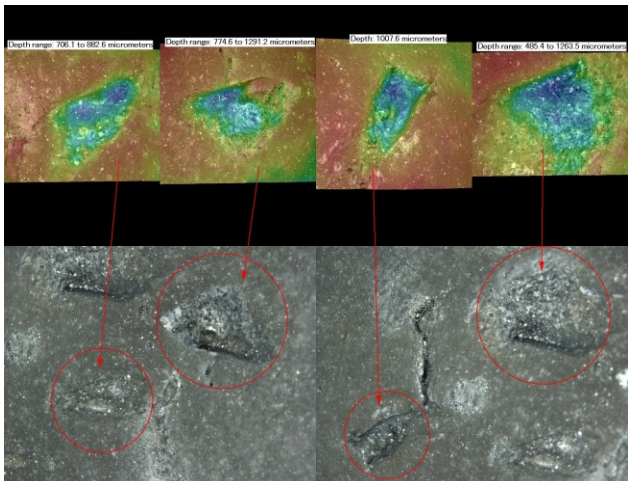

FIG. 4.18 shows a series of stab wounds on a calotte (T21).

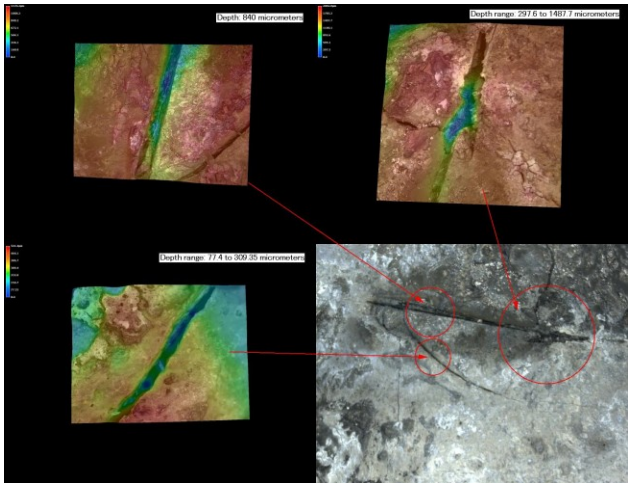

FIG. 4.19 shows two portions of a SFT slash wound and one additional fracture formed at the time of impact (T21).

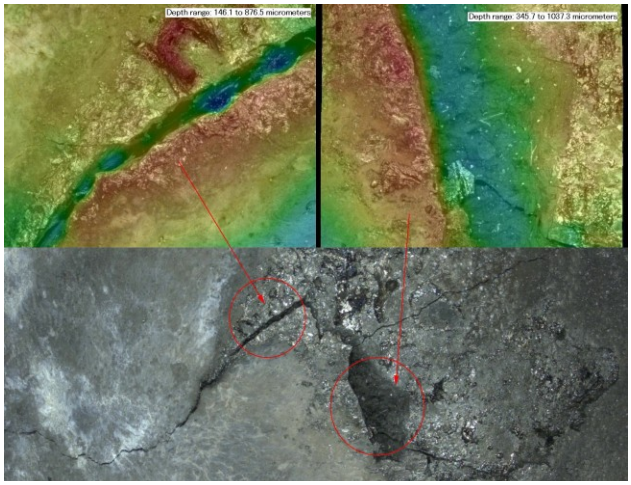

FIG. 4.20 shows two heat fractures on a calotte, causing the lamina to peel (T21).

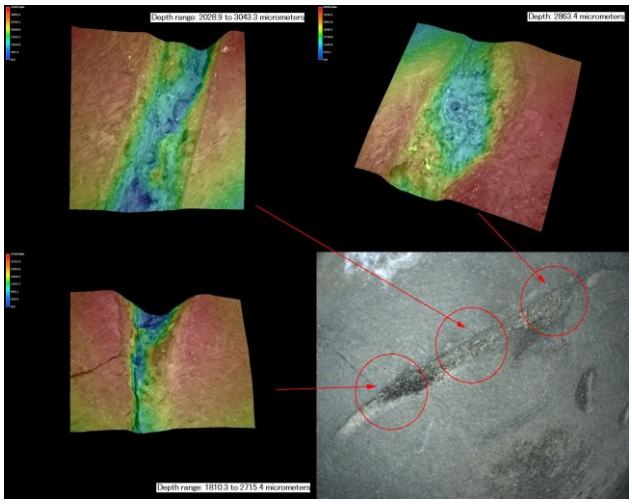

FIG. 4.21 shows a series of various SFT slash wound markers on a calotte (T20).

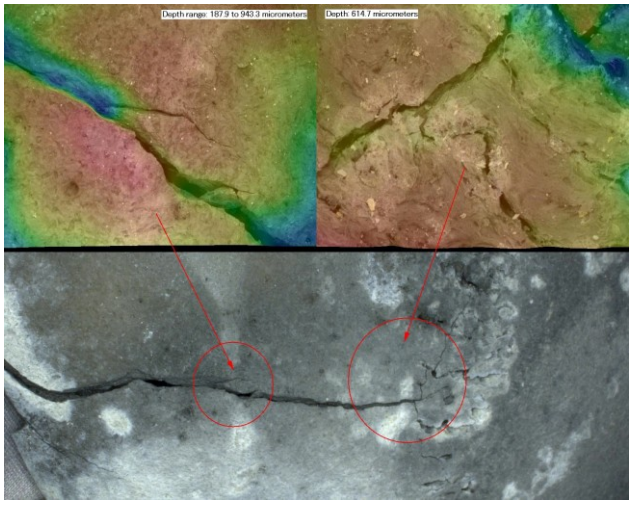

FIG. 4.22 shows a series of heat fractures on the occipital of a calotte (T20).

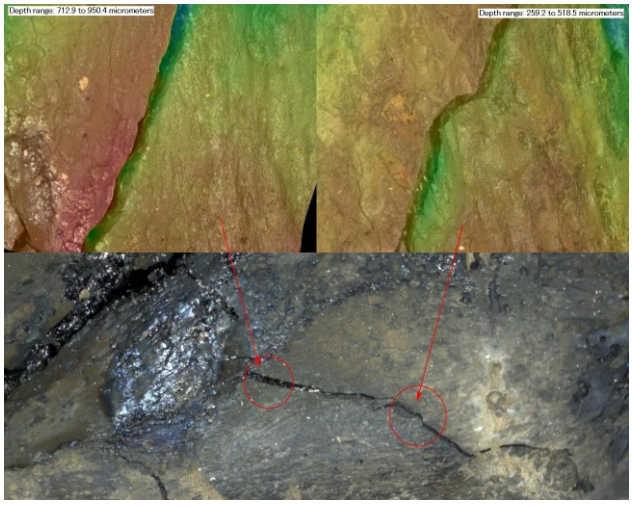

FIG. 4.23 shows a series of heat fractures on a hemipelvis (T29).

various colors that scale down the trabecular center of the iliac blade. Figure 4.26 shows residual heat fractures stemming off the original point of impact for the BFT, moving superiorly towards the iliac crest. More damage from heat can be seen on hemipelvis T13 as the anterior surface of iliac blade, near the BFT trauma, shifted so one layer of cortical bone is higher than the other. This is seen in Figure 4.27 via the red plateaus and blue plateaus. Hemipelvis T26 also underwent BFT via a tire iron. This hemipelvis, like T13, did not have a high survival rate post-cremation. Again, the bone fragments around the point of trauma were lost as the hemipelvis musculature burned away; however, the Keyence VHX-2000 was once again able to show the depth of the iliac blade, and the sloped fracture walls from the point of impact (FIG. 4.28).

The hemipelves that experienced SFT had a greater rate of survivability than the BFT samples. This is most likely due to less extensive trauma from a knife than a tire iron. Hemipelvis T21 shows a distinct stab wound, complete with sloped edges and two heat fractures stemming off the site of impact (FIG. 4.29). A slash wound inflicted on hemipelvis T21 is shown in Figure 4.30, with curved edges, which can be directly compared to a heat fracture shown in the same image. The heat fractures of this hemipelvis still have sharp edges, though they are not as defined

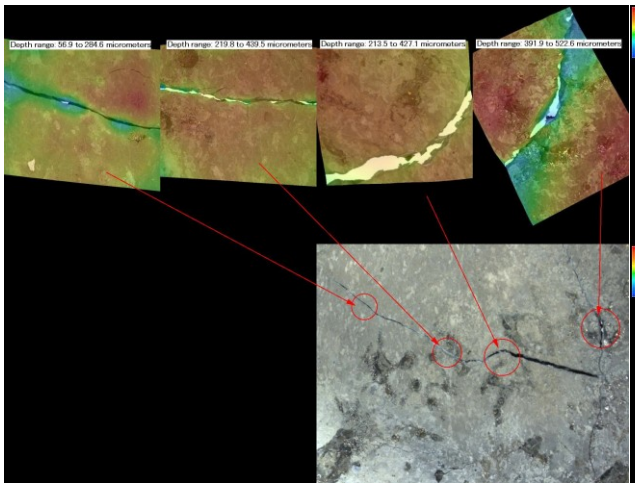

FIG. 4.24 shows a series of heat fractures near the middle of the iliac blade on a hemipelvis (T29).

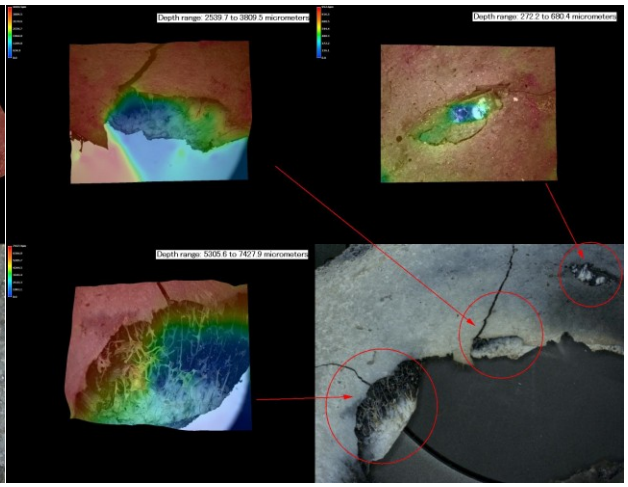

FIG. 4.25 shows BFT on a hemipelvis, including the complete collapse of the cortical and trabecular portions of the bone (T13).

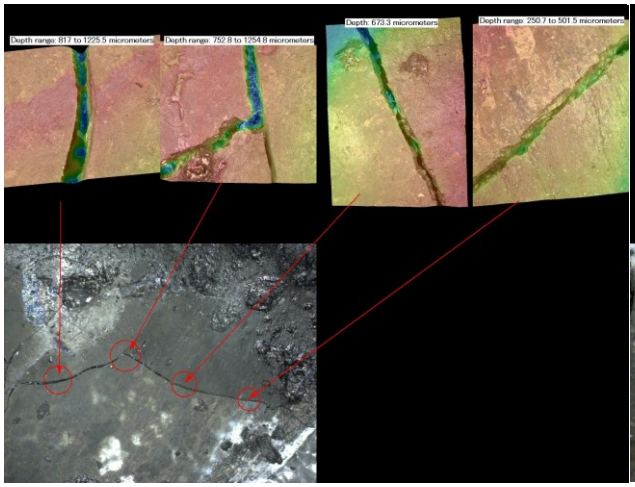

FIG. 4.26 shows a set of heat fractures stemming from the original point of impact via BFT (T13).

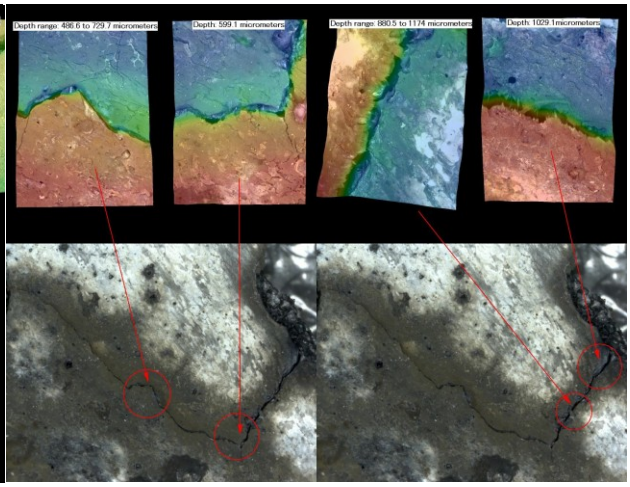

FIG. 4.27 shows a series of heat fractures on a hemipelvis, splitting the cortical bone into two sections – one elevated slightly higher than the other (T13).

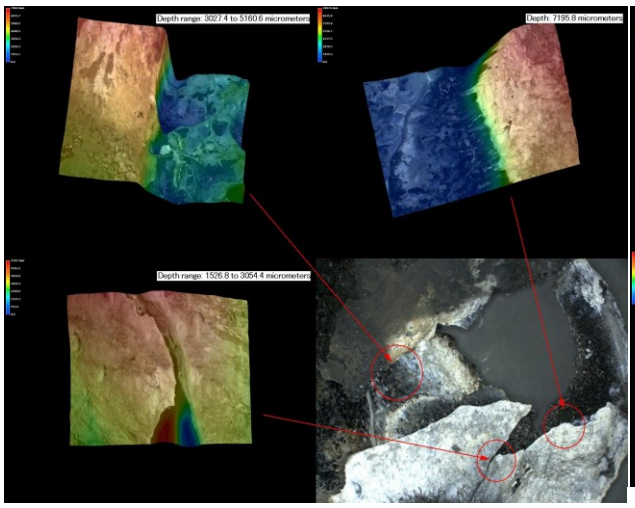

FIG. 4.28 shows another series of the impact of BFT on a hemipelvis, once again collapsing all layers of bone (T26).

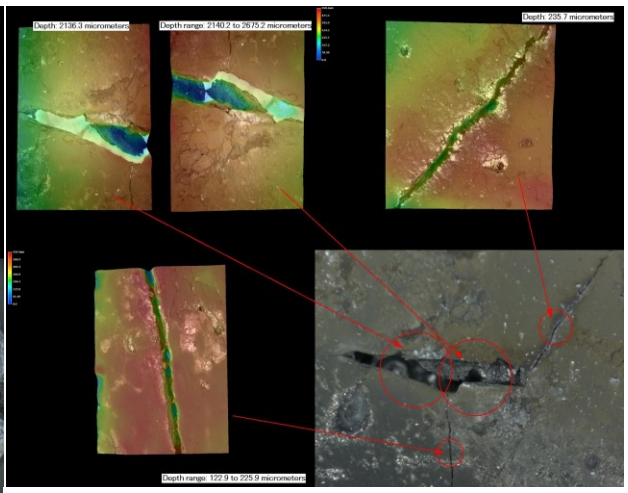

FIG. 4.29 shows the front and back half of the same stab wound and two heat fractures stemming from the SFT (T21).

as the calotte (FIG. 4.31). Hemipelvis T20 was the other sample inflicted with SFT was mostly recovered, sans minor bone flakes and ash. The main slash wound, combined with residual trauma fractures can be seen in Figure 4.32 – there is one notable sloped wall and one more straight edge. This is most likely caused from the angle at which the knife was held as it impacted the hemipelvis. A stab wound (FIG. 4.33) also shows similar traits, as do the other two fractures in this image. Finally, the heat fractures from hemipelvis T20 largely disrupt the iliac blade (FIG. 4.34), shifting the cortical bone on the anterior surface into non-level segments. Once witnessed under the Keyence VHX-2000, it was evident that the trauma fractures maintained their sloped walls as predicted. The heat fractures did indeed appear to be more upright and have sharp edges. This is seen in both the calottes and hemipelves.

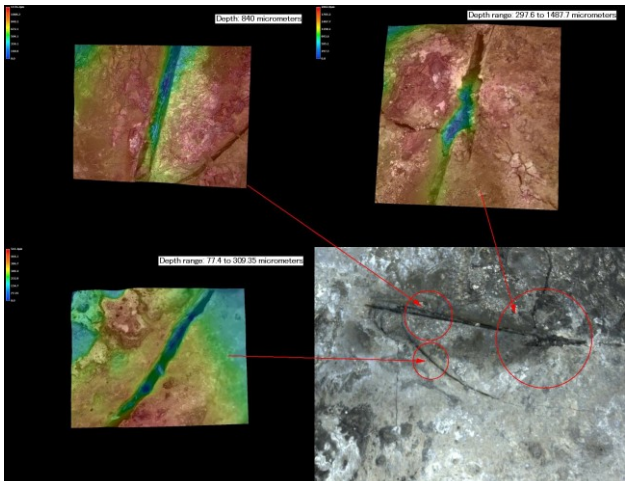

FIG. 4.30 shows the front and back half of the same slash wound and one heat fracture stemming from the SFT impact site (T21).

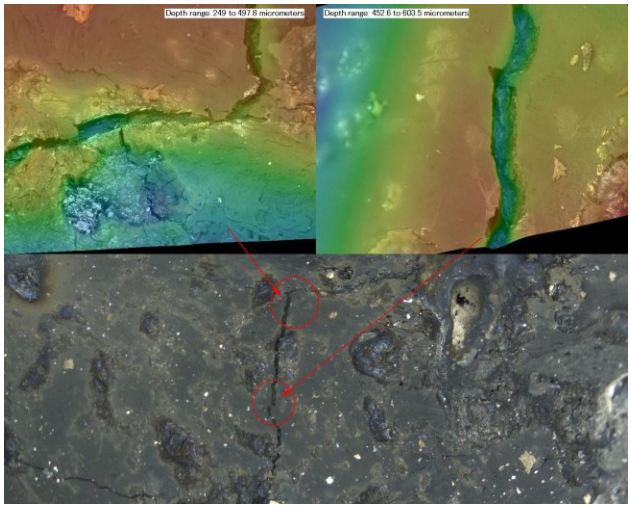

FIG. 4.31 shows heat fractures on a hemipelvis (T21).

4.4 Discussion

4.4.1 Geomagic Software

Once the Keyence VHX-2000 point clouds were converted to .csv files and imported into Geomagic software for the creation of 3D virtual models, greater distinctions were evident between the traumatic fractures and heat fractures in the calottes and hemipelves. BFT markers in both samples showed drastic one-walled models (FIG. 4.5) that contained various

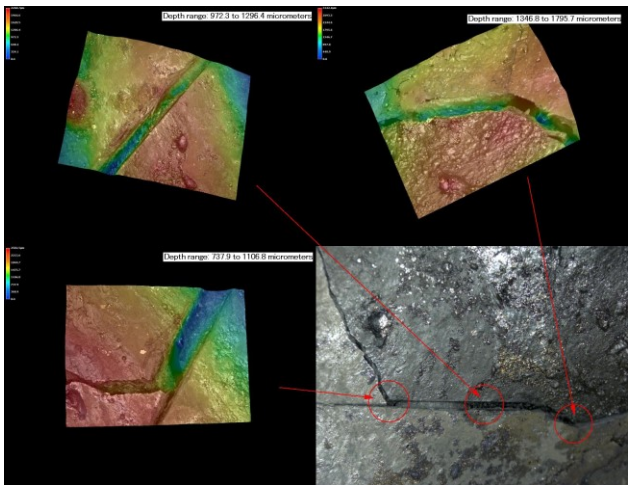

FIG. 4.32 shows a set of images with a SFT slash wound in combination with an extending trauma fracture from the force of impact (T20).

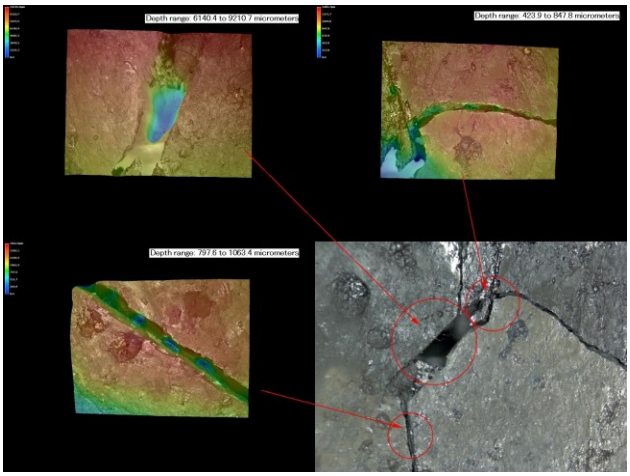

FIG. 4.33 shows a series that represents SFT stab wounds on a hemipelvis, including extending trauma fractures from the impact site (T20).

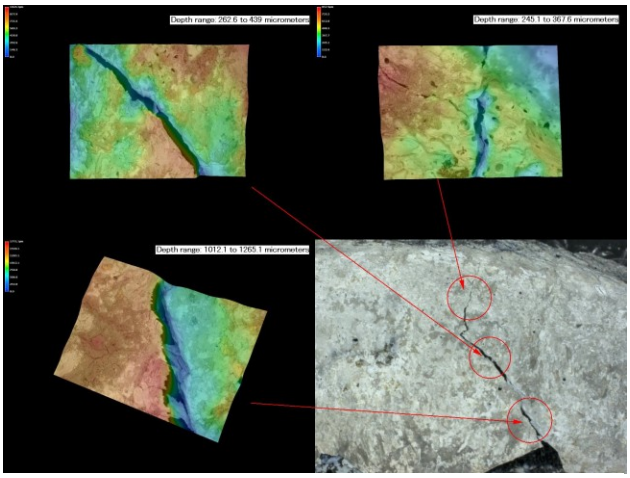

FIG. 4.34 shows a series of heat fractures from the SFT impact site (T20).

colors. There are no other images like these. SFT markers on both the calottes and hemipelves show a few distinct patterns. The first notable characteristic is a double reverse curvatur[5] (FIG. 4.6) The double reverse curvature can be seen in shallow SFT wounds, such as stab wounds, leaving a rippled, bubbled pattern[6] (FIG. 4.5). In traumatic fracture lines that stem from the main point of impact, there are two main CCM's that are seen: the 'island' of color[6] situated between fracture walls, and gradual color transitions[6] from dark red to dark blue (FIG. 4.5, FIG. 4.8). Heat fractures are vastly different from the traumatic fractures on both calottes and hemipelves. They are categorized in one of two ways: drastic color change from dark red to dark blue[6] (FIG. 4.10) or varied color with a distinct pinching pattern at the base of the fracture walls where they meet[6] (FIG. 4.11).

It is suggested these CCM's occur because the fractures are being made in fresh bone that reacts as a viscoelastic material. The collagen fibrils separate around the site of impact as mechanical failure occurs, and the double reverse curvature marks the peeling of collagen fibrils or possibly the edges of the lamellar bone being torn. The elongated color range in trauma fracture walls, with a thin line of dark red and dark blue and a larger portion of light blue, yellow, and orange is suggested to represent the peeling of the collagen fibers or bone curl that occurs when blunt and sharp force implements contact bone and are pulled out. Fresh bone caves in, leaving ragged edges that appear worn which is seen in diverse colors on a curve analysis scale.

Heat fractures are differentiated from trauma fractures because of their lack of color gradient on the accuracy analyzer scale presented by Geomagic Design X 2016 (Geomagic®, Morrisville,

[5] Previously discussed in Chapter 4.3

North Carolina; USA). The analysis shows heat fractures are largely represented by the darker red and blue with minimal orange, yellow, and light blue (FIG. 4.10). This occurs because heat impacts bone as a brittle substance, where the fracture goes straight through the bone without resistance, creating sharp edges and more vertical fracture walls. In addition, heat fractures show a pinching or gathering at the base of the fracture sporadically throughout the length of the fracture (FIG. 4.11). This almost looks like a bridging of the fracture walls where the bone was not completely split during fracturing. It is suggested that this is happening as the interstitial fluids expand during the heating process and dehydration occurs, creating ripples in the base of the fractures. Since dehydration does not occur evenly as bones burn, it is possible that heat fractures do not have even bases where the fracture walls meet when they do not fully extend through the bone.

4.4.2 Mineral and Organic Changes

The patterns seen on the Geomagic 3D virtual models are representative of the biomechanical differences seen between fresh and brittle (burned) bone. Trauma, in fresh bone, disrupts the bone structure, causing a failure of the entire bone structure when the force is too much for the bone to rebound from. The forces pushed onto the bone are unable to be redirected (Klepinger 2006). Interstitial fluids are a major component of this, as they shift the force throughout the bone structure in attempt to minimize damages and prevent plastic deformation. Interstitial fluids move the forces through cement lines, around osteonal systems (Gupta and Zioupos 2008, Nalla *et al.*, 2005, Peterlik *et al.*, 2005, Zimmermann and Ritchie 2015). As the force moves throughout the bone, the collagen fibrils, oriented in a way to deter crack tip propagation, are pulled and strained. When a fracture does occur, the collagen fibrils are mangled and torn, resulting in a jagged, sloped edge. Since most fractures follow the path of least resistance, collagen fibrils that are able to deflect the crack tip will largely stay intact, whereas others break under strain. This is why, on the Geomagic models showing SFT sites of impact and residual fractures from BFT and SFT impact sites, there is a distinct double reverse curvature or island motif. The elongated gradient from these fractures is noted because they were made in fresh bone, i.e. the slope (seen in the Keyence VHX-2000 images) is still evident post-cremation. The gradual changes in color represent the osteonal pullout and uneven surface seen in perimortem trauma.

Heat highly alters the bones' biomechanical structure. Perimortem trauma shows collagen bounce-back, or elasticity, in response to bone deformation; postmortem trauma does not (Klepinger 2006). This concept extends to the impact of heat on bone. Heat causes bones to shrink and warp as

the interstitial fluid dries up and can no longer divert forces; collagen fibrils break down and cannot divert crack tip propagation. The crystal bonds and proteins that ultimately hold bones together break down and the entire system deteriorates (Marella *et al.*, 2012). For this reason, in the Geomagic models showing heat fractures, there are very clear, thin lines of color change, as the bone is being ripped apart and drastic colors are seen. There is no osteonal pullout, no crack tip divergence via collagen fibrils, and no force dispersal from interstitial fluids. As for the second model seen with heat fractures, the general pinching nature theoretically arises from the organic components that are still present in the bone. These remains were only partially cremated, meaning there are still organic components present (Baby 1954). It is possible that the remaining organic components in these instances were existent to the point where they were able to marginally deflect or hinder the heat fractures from fully forming.

The mineral and organic changes seen in these 10 samples is anticipated, as bone break down in heat exposure has already been studied (Forbes 1941, Marella *et al.* 2012, Mayne Correia 1997). The trauma fractures, appearing eroded, rounded, and warped, were expected as the protein structures, hydroxyapatite crystals, collagen fibers, and interstitial fluid disintegrated. Studies on human long bones and animal remains have given some indication as to how BFT and SFT trauma would react with heat exposure (Kimmerle and Baraybar 2008, Klepinger 2006, Mayne 1990, Pope and Smith 2004, Symes *et al.*, 2008, Wedel and Galloway 1999). What was unknown, however, was how BFT and SFT fractures would be characteristically different from heat fractures after cremation of cranial and irregular bones due to the lack of research in this area. For these reasons, when viewed microscopically, there are distinct differences seen from long bone and animal bone, and there is a way to differentiate perimortem trauma from heat fractures on cranial and irregular bones in cases of cremation.

4.4.3 Quantitative Analysis

Quantitative analysis was completed by taking isolated 2D curve models from the Geomagic Studio 2014 (Geomagic®, Morrisville, North Carolina; USA) software and by comparing them to one another. 15 curves were created perpendicular to the fracture lines at 300 μm spacing. The curves were isolated and studied. Distinct differences in the curvature, or slope, from the top cortical bone layer into the fracture wall were compared to see if a numerical degree could be used to determine what curvature was predominately seen in trauma fractures versus heat fractures. Unfortunately, the 2D

models were indiscernible from one another, making it impossible to draw conclusions on curvature without the color map. More work in this area needs to be done to find a way to quantify what is being seen in the CCM's from the 3D virtual models.

4.5 Conclusion

The research in this study utilized novel qualitative analytical techniques to differentiate perimortem trauma fractures from heat fractures. It was hypothesized that perimortem trauma fractures would be able to be differentiated from heat fractures post-cremation. The Keyence VHX-2000 illuminated on a microscopic level the differences between trauma fractures and heat fractures on cremated cranial and irregular bones. This is an extremely valuable finding in the world of forensic anthropology, as it opens new avenues of research and charts mostly unexplored territory with how trauma and heat fractures act on cranial and irregular bones. Extending further, the work done on Geomagic Studio and Design X 2016 (Geomagic®, Morrisville, North Carolina; USA) helped to put defined methods of qualitative analysis together for forensic anthropologists to use. Being able to look at trauma and heat fractures as 3D models with curvature color scales helps to illuminate further the differences between the fracture types. This is critical to furthering this field of study and providing a new point, microscopically, in which further research can stem from.

Blunt and sharp force traumas are noted by the heavy double reverse curvature noted at the site of impact from the blunt or sharp force object. The sites of impact from blunt and sharp force objects are easily discerned from trauma fractures stemming off of the site of impact, as well as heat fractures. Residual fractures coming off the site of impact can be separated from heat fractures with confidence. These are defined by minimal double reverse curvature, which looks like an island in the middle of the fracture. Heat fractures, which are readily differentiated, show minimal gradient changes on the accuracy analyzer scale. They show a pinching or bubbled nature along the base of the fracture walls of the CCM's. This microscopic analysis gives preliminary conclusions for the differentiation of perimortem trauma from heat fractures.

We present these findings as evidence for differentiation of perimortem trauma fractures from heat fractures in cases of cremation. Fresh bone and burned bone show distinctive differences in bone properties on a basic molecular level, meaning they should show unique characteristics. Once ethics approval is obtained, inter-observer error will be tested before this research is submitted for publication. A survey has been created (see Appendix 1) that asks participants to identify thirty models from the process described above as either trauma or heat fractures. Detailed description of how each

type of fracture should appear, as well as photo examples highlighting descriptors, will be given to each participant. This will be done to combat inter-observer errors that may have been present in this study. Further development of this theory needs to be studied in order to provide confidence in the qualitative study results, as well as positive quantitative analysis results, with intensive analysis regarding patterns seen on the fracture wall slope and the curves between the outer cortical bone layer and the fracture walls.

Appendix 1: Inter-observer Error Survey

Qualitative Analysis of Trauma Fractures from Heat Fractures using Curvature Analysis of 3D Fracture Models

Welcome to the Qualitative Analysis of Trauma Fractures from Heat Fractures using Curvature Analysis of 3D Fracture Models survey page!

This survey is being sent out on behalf of Hanna Friedlander, a Master's candidate in the Department of Anthropology at the University of Alberta. I am conducting a survey as part of my thesis research on fractures in bone. This research involved creating 3D models of traumatic fractures and heat fractures present on human bone – not images of the bones themselves, but rendered models to provide information about bone type, morphology, and other characteristics of the individuals in the study. The goal of this work is to be able to differentiate traumatic fractures from heat fractures in these images by following simple guidelines. In order to demonstrate the utility of the method I've developed, I need to ensure that repeatability of the study is possible in future research.

Your information will NOT be recorded or kept as part of the study. That being said, once you have given consent and submitted the survey, there is no way to withdraw from the study as I will not know which responses are yours. You will be quickly briefed on the study itself and given examples of what to look for in traumatic fractures versus heat fractures. There will be 30 questions asking you to assess whether the 3D models presented are trauma or heat related in nature – this will take approximately 10 minutes to read through and fill out. Using the provided examples and descriptions of the different fracture types, you will be asked to select "Trauma" or "Heat" for each question. The data collected from this survey will be analyzed for inter-observer error. The statistics gathered will be presented in published articles and future presentations at forensic and anthropology conferences describing this method of analysis, as well as its accuracy and repeatability.

By clicking the "NEXT" button, you agree to participate in the survey, with the understanding that you can stop participating by closing the window at any time or choosing not to submit your response. Once again, as your participation is anonymized, once you have submitted your responses, they cannot be pulled from the study. The Research Ethics number for this study is: Pro00070625, approved by the University of Alberta Research Ethics Management Online (REMO). If you have questions about the research, now or later, or experience technical issues, please send an email to hrfriedl@ualberta.ca. If you have questions regarding your rights as a research participant, you may contact the Health Research Ethics Board at 780-492-2615. This office is independent of the study investigators.

Thank you for your participation in this survey – please take these questions seriously and do your best to answer every question to the best of your ability.

By clicking the "NEXT" button below, I am consenting to participate in this study.

About the Study

Differentiation of trauma fractures from heat fractures is an area of study within forensic anthropology that needs to be better understood. The fractures themselves have different visual

properties, extending from the way they were created to the material composition at time of formation. Trauma fractures are typically formed on fresh bone, characterized by compression on both sides of entry and a raised edge forming upon object removal. This allows the bone to bend and react as the force from the blow is transferred throughout the bone, generating cracks. However, in instances of heat fractures, the bone is a dry and brittle substance. Having lost its organic components from an elevated temperature, the bone will crack with less resistance; there will be no compression upon entry or raised edge upon removal of the implement. Think about breaking a glass – the edges are sharp and the fractures are clean in nature.

A study recently done at the University of Alberta has taken fresh bone and traumatized it. The bones were then burned until most of the organic components were lost and a brittle structure was noted. The fractures were then photographed under a Keyence VHX-2000 microscope, generating 3D models which were imported into Geomagic Studio and Geomagic Design X 64. Auto-surfaced models were created with a curvature analysis overlay to create vibrant images. The images show color scales ranging from red to blue. Red, indicating the high point of a fracture, and blue being the base, are color delineated through orange, yellow, and light blue. The images have been broken down based on perceived differences in color gradient and known fracture types.

When looking at trauma fractures, the models show a definitive reverse double curvature inside the fracture walls. This means we see a color scale that transitions from red to blue and back to red again. This can occur once or multiple times depending on whether the trauma was caused by a blunt or sharp force object. The orange, yellow, and light blue can be seen in the gradient changes between these 'waves.'

It is critical when looking at the images to only focus on the fracture itself, not the area surrounding fracture walls, which may appear granular or bumpy in nature.

In this trauma fracture, you can see a definite reverse double curvature where the colors changes from red to blue and back again creating a 'wave' of color. This is very typical of a traumatic fracture at the site of impact.

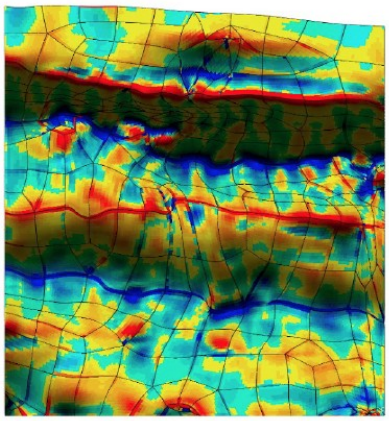

Trauma fractures

In more shallow trauma fractures, the color gradient will be seen, encompassing the range between red and blue. In some instances, there will be various 'bubbles' of color change. However, there will not necessarily be a reverse double curvature in others. Here, it is important to look at how the colors are projected and what variety of color can be seen, especially on the sides, or slopes, of the fracture

lines. Commonly seen in addition to the large color gradient in the slopes of the fracture walls are 'islands' of reverse curvature (Image 2 below).

The image below shows the double reverse curvature running through the center of the shallow fracture model. This is represented by the bubbled effect of color change throughout the model.

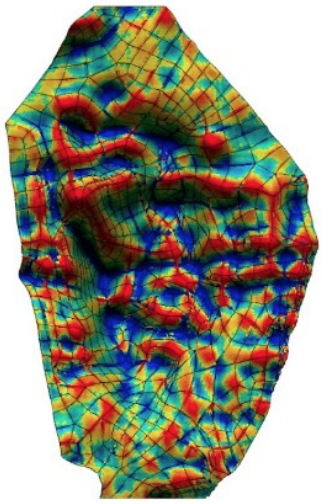

In this image, you can see a small but definitive double reverse curvature inside of the white circle. This is denoted by the abrupt 'island' in the middle of the fracture. There is also a large gradient change noted on the sides or slopes of the fractures. Evidence of the gradual change from red to dark blue is seen with orange, yellow, and light blue between the extreme colors at the top of the fracture wall and the base.

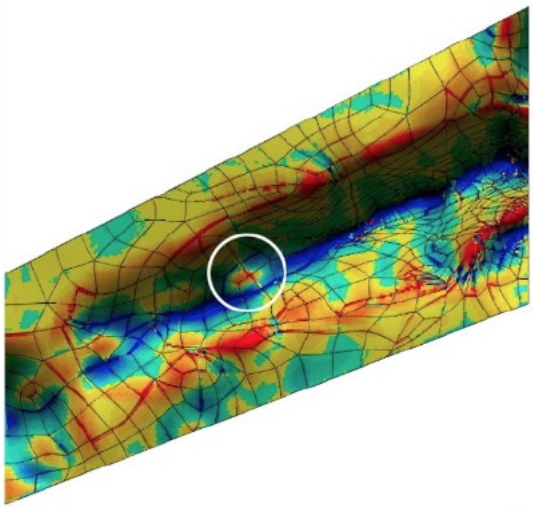

Heat Fractures

When looking at heat fractures, however, there is no reverse double curvature inside the fracture walls and limited color gradient changes. Instead, the images show drastic transitions from red to blue coloring. There is a limited change in the color gradient noted between red and blue colors.

In this image, there is no double reverse curvature. Ignoring the light blue/teal color surrounding the fracture, you can see the fracture itself is outlined in dark blue. This image shows a drastic shift from blue to red as you transition your gaze from the dark blue at the top of the fracture to the dark red at the base of the fracture walls. The color change between blue and red (light blue, yellow, and orange) is hardly noticeable within the fracture walls.

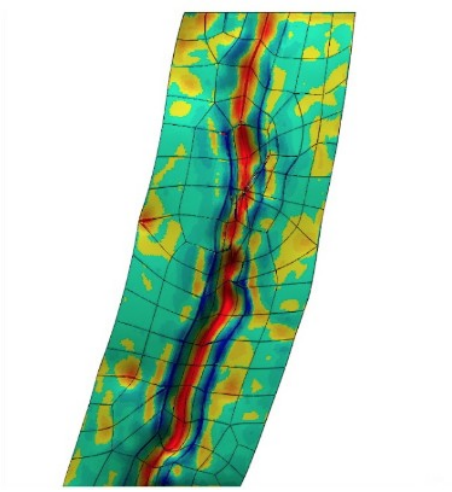

The heat fracture below shows the extremes of the color scale with red lining the top of the fracture wall, and dark blue at the base of the fracture walls. As you can see going down the fracture walls, from the dark red bands inward, there is very little deviation in color, i.e. a lack of oranges, yellows, and light blue. There are also indents or 'pinching' along the base of the fracture walls indicated inside the white ovals. This is denoted by the sharp lines of red that cross the fracture perpendicularly.

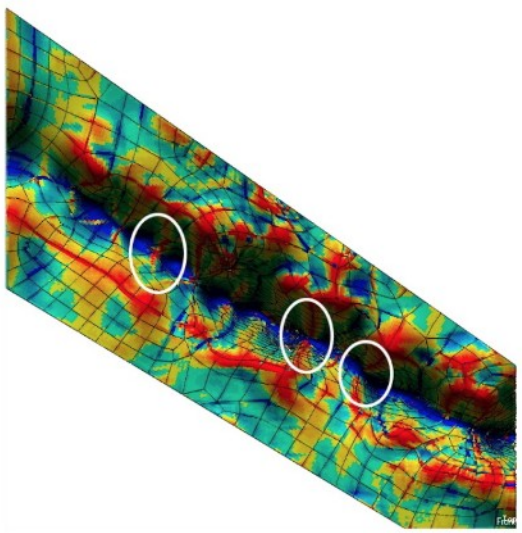

In the heat fracture below, please note that though it is not shallow and you can see color variation along the fracture wall (depicted in the white circle), there is not a large gradient or wide bar of color spanning from orange to yellow to light blue. There is a thin band of color separating the dark red from dark blue.

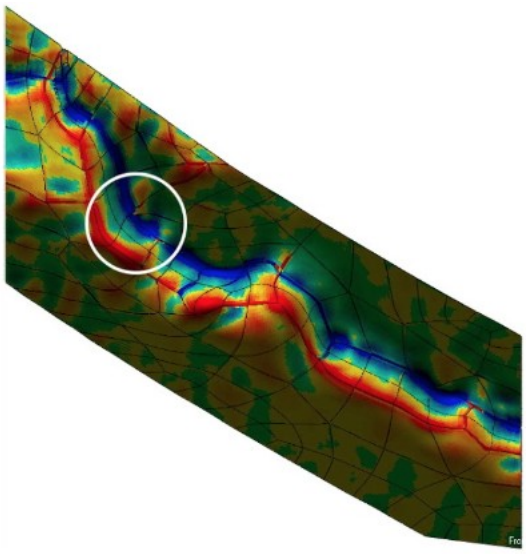

Can you answer these questions based off the prior descriptions?

Please refer to the prior examples and descriptions for help throughout the answering process. Please be sure to only look at the fractures themselves, not the surrounding area depicted in blues and yellow.

Is this a trauma fracture or heat fracture?

* Remember the basics of fracture differentiation: For traumatic fractures, you will typically see a double reverse curvature and a wide variation in color. This can be indicated by waves of color or a bubbled, rough looking surface. In some instances, there is minor reversal of color noted by and island of color change as seen in example 3. There is also a wide variation in color, scaling from dark red to orange, yellow, light blue, and finally to dark blue along the fracture walls and within the fracture itself. In heat fractures, there is no double reverse curvature and a drastic change from dark red to dark blue, or vice versa as seen in example 4. You may also see a pinching of colors at the base of the fracture as evident in example 5.

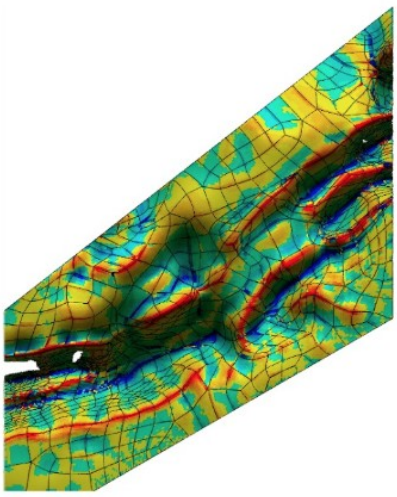

Trauma

Heat

Is this a trauma fracture or heat fracture?

* Remember the basics of fracture differentiation: For traumatic fractures, you will typically see a double reverse curvature and a wide variation in color. This can be indicated by waves of color or a bubbled, rough looking surface. In some instances, there is minor reversal of color noted by and island of color change as seen in example 3. There is also a wide variation in color, scaling from dark red to orange, yellow, light blue, and finally to dark blue along the fracture walls and within the fracture itself. In heat fractures, there is no double reverse curvature and a drastic change from dark red to dark blue, or vice versa as seen in example 4. You may also see a pinching of colors at the base of the fracture as evident in example 5.

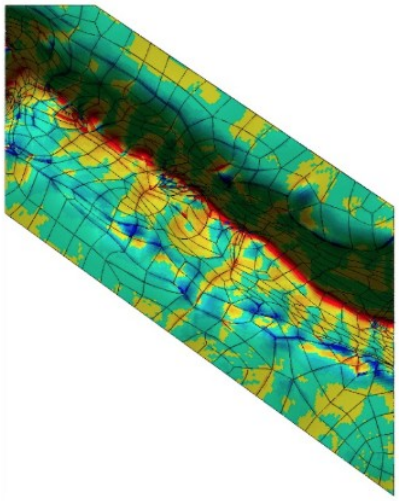

- Trauma
- Heat

Is this a trauma fracture or heat fracture?

* Remember the basics of fracture differentiation: For traumatic fractures, you will typically see a double reverse curvature and a wide variation in color. This can be indicated by waves of color or a bubbled, rough looking surface. In some instances, there is minor reversal of color noted by and island of color change as seen in example 3. There is also a wide variation in color, scaling from dark red to orange, yellow, light blue, and finally to dark blue along the fracture walls and within the fracture itself. In heat fractures, there is no double reverse curvature and a drastic change from dark red to dark blue, or vice versa as seen in example 4. You may also see a pinching of colors at the base of the fracture as evident in example 5.

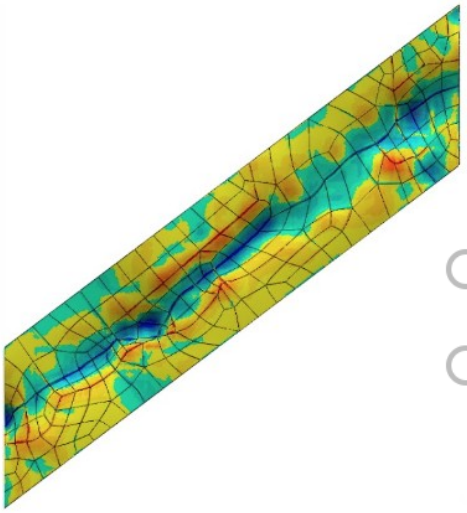

- Trauma
- Heat

Is this a trauma fracture or heat fracture?

* Remember the basics of fracture differentiation: For traumatic fractures, you will typically see a double reverse curvature and a wide variation in color. This can be indicated by waves of color or a bubbled, rough looking surface. In some instances, there is minor reversal of color noted by and island of color change as seen in example 3. There is also a wide variation in color, scaling from dark red to orange, yellow, light blue, and finally to dark blue along the fracture walls and within the fracture itself. In heat fractures, there is no double reverse curvature and a drastic change from dark red to dark blue, or vice versa as seen in example 4. You may also see a pinching of colors at the base of the fracture as evident in example 5.

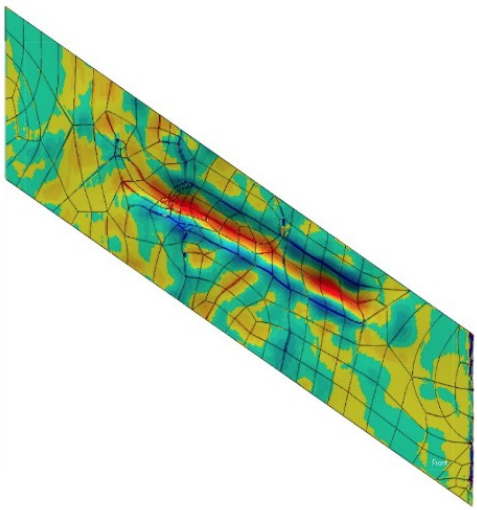

- Trauma
- Heat

Is this a trauma fracture or heat fracture?

* Remember the basics of fracture differentiation: For traumatic fractures, you will typically see a double reverse curvature and a wide variation in color. This can be indicated by waves of color or a bubbled, rough looking surface. In some instances, there is minor reversal of color noted by and island of color change as seen in example 3. There is also a wide variation in color, scaling from dark red to orange, yellow, light blue, and finally to dark blue along the fracture walls and within the fracture itself. In heat fractures, there is no double reverse curvature and a drastic change from dark red to dark blue, or vice versa as seen in example 4. You may also see a pinching of colors at the base of the fracture as evident in example 5.

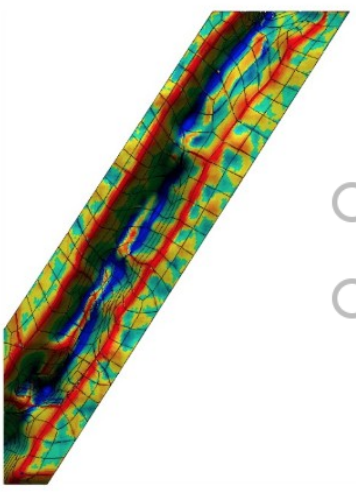

- Trauma
- Heat

Is this a trauma fracture or heat fracture?

* Remember the basics of fracture differentiation: For traumatic fractures, you will typically see a double reverse curvature and a wide variation in color. This can be indicated by waves of color or a bubbled, rough looking surface. In some instances, there is minor reversal of color noted by and island of color change as seen in example 3. There is also a wide variation in color, scaling from dark red to orange, yellow, light blue, and finally to dark blue along the fracture walls and within the fracture itself. In heat fractures, there is no double reverse curvature and a drastic change from dark red to dark blue, or vice versa as seen in example 4. You may also see a pinching of colors at the base of the fracture as evident in example 5.

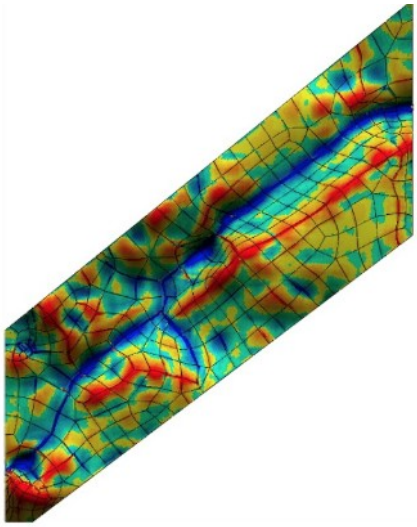

- Trauma
- Heat

Is this a trauma fracture or heat fracture?

* Remember the basics of fracture differentiation: For traumatic fractures, you will typically see a double reverse curvature and a wide variation in color. This can be indicated by waves of color or a bubbled, rough looking surface. In some instances, there is minor reversal of color noted by and island of color change as seen in example 3. There is also a wide variation in color, scaling from dark red to orange, yellow, light blue, and finally to dark blue along the fracture walls and within the fracture itself. In heat fractures, there is no double reverse curvature and a drastic change from dark red to dark blue, or vice versa as seen in example 4. You may also see a pinching of colors at the base of the fracture as evident in example 5.

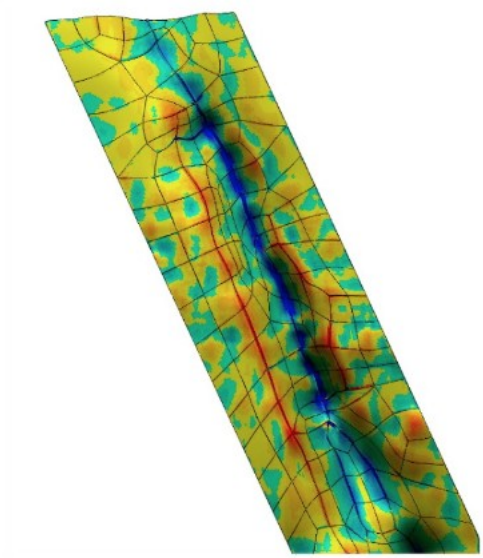

- Trauma
- Heat

Is this a trauma fracture or heat fracture?

* Remember the basics of fracture differentiation: For traumatic fractures, you will typically see a double reverse curvature and a wide variation in color. This can be indicated by waves of color or a bubbled, rough looking surface. In some instances, there is minor reversal of color noted by and island of color change as seen in example 3. There is also a wide variation in color, scaling from dark red to orange, yellow, light blue, and finally to dark blue along the fracture walls and within the fracture itself. In heat fractures, there is no double reverse curvature and a drastic change from dark red to dark blue, or vice versa as seen in example 4. You may also see a pinching of colors at the base of the fracture as evident in example 5.

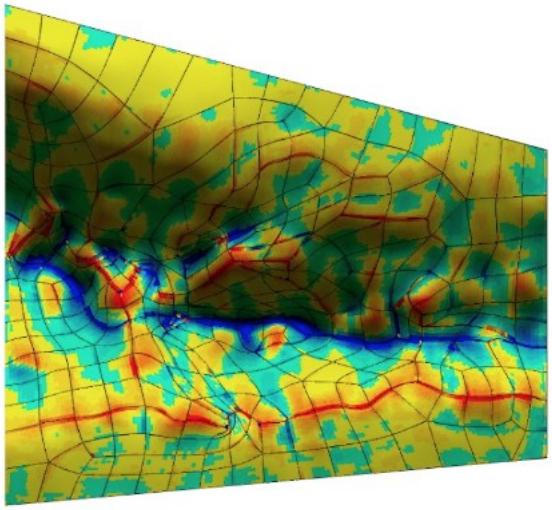

- ○ Trauma
- ○ Heat

Is this a trauma fracture or heat fracture?

* Remember the basics of fracture differentiation: For traumatic fractures, you will typically see a double reverse curvature and a wide variation in color. This can be indicated by waves of color or a bubbled, rough looking surface. In some instances, there is minor reversal of color noted by and island of color change as seen in example 3. There is also a wide variation in color, scaling from dark red to orange, yellow, light blue, and finally to dark blue along the fracture walls and within the fracture itself. In heat fractures, there is no double reverse curvature and a drastic change from dark red to dark blue, or vice versa as seen in example 4. You may also see a pinching of colors at the base of the fracture as evident in example 5.

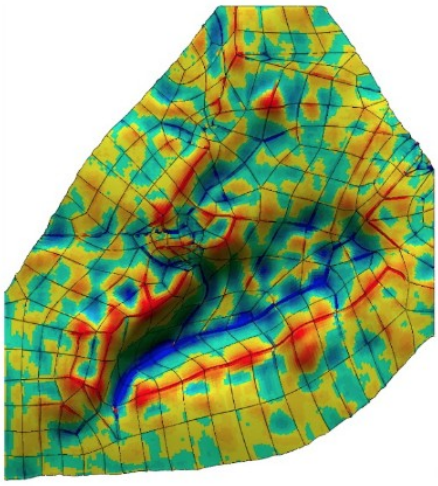

- ○ Trauma
- ○ Heat

Is this a trauma fracture or heat fracture?

* Remember the basics of fracture differentiation: For traumatic fractures, you will typically see a double reverse curvature and a wide variation in color. This can be indicated by waves of color or a bubbled, rough looking surface. In some instances, there is minor reversal of color noted by and island of color change as seen in example 3. There is also a wide variation in color, scaling from dark red to orange, yellow, light blue, and finally to dark blue along the fracture walls and within the fracture itself. In heat fractures, there is no double reverse curvature and a drastic change from dark red to dark blue, or vice versa as seen in example 4. You may also see a pinching of colors at the base of the fracture as evident in example 5.

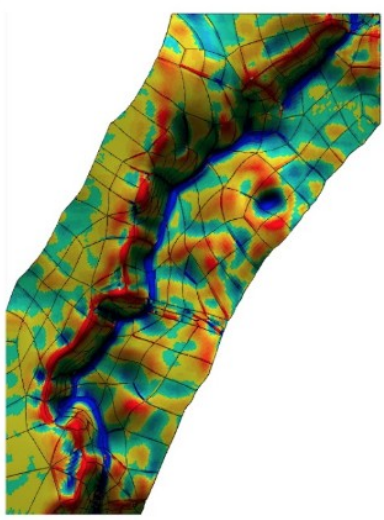

- ○ Trauma
- ○ Heat

Is this a trauma fracture or heat fracture?

* Remember the basics of fracture differentiation: For traumatic fractures, you will typically see a double reverse curvature and a wide variation in color. This can be indicated by waves of color or a bubbled, rough looking surface. In some instances, there is minor reversal of color noted by and island of color change as seen in example 3. There is also a wide variation in color, scaling from dark red to orange, yellow, light blue, and finally to dark blue along the fracture walls and within the fracture itself. In heat fractures, there is no double reverse curvature and a drastic change from dark red to dark blue, or vice versa as seen in example 4. You may also see a pinching of colors at the base of the fracture as evident in example 5.

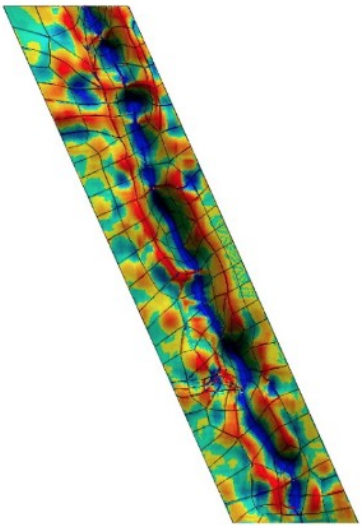

- ○ Trauma
- ○ Heat

Is this a trauma fracture or heat fracture?

* Remember the basics of fracture differentiation: For traumatic fractures, you will typically see a double reverse curvature and a wide variation in color. This can be indicated by waves of color or a bubbled, rough looking surface. In some instances, there is minor reversal of color noted by and island of color change as seen in example 3. There is also a wide variation in color, scaling from dark red to orange, yellow, light blue, and finally to dark blue along the fracture walls and within the fracture itself. In heat fractures, there is no double reverse curvature and a drastic change from dark red to dark blue, or vice versa as seen in example 4. You may also see a pinching of colors at the base of the fracture as evident in example 5.

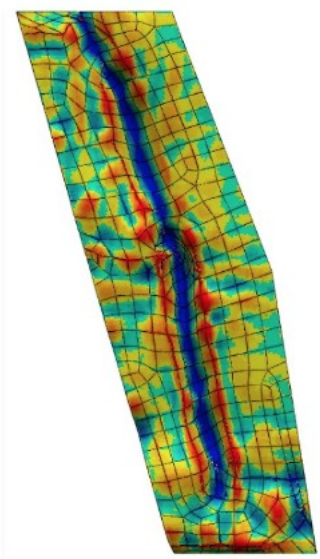

- Trauma
- Heat

Is this a trauma fracture or heat fracture?

* Remember the basics of fracture differentiation: For traumatic fractures, you will typically see a double reverse curvature and a wide variation in color. This can be indicated by waves of color or a bubbled, rough looking surface. In some instances, there is minor reversal of color noted by and island of color change as seen in example 3. There is also a wide variation in color, scaling from dark red to orange, yellow, light blue, and finally to dark blue along the fracture walls and within the fracture itself. In heat fractures, there is no double reverse curvature and a drastic change from dark red to dark blue, or vice versa as seen in example 4. You may also see a pinching of colors at the base of the fracture as evident in example 5.

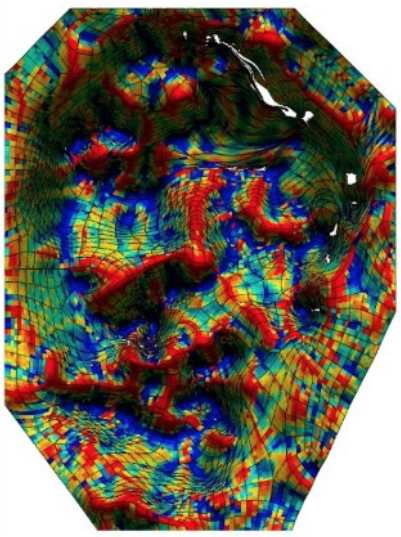

- Trauma
- Heat

Is this a trauma fracture or heat fracture?

* Remember the basics of fracture differentiation: For traumatic fractures, you will typically see a double reverse curvature and a wide variation in color. This can be indicated by waves of color or a bubbled, rough looking surface. In some instances, there is minor reversal of color noted by and island of color change as seen in example 3. There is also a wide variation in color, scaling from dark red to orange, yellow, light blue, and finally to dark blue along the fracture walls and within the fracture itself. In heat fractures, there is no double reverse curvature and a drastic change from dark red to dark blue, or vice versa as seen in example 4. You may also see a pinching of colors at the base of the fracture as evident in example 5.

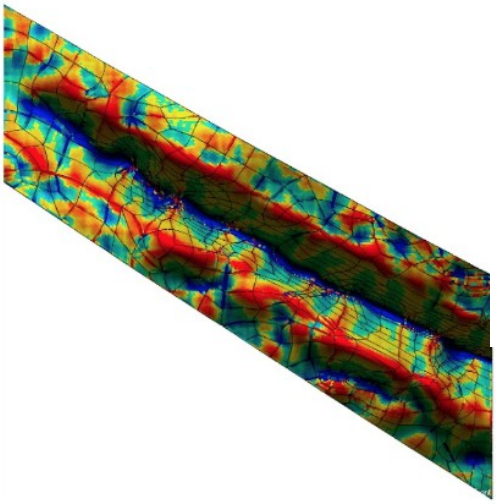

- Trauma
- Heat

Is this a trauma fracture or heat fracture?

* Remember the basics of fracture differentiation: For traumatic fractures, you will typically see a double reverse curvature and a wide variation in color. This can be indicated by waves of color or a bubbled, rough looking surface. In some instances, there is minor reversal of color noted by and island of color change as seen in example 3. There is also a wide variation in color, scaling from dark red to orange, yellow, light blue, and finally to dark blue along the fracture walls and within the fracture itself. In heat fractures, there is no double reverse curvature and a drastic change from dark red to dark blue, or vice versa as seen in example 4. You may also see a pinching of colors at the base of the fracture as evident in example 5.

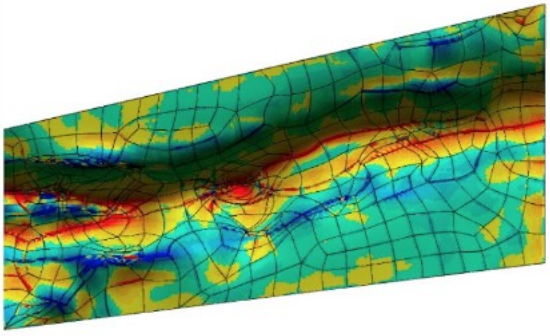

- Trauma
- Heat

Is this a trauma fracture or heat fracture?

* Remember the basics of fracture differentiation: For traumatic fractures, you will typically see a double reverse curvature and a wide variation in color. This can be indicated by waves of color or a bubbled, rough looking surface. In some instances, there is minor reversal of color noted by and island of color change as seen in example 3. There is also a wide variation in color, scaling from dark red to orange, yellow, light blue, and finally to dark blue along the fracture walls and within the fracture itself. In heat fractures, there is no double reverse curvature and a drastic change from dark red to dark blue, or vice versa as seen in example 4. You may also see a pinching of colors at the base of the fracture as evident in example 5.

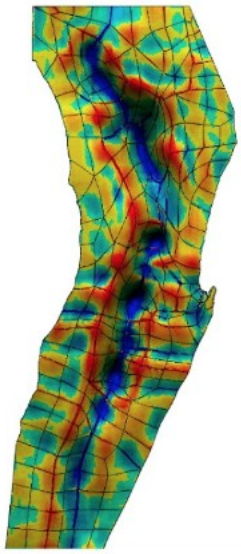

- Trauma
- Heat

Is this a trauma fracture or heat fracture?

* Remember the basics of fracture differentiation: For traumatic fractures, you will typically see a double reverse curvature and a wide variation in color. This can be indicated by waves of color or a bubbled, rough looking surface. In some instances, there is minor reversal of color noted by and island of color change as seen in example 3. There is also a wide variation in color, scaling from dark red to orange, yellow, light blue, and finally to dark blue along the fracture walls and within the fracture itself. In heat fractures, there is no double reverse curvature and a drastic change from dark red to dark blue, or vice versa as seen in example 4. You may also see a pinching of colors at the base of the fracture as evident in example 5.

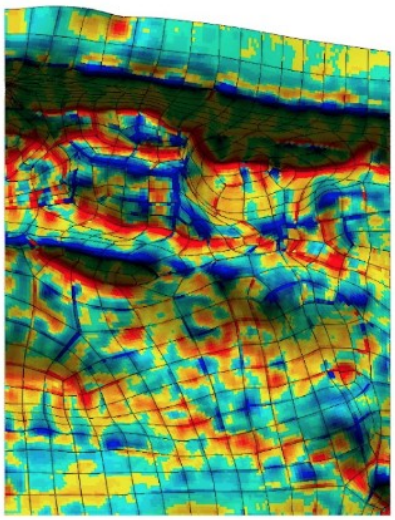

- Trauma
- Heat

‘

Is this a trauma fracture or heat fracture?

* Remember the basics of fracture differentiation: For traumatic fractures, you will typically see a double reverse curvature and a wide variation in color. This can be indicated by waves of color or a bubbled, rough looking surface. In some instances, there is minor reversal of color noted by and island of color change as seen in example 3. There is also a wide variation in color, scaling from dark red to orange, yellow, light blue, and finally to dark blue along the fracture walls and within the fracture itself. In heat fractures, there is no double reverse curvature and a drastic change from dark red to dark blue, or vice versa as seen in example 4. You may also see a pinching of colors at the base of the fracture as evident in example 5.

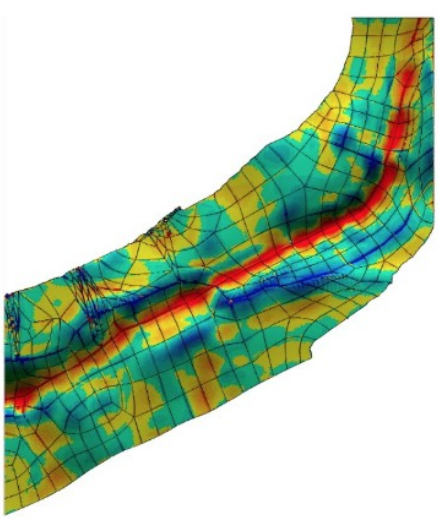

- Trauma
- Heat

Is this a trauma fracture or heat fracture?

* Remember the basics of fracture differentiation: For traumatic fractures, you will typically see a double reverse curvature and a wide variation in color. This can be indicated by waves of color or a bubbled, rough looking surface. In some instances, there is minor reversal of color noted by and island of color change as seen in example 3. There is also a wide variation in color, scaling from dark red to orange, yellow, light blue, and finally to dark blue along the fracture walls and within the fracture itself. In heat fractures, there is no double reverse curvature and a drastic change from dark red to dark blue, or vice versa as seen in example 4. You may also see a pinching of colors at the base of the fracture as evident in example 5.

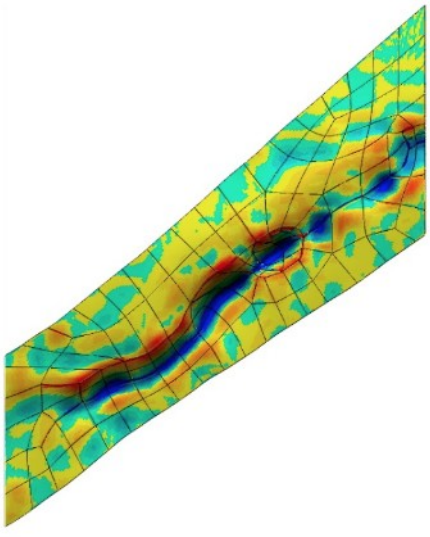

- Trauma
- Heat

Is this a trauma fracture or heat fracture?

* Remember the basics of fracture differentiation: For traumatic fractures, you will typically see a double reverse curvature and a wide variation in color. This can be indicated by waves of color or a bubbled, rough looking surface. In some instances, there is minor reversal of color noted by and island of color change as seen in example 3. There is also a wide variation in color, scaling from dark red to orange, yellow, light blue, and finally to dark blue along the fracture walls and within the fracture itself. In heat fractures, there is no double reverse curvature and a drastic change from dark red to dark blue, or vice versa as seen in example 4. You may also see a pinching of colors at the base of the fracture as evident in example 5.

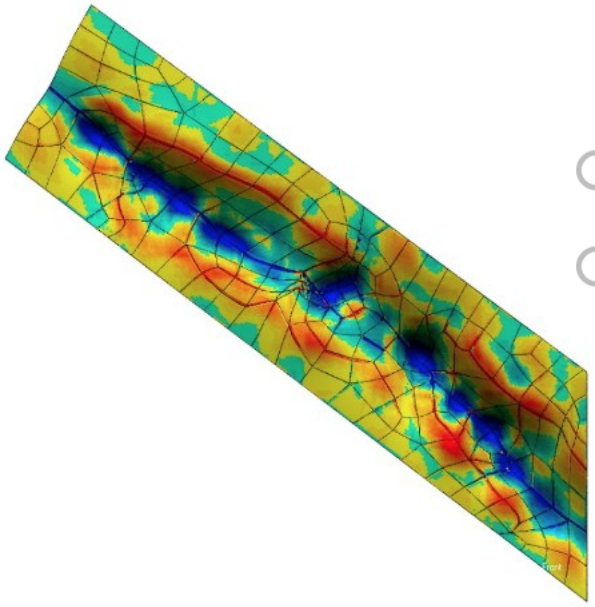

- Trauma
- Heat

Is this a trauma fracture or heat fracture?

* Remember the basics of fracture differentiation: For traumatic fractures, you will typically see a double reverse curvature and a wide variation in color. This can be indicated by waves of color or a bubbled, rough looking surface. In some instances, there is minor reversal of color noted by and island of color change as seen in example 3. There is also a wide variation in color, scaling from dark red to orange, yellow, light blue, and finally to dark blue along the fracture walls and within the fracture itself. In heat fractures, there is no double reverse curvature and a drastic change from dark red to dark blue, or vice versa as seen in example 4. You may also see a pinching of colors at the base of the fracture as evident in example 5.

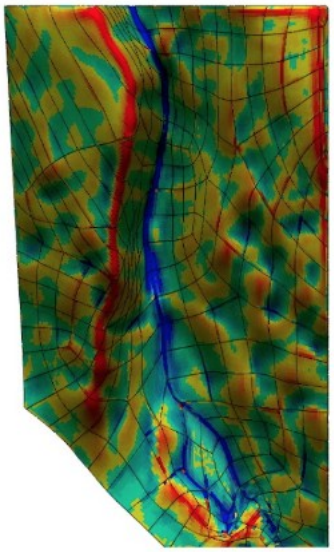

- Trauma
- Heat

Is this a trauma fracture or heat fracture?

* Remember the basics of fracture differentiation: For traumatic fractures, you will typically see a double reverse curvature and a wide variation in color. This can be indicated by waves of color or a bubbled, rough looking surface. In some instances, there is minor reversal of color noted by and island of color change as seen in example 3. There is also a wide variation in color, scaling from dark red to orange, yellow, light blue, and finally to dark blue along the fracture walls and within the fracture itself. In heat fractures, there is no double reverse curvature and a drastic change from dark red to dark blue, or vice versa as seen in example 4. You may also see a pinching of colors at the base of the fracture as evident in example 5.

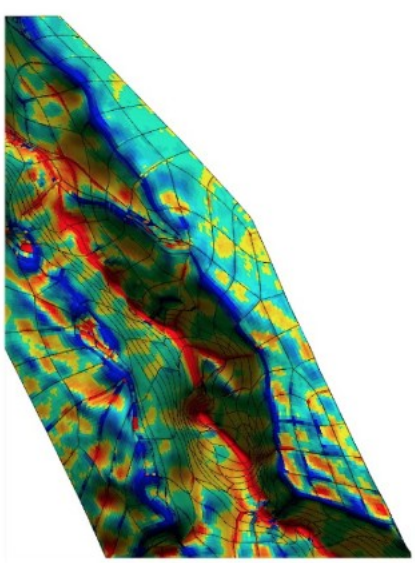

- Trauma
- Heat

Is this a trauma fracture or heat fracture?

* Remember the basics of fracture differentiation: For traumatic fractures, you will typically see a double reverse curvature and a wide variation in color. This can be indicated by waves of color or a bubbled, rough looking surface. In some instances, there is minor reversal of color noted by and island of color change as seen in example 3. There is also a wide variation in color, scaling from dark red to orange, yellow, light blue, and finally to dark blue along the fracture walls and within the fracture itself. In heat fractures, there is no double reverse curvature and a drastic change from dark red to dark blue, or vice versa as seen in example 4. You may also see a pinching of colors at the base of the fracture as evident in example 5.

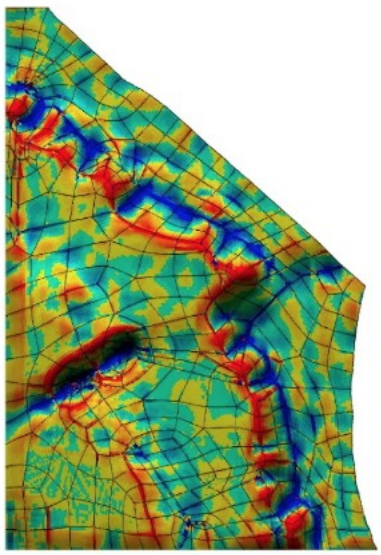

- Trauma
- Heat

Is this a trauma fracture or heat fracture?

* Remember the basics of fracture differentiation: For traumatic fractures, you will typically see a double reverse curvature and a wide variation in color. This can be indicated by waves of color or a bubbled, rough looking surface. In some instances, there is minor reversal of color noted by and island of color change as seen in example 3. There is also a wide variation in color, scaling from dark red to orange, yellow, light blue, and finally to dark blue along the fracture walls and within the fracture itself. In heat fractures, there is no double reverse curvature and a drastic change from dark red to dark blue, or vice versa as seen in example 4. You may also see a pinching of colors at the base of the fracture as evident in example 5.

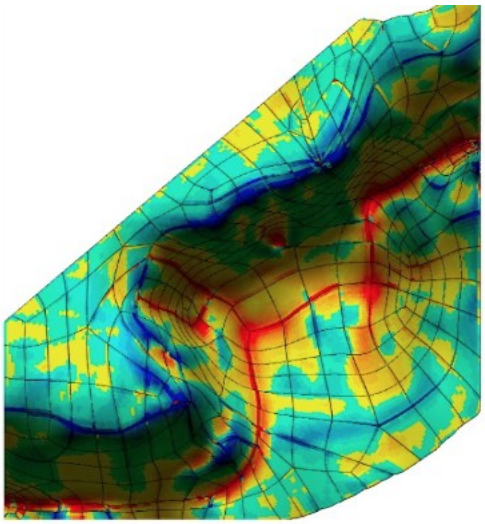

- ○ Trauma
- ○ Heat

Is this a trauma fracture or heat fracture?

* Remember the basics of fracture differentiation: For traumatic fractures, you will typically see a double reverse curvature and a wide variation in color. This can be indicated by waves of color or a bubbled, rough looking surface. In some instances, there is minor reversal of color noted by and island of color change as seen in example 3. There is also a wide variation in color, scaling from dark red to orange, yellow, light blue, and finally to dark blue along the fracture walls and within the fracture itself. In heat fractures, there is no double reverse curvature and a drastic change from dark red to dark blue, or vice versa as seen in example 4. You may also see a pinching of colors at the base of the fracture as evident in example 5.

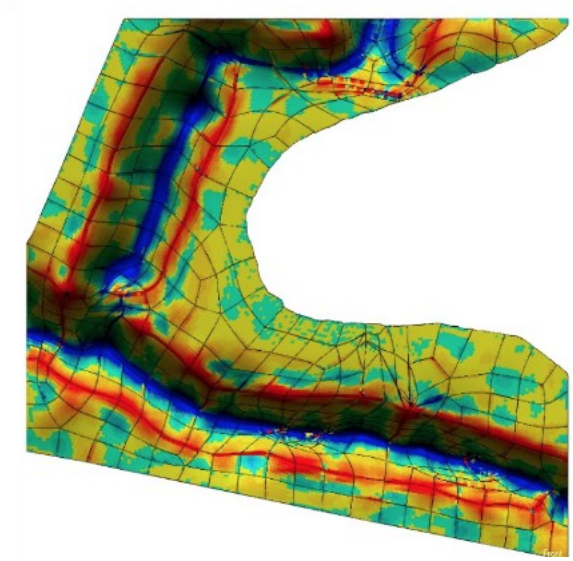

- ○ Trauma
- ○ Heat

Is this a trauma fracture or heat fracture?

* Remember the basics of fracture differentiation: For traumatic fractures, you will typically see a double reverse curvature and a wide variation in color. This can be indicated by waves of color or a bubbled, rough looking surface. In some instances, there is minor reversal of color noted by and island of color change as seen in example 3. There is also a wide variation in color, scaling from dark red to orange, yellow, light blue, and finally to dark blue along the fracture walls and within the fracture itself. In heat fractures, there is no double reverse curvature and a drastic change from dark red to dark blue, or vice versa as seen in example 4. You may also see a pinching of colors at the base of the fracture as evident in example 5.

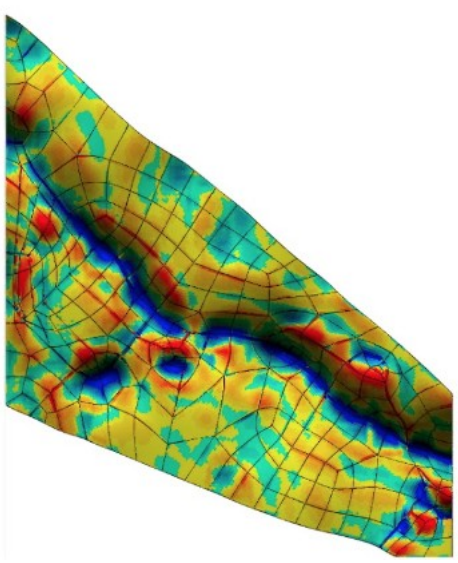

- ○ Trauma
- ○ Heat

Is this a trauma fracture or heat fracture?

* Remember the basics of fracture differentiation: For traumatic fractures, you will typically see a double reverse curvature and a wide variation in color. This can be indicated by waves of color or a bubbled, rough looking surface. In some instances, there is minor reversal of color noted by and island of color change as seen in example 3. There is also a wide variation in color, scaling from dark red to orange, yellow, light blue, and finally to dark blue along the fracture walls and within the fracture itself. In heat fractures, there is no double reverse curvature and a drastic change from dark red to dark blue, or vice versa as seen in example 4. You may also see a pinching of colors at the base of the fracture as evident in example 5.

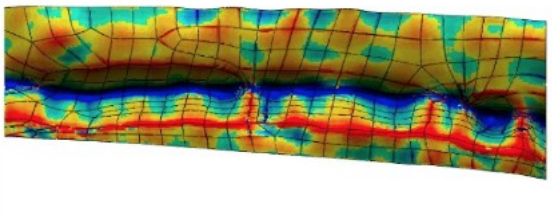

- ○ Trauma
- ○ Heat

Is this a trauma fracture or heat fracture?

* Remember the basics of fracture differentiation: For traumatic fractures, you will typically see a double reverse curvature and a wide variation in color. This can be indicated by waves of color or a bubbled, rough looking surface. In some instances, there is minor reversal of color noted by and island of color change as seen in example 3. There is also a wide variation in color, scaling from dark red to orange, yellow, light blue, and finally to dark blue along the fracture walls and within the fracture itself. In heat fractures, there is no double reverse curvature and a drastic change from dark red to dark blue, or vice versa as seen in example 4. You may also see a pinching of colors at the base of the fracture as evident in example 5.

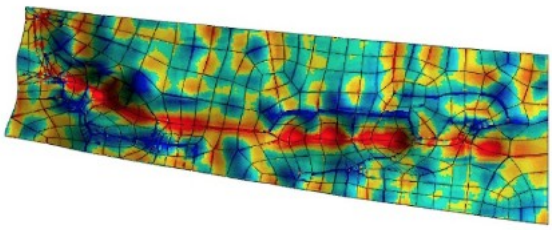

- ○ Trauma
- ○ Heat

Is this a trauma fracture or heat fracture?

* Remember the basics of fracture differentiation: For traumatic fractures, you will typically see a double reverse curvature and a wide variation in color. This can be indicated by waves of color or a bubbled, rough looking surface. In some instances, there is minor reversal of color noted by and island of color change as seen in example 3. There is also a wide variation in color, scaling from dark red to orange, yellow, light blue, and finally to dark blue along the fracture walls and within the fracture itself. In heat fractures, there is no double reverse curvature and a drastic change from dark red to dark blue, or vice versa as seen in example 4. You may also see a pinching of colors at the base of the fracture as evident in example 5.

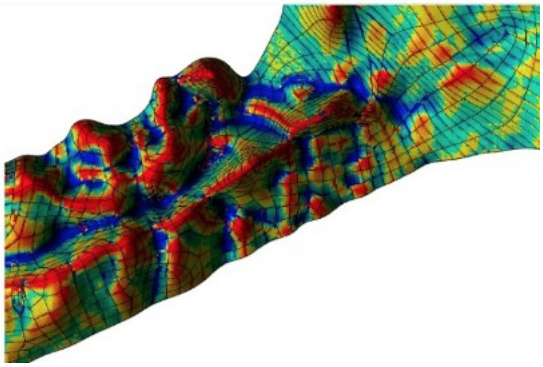

- ○ Trauma
- ○ Heat

Is this a trauma fracture or heat fracture?

* Remember the basics of fracture differentiation: For traumatic fractures, you will typically see a double reverse curvature and a wide variation in color. This can be indicated by waves of color or a bubbled, rough looking surface. In some instances, there is minor reversal of color noted by and island of color change as seen in example 3. There is also a wide variation in color, scaling from dark red to orange, yellow, light blue, and finally to dark blue along the fracture walls and within the fracture itself. In heat fractures, there is no double reverse curvature and a drastic change from dark red to dark blue, or vice versa as seen in example 4. You may also see a pinching of colors at the base of the fracture as evident in example 5.

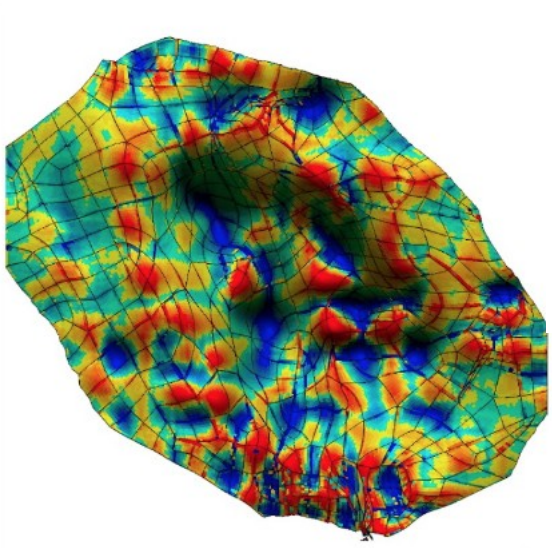

- ○ Trauma
- ○ Heat

Chapter 5: Technical Note: Virtual Reconstruction and Identification of Traumatic Fractures and Heat Fractures[6]

5.1 Introduction

Skeletal analysis in forensic and archaeological cases is crucial to writing an osteobiography. These reports include trauma analysis that attempts to determine if injuries are antemortem, perimortem, and postmortem. Fracture analysis is a major component of this, as fractures can be broken down into the aforementioned categories. Antemortem injuries will show signs of healing, a callus or line on the bone where the injury occurred (Kimmerle and Baraybar 2008). These injuries occur prior to death and with no direct relation to the cause of death (Kimmerle and Baraybar 2008). Postmortem injuries are distinguished by taphonomic processes, such as sun bleaching, water erosion, fire exposure, carnivore tooth marks, root etching, and breakage (Dupras and Schultz 2014, Klepinger 2006, Mayne Correia 1997).

Perimortem fractures, on the other hand, are more complicated. They show no signs of healing or new bone growth around areas of damage (Dzierzykray-Rogalski 1967, Herrmann 1977, Mayne Correia 1997). The main difference between postmortem and perimortem injuries is that perimortem trauma shows collagen bounce-back, or elasticity in response to deformation of the bone (Klepinger 2006). These fractures can be caused by sharp force trauma or blunt force trauma, sometimes a combination of both; however, since these fractures occur around the time of death, there is no definitive way to determine whether the injury occurred before or after death. This is important because when injury times overlap, there needs to be a way to distinguish them. This is incredibly crucial in cases involving cremation.

In forensic investigations, accidental fires can result in cremated remains. In other instances, fire can be used as an attempt to hide another crime. In the latter situations, it is imperative to be able to differentiate perimortem fractures from those caused by heat. As of yet, there is limited research on the identification and differentiation of the two. Mayne (1990) worked on identifying pre-cremation trauma in cremated animal long bones, showing how animal long bones break down post traumatization and under duress of heat. Furthermore, research involved on cremated remains

[6] A version of this chapter is ready for submission for publication to the Journal of Forensic Sciences.

typically revolves around long bones – there is limited research on how heat impacts irregular bones such as the cranium and os coxa (Pope and Smith 2004). Other authors discuss cranium destruction as heat alters remains, but do not discuss trauma degradation (Baby 1954, Bohnert *et al.*, 1997, Dokládal 1971, Fairgrieve and Molto 1994, Holland 1989).

Traditionally, research uses human or animal long bones in place of irregular bones, especially with regards to cremation studies. This includes looking at where the main fractures stem from and how they move across the bone. Longitudinal fractures along the main axis of the bone, as well as curved and straight transverse fractures, are seen on long bones (Baby 1954, Binford 1963). Traumas, which can be intermingled, are broken down into sharp and blunt force trauma (see Chapters 1.3, 1.4, 2.3.1, 4.1.1, and 4.1.2 for more detailed information). These different types of trauma can be seen post cremation in many instances. The larger question at hand is how do these two types of fractures interact on irregular bones and how can they be distinguished?

Reverse engineering technologies can help to improve the ability to differentiate perimortem trauma from heat fractures. This study's results show discernable differences in traumatic fractures and heat fractures via 3D modeling. Using virtual reconstruction of perimortem trauma fractures and heat fractures can assist in sorting fracture types found on cremated remains. The 3D models based off depth analysis scans show distinct patterns in the floors and walls of different fracture types. Due to the limited information on how perimortem trauma fractures break down on irregular bones once exposed to heat, this work was done on calottes and hemipelves.

5.2 Materials

The University of Alberta Anatomical Gifts Program (AGAP) generously donated five human calottes and five human hemipelves to this project (University of Alberta Research Ethics Management Online file No. Pro00070625). One female and four males were selected based on health and age criteria. All individuals were chosen based on the lack of pathological diseases that would impede this study, other than natural skeletal age markers, such as osteoporosis. The ages ranged from 77 years to 86 years old. No other information on these individuals was given.

The calottes were free of soft tissues when taken from cadavers due to medical dissections that had previously taken place. The hemipelves, however, had to be dissected from the individuals. Scalpels and medical scissors were used to remove flesh, musculature, and ligaments. Some tissues were left on as to not mark the bone with dissection tools. A band saw was then used to separate the

hemipelvis from the ischium and lower portion of the ilium, as well as the sacrum and femoral head. Aside from autopsy marks on the calottes and saw marks on the lower hemipelvis boarders, no other trauma markers were noted on the remains.

5.3 Methods

The remains were transferred to the Office of the Chief Medical Examiner where one calotte and one hemipelvis were left undamaged. Two calottes and two hemipelves were then exposed to sharp force trauma via a 10 inch chef's knife. The SFT includes stab and slash wounds. The other two calottes and hemipelves were bludgeoned with a tire iron, producing BFT. The remains were then transferred to a local crematorium where they were burned between 350°C and 550°C for just over 6 minutes. All remains were left to cool overnight, divided into piles representative of each respective individual. When necessary, remains were glued back together with common, dissolvable white glue.

The remains were all placed under a Keyence VHX-2000 microscope for depth analysis photography, with automatic adjustments to view the lowest and highest points of the fracture walls. Portions of fractures were magnified between 20x and 50x, depending on the visibility and depth of the fracture. The Keyence VHX-2000 displays captured 2D images in a 3D manner, allowing for a full analysis of the depth, width, and characteristics of each fracture type. The microscopes camera was then auto-focused and the 3D depth up function was accessed once the lowest visible level of the fracture was found. 3D depth analysis was manually stopped when the top of the fracture was in focus on the camera. The Keyence WHX-2000 automatically creates 3D images at this point, as color models highlighting various depths in different colors. The point clouds for each image were exported as .csv files from the Keyence VHX-2000.

Further analysis was carried out by Geomagic Studio and Geomagic Design X software packages used for engineering, taking 3D data from premade scans and allowing for reverse engineering analyses through the creation of 3D models. Courtesy of Dr. Samer Adeeb and Devon Stone, B.Sc., CAD models were then created using various software programs to further analyze the fracture walls and floors, with curvature analysis and pattern recognition. Geomagic created CAD models which process point clouds, allowing for mesh editing, polygon manipulation, and model manipulation (Geomagic Design X 64). Individually, each .csv file was uploaded to Geomagic Studio 2014. Geomagic converted the point clouds into polygon models which could be manipulated to show high end virtual scans of the original files. The point clouds were formatted so the X coordinates

occupied the first column of the .csv file, with the corresponding Y and Z coordinates occupying the second and third columns, respectively. These files were imported into Geomagic Studio 2014 (Geomagic®, Morrisville, North Carolina; USA) with a 100% sample rate. Once imported, each .csv file underwent surface wrapping via the wrap command, with the Performance-Quality slider set all the way to "Quality." If holes were present in the model, the "fill holes by curvature option" under the Polygons ribbon was used to re-render the information and fill the holes. The images were saved as .stl binary files. The .stl files were uploaded to Geomagic Design X 2016 (Geomagic®, Morrisville, North Carolina; USA), where each polygon object was created into a NURBS (non-uniform rational basis spline) surface. NURBS are used by computers graphics programs to generate curvature analysis on surfaces of models. Each model was then converted to an exact surface by using the Auto-surface function, where each model was auto-surfaced using a mechanical mesh, auto-estimated patch count method, and an adaptive fitting method with the fitting options slider set to "Maximum Geometry Capture Accuracy." Afterwards, the Accuracy Analyzer™ tool was used to display the surface curvatures. The resulting curvature color maps (CCM's) can then be used for analysis.

Aside from qualitative work, this research attempted to gather quantitative data. To do so, 2D curves were placed perpendicular to the fractures throughout the models. This was done to best fit as fracture lines are not straight. To do so, "Create Curves" was selected under the Curves ribbon, creating cross-sectional curves across the traumatic and heat fractures. The "Sections" and "Spacing" dialogue boxes were used to create 15 planes with 300 μm spacing. Screen captures were taking using the "Capture Graphics Only Function" under the Tools ribbon, ensuring that the image captured was perpendicular with the curves so the parallax was minimized. The curves were isolated from the models and the slope of the curvatures was visually analyzed; however, when separated from their 3D counterparts, the 2D models were indiscernible from one another. There was no way to distinguish trauma fractures from heat fractures from the 2D curve models alone. More research needs to be done in this area to produce quantitative data. This is necessary in order to positively identify perimortem trauma fractures from heat fractures.

5.4 Results

Based on the images alone, qualitative analysis show direct differences in traumatic fractures from heat fractures. For purposes of differentiation, traumatic fractures have been broken down into two categories: point of impact and residual fractures from force dispersal. The images showing point of impact are known to have a reverse double curvature where the color gradient travels from red to

dark blue, showing the color scale in between. This pattern repeats itself where the colors will reverse and reoccur between the fracture walls. In shallow trauma points of impact, from a knife tip for example, a clear rough surface is noted, showing a vast display of colors hitting peaks and valleys. In more shallow trauma fractures, or those resulting from expelling force across the bone, a distinct reverse double curvature may or may not be seen. What is key to look for in these fractures are the way the color gradient is projected. A larger gradient scale, showing gradual changes from red to dark blue, is consistent with trauma fractures. There are also noted 'islands' in portions of the fractures were a double reverse curvature can indeed be seen. This is not always the case, but is evident in a large portion of the trauma fractures. These methods of recognition are opposite of heat fractures, where the color gradient drastically changes from red to dark blue. There are minimal segments of orange, yellow, and light blue noticed in the fracture walls. At the base of heat trauma fracture walls are pinched portions where it appears the two walls are connected by a thin line of red. This is a distinctive quality in the majority of the heat fractures (see Chapter 4.3 for a more detailed explanation).

Having not known inter-observer error would be integral to validating the CCM's of the models, ethics approval has yet to be given to disseminate the survey (see Chapter 4, Appendix 1). Once ethics approval is granted, we will test the inter-observer error of this study by allowing the general public a chance to look at select models from this study and having them attempt to identify the fractures off of predetermined descriptors. The inter-observer test will utilize novices, trained individuals, and professionals and give them a chance to practice differentiating these fractures. With this test, we can test the applicability of our observations in a practical setting. This is a crucial step in ensuring qualitative data is accurate and repeatable.

5.5 Conclusion

Based off the results generated from this study, it is evident that qualitative analysis alone can be useful at describing the known types of fractures from this study. By giving definitive models with guidelines for how to identify fractures, blunt and sharp force trauma can be distinguished from heat fractures in cases of cremation. Though these images were tested on whole remains, there is no evidence to suggest similar studies on fragmentary remains would differ. This is important because in majority of forensic and archaeological cases, full skeletal remains are not found.

The implications of this research are numerous. Not only does this work pioneer new ways to look at fracture analysis, but it creates a working database in which patterns can be identified and

linked to direct types of fractures, i.e. trauma or heat. Future researchers can continue to build this repertoire by using the same process in attempt to distinguish various types of sharp force trauma from one another, or blunt force trauma. The research could potentially be used to catalogue bite mark differences left on bone from scavenging, or even pathological diseases. Using this method of analysis opens new avenues of research that could further enhance how forensic anthropologists look at fractures and damage to skeletal remains. Not only can general blunt force trauma and sharp force trauma be looked at, but more in-depth characteristics of specific implements can be viewed and analyzed. In addition to this, fractures on compact bone of humans and animals can be examined to further back up the results from this study. It is possible to even look at pathologies noted on human and animal remains, or taphonomic changes by means of scavenging to differentiate animal gnaw marks. The work done in this study is only the beginning of where this methodology can be used to further research within the field of anthropology. A working database cataloging how different traumas, fracture types, etc. look based on virtual recreations could lead to a new way of identifying perimortem and postmortem damage to human remains in both forensic and archaeological settings.

Chapter 6: Conclusions

After reviewing the information provided in this thesis, it is critical to reconsider the discussion in chapter one. The goal of this research was to discern a method to differentiate perimortem trauma fractures from heat fractures in cases of cremation involving crania and irregular bones. The analysis shows that it is possible to use qualitative data from multiple fractures to discern the two. These observations and new methods using advanced technologies are imperative to advancing the study around cremated remains.

The majority of the research surrounding heat fractures relies on data collected from long bones. This is illustrated by the lack of information in the literature about fracture identification on cranial and irregular bones. In cases involving human skeletal remains, a forensic anthropologist must be able to create the most full and accurate osteobiography possible. In part, this entails listing any evidence of trauma and taphonomy. Trauma and taphonomy have been well studied for the most part; however, animal remains are frequent substitutions for human remains in experiments to further these studies. When human remains are used, the bulk of research is done on long bones. Animal crania or human long bones are not interchangeable substitutes with human crania and irregular bones.

In order to clarify, a review of information from Chapter 1 is required. As a community of anthropologists, scientists, and medico-legal investigators, it is important to understand that bones are structurally different based on species and bone type, i.e. long bones, cranial bones, or irregular bones. Substituting one for another is not always acceptable because there are vast differences between the categories aforementioned. In utero, bones are developed through intramembranous and endochondral ossification. Cortical bone of long bones develop via intramembranous ossification – perichondral – which is derived from mesenchymal origin. The cancellous center is also mesenchymal in origin, but comes from endochondral ossification. The cortical portions of cranial bones develop from endochondral ossification and intramembranous – perichondral ossification. This varies based on the type of cranial bone, i.e. flat bone or smaller bones of the face. The diploic center is intramembranous in origin, however, it is dermal in nature, not perichondral. Diplöe comes from neural crest cell origins as a protective maneuver to the developing brain case. This creates a thin, protective layer to the developing embryo. The combination of intramembranous ossification and endochondral ossification allows cranial and irregular bones to react differently to onset forces because they are structurally different. Instead of breaking down in zones like long bones, cranial and irregular

bones become largely deformed as they compress together because of their thinner cortical layer in relation to the diploic (cranial bone) and trabecular (irregular bone) portions.

The basic multicellular units of bone help to give bone its lightweight, yet strong structure. Identifying differences between long bones, cranial bones, and irregular bones is the first aspect that needs to be discussed. Long bones, comprised mostly of cortical bone, are arranged via lamellae, composed of minerals, and collagen fibrils laid down in adjacent sublayers. This creates a stable plywood structure to help hinder crack propagation throughout daily wear of bones. The lamellar bone is arranged around Haversian canals, Volkmann's canals, lacunae, and canaliculi to allow for proper vascularization and nutrient flow. This bone is constantly being remodeled by osteoblasts and osteoclasts to ensure the bone is metabolically sound and maintained throughout life. In the medullary cavity of long bones lies trabecular bone, which is less organized and more haphazard in nature. The bony spicules of trabecular bone is comprised of hydroxyapatite crystals and organic collagen proteins, like cortical bone. Trabeculae, however, allows bones to remain lightweight and flexible in nature.

This more rigid, cylindrical structure is vastly different from the biomechanical structure of cranial bones and irregular bone. Cranial bone and irregular bone, much like long bones, have a distinctive layer of cortical bone. However, in cranial and irregular bones, the cortical bone is much thinner in ratio to the spongy bone center. In crania, the large, flat bones are composed in a sandwich like structure with an inner and outer cortical bone layer, filled with a diploic center. The diplöe acts like trabecular bone but is only found in the bones of the cranium. Diplöe is highly vascularized and more dense than typical trabecular bone. Irregular bones, which have an even thinner layer of cortical bone, are filled with thick section of trabecular bone. These bones are extremely lightweight in nature.

Knowing the embryological and structural differences of various bone types gives context to fracture mechanics which need to be well understood. Long bones can deflect fractures via the plywood model. The lamellar fibrils are bonded together via a natural organic matrix, which helps to propagate outside forces and redirect them elsewhere. Being hypertrophic, bone has to ability to regrow and remodel as stressors are applied. Long bones break down as the stress/strain yield is reached and plastic deformation occurs. These final stressors break the bone as the molecular bonds that hold the bone together are broken. Crack tips, caused from a fail point being reached, advance throughout the lamellar bone structure and circumnavigate osteons, instead travelling along cement

lines. This is done in attempt to stop the crack tip from further advancing. Once plastic deformation is reached, however, the bones overall ability to absorb and reduce the force is hindered.

Cranial and irregular bones fracture differently from long bones. In cranial bones, depending on the type of fracture witnessed, the bone will react in different ways. Linear fractures react by following the path of least resistance and can form either a straight line or result in radiating/concentric fractures. Diastatic fractures work like linear fractures but are frequently pushed into sutural lines. Depression fractures cause the inner and outer tables of bone to collapse and radiating fracture to grow from site. Stellate fractures form like depression fractures but cause a star-like depression instead of a hole. Finally, comminuted fractures form like stellate fractures but produce heavy fragmentation and circular fractures around the point of impact. In all cases, the diploic bone attempts to redistribute forces applied throughout the crania to minimize damage. Irregular bones are theorized to fracture in similar ways, however, instead of compressing the inner and outer tables of bone, general depressions are created that collapse the trabecular structure and the encompassing cortical bone layer.

Trauma, responsible for causing fractures and plastic deformation, is broken down into two sub categories: sharp force trauma (SFT) and blunt force trauma (BFT). Sharp force trauma is classified by objects that chop, cut, incise, or puncture tissues. Different bone types, i.e. long bones, cranial bones, and irregular bones, show sharp force trauma differently based on the overall thickness of the bone. For example, a knife is more likely to pierce all the way through cranial bone than it is a long bone when used in a stabbing motion. Blunt force trauma, on the other hand, is categorized via the use of a wide implement that crushes or tears the bone, collapsing the overall structure. Again, depending on the type of bone used and the force, varying levels of damage will occur. An example of this is the trauma left behind by the tire iron in this experiment. In the calottes, the inner and outer tables collapsed causing depression fractures. There are distinctive holes in the bones. On the hemipelves, however, though the bone is thinner and a hole was created, there are many more radiating and circumferential fractures around the point of impact. It should be noted that both types of trauma can remain visible post burning.

Fracture differentiation is important to gathering more information on the types of trauma seen, and understanding what structural properties of each bone type leads to failure is also critical. However, when heat is introduced, there are more complications. Understanding fully how the

fracture mechanics of burned bone work is important to understanding why and how fracture differentiation of perimortem trauma fracture and heat fractures can be determined. Heat impacts bones via breaking down the basic molecular units of bone. Burned bone does not have the interstitial fluid or responsive osteocytes to signal bone to react to fractures – there is simply no way for the bone to deflect fracture propagation. Long bones break down by zones, starting in the metaphyseal portions and working down the diaphysis. There is rarely any trabecular bone left and only a thin shell of cortical bone. The breakdown of long, cranial and irregular bones depends on the amount of insulative fats, muscles, and ligaments that surround them.

It is of importance to note that fracture propagation is different in humans versus animal counterparts as well. The biomechanical structure of animal bones varies greatly across species, especially with respect to Haversian canal size, osteonal growth and vascularization. Animal bone structure, unlike human bones, distribute Haversian canal size based on the size and growth of that particular species. This is crucial to understand because a thin section of horse femur, for example, would be drastically different than that of a mouse. In addition, the types of tissues that make up animal bones are referred to as plexiform and woven bone. Plexiform bone is built in a brick wall pattern, which is layered longitudinally around primary osteons. This is vastly different from the human plywood structure. Plexiform bone is also more dense and highly vascularized, constantly being remodeled to accompany animal growth and daily micro-crack repairs. The remodeling of larger animal bones is done at sites of contact, stressors, and cracks; whereas in small animals, most remodeling occurs around ligament and tendon attachment sites. In the medullary cavity and epiphyseal ends lies trabecular bone. This functions very similarly to human cancellous bone.

The trabecular bone of animal crania is different than human diplöe. Animal cranial trabeculae are developed in long lines throughout the three inner layers of bone between the inner and outer tables. This is different from the human counterparts in which diplöe grows in small, dense circles. As mentioned with the trabeculae of animal crania, there are five distinct layers of bone in animal crania: the outer table, three diploic center portions, and an inner table. These inner portions are mostly composed of fibers of cells which connect the periosteum of the outer surface to the periosteum of the inner surface. When sectioned, animal cranial bones show little evidence of the sandwich like structure seen in human crania. Humans are the "unusual animals" in this case. Reasons for this are unknown.

In addition to the bone structural differences, the locomotive qualities needed for animal bones differ from human bones. Animal bones must remodel based on locomotive and mechanical stressors that are applied to the limbs more regularly than human bones. There are constant mineral changes between old animal bone, new growth, and surrounding tissues. This makes the overall remodeling process less efficient than that of human bone. The vascularization and brick wall appearance of animal bones changes the way in which fractures disseminate throughout animal bone. There are more clear-cut paths for fractures to follow, increasing the speed and efficiency of fracture propagation. This, in combination with the overall structural differences noted between human and animal bones, make it difficult to successfully swap animal bones for human bones in forensic recreations. The accuracy of the results will not be as high when the tests are not done on human bone. This complicates the ability for forensic recreations to be done though because fresh human remains are difficult to obtain. Here lies the reason for the preliminary work of this project, testing the viability of formalin fixed cadavers as substitutes for fresh human bone in forensic experiments.

Formalin has been tested in this study to determine the use of medical cadavers in forensic recreations. The chemical is known to react to the lysine of collagen altering the ability for bone tissues to respond to stressors; however, there is no proof that the stiffness of collagen is indeed impacted by formalin. Formalin binds to the basic molecular units of bone, especially hydroxyapatite. In doing so, the underlying minerals of bone are altered and formalin reacts with the ε-amino groups of collagen. Collagen fibrils are noted to enlarge with prolonged exposure to formalin, changing the highly regulated and symmetrical nature of lamellar bone, making it thin and uneven in nature. This causes the bone, on a microscopic level, to appear dehydrated with what appears to be enlarged canaliculi. When this is further impacted with heat, the flammability of formalin needs to be considered. It was hypothesized that formalin's increased flammability would cause rapid bonds with bone mineral content as it evaporates from the bone during the dehydration stage of heat alteration. This would cause an increase in the flash point of formalin fixed remains, but the heating would be the same once the formalin burned off.

To allow easier access to human remains in cases of forensic recreation, this thesis first tested the aforementioned theories and reliability of using formalin fixed cadavers as substitutes for fresh human remains. As of yet, there is limited information as to how formalin impacts the bone structure on a microscopic level. Chapter 2 of this study looks directly at implicating factors around this concept by taking femoral sections from formalin fixed cadavers and burning them. The femoral segments

were taken from an 86 year old male; the sample was divided it into three portions. One portion was left unburned as a control, the other two were burned individually – one at 600°C, the other at 800°C. Once complete, the samples were embedded in an epoxy resin to stabilize the bone structure, as burned bone is extremely fragile. Thin sections were taken of each sample in order to study the histological structure of formalin fixed bone. These were compared to a study involving similar work with non-formalin fixed femoral bone. Microscopically, the histological differences between remains fixed with formalin and not fixed with formalin were null at the 600°C level, but distorted at 800°C. The control samples in each study showed similar results, as did the burn at 600°C. However, the 800°C thin sections from the formalin fixed femoral bone more closely mirrored the histological components of non-formalin fixed bone that was burned at 1000°C. This suggests that the formalin impacts the bone at higher heat rates, potentially due to increased dehydration of the collagen fibrils.

Having accomplished the aforementioned study, it was possible to proceed with using formalin fixed cadavers, assuming the heating process would not exceed 600°C. This was done to ensure the histology and bone structure was not overtly altered to keep the bulk of the study in line with common house fires. Knowing that previous work with regards to cremation largely focuses on animal surrogates or long bones, studying fracture patterning and heat on cranial and irregular bones allows for new techniques of analysis to arise, as well as a greater breadth of information in the areas of cremation and fracture analysis. It is critical to expand upon these concepts, as investigations involving cremated remains is abundant, especially in the modern world as technology is advancing, new warfare techniques are developing, and mass disasters are inevitable given the climate in which we live in. Forensically relevant, it is imperative to better understand trauma on cremated remains and differentiation of fractures because fire is often used to hide evidence of crime. With the cranium being a frequent target of attack in cases of homicide, understanding how cranial bones react to trauma and then heat is important to discerning if foul play is at hand. With regards to irregular bones, there is limited research in this field as a whole, so it is important to assess the variables that alter irregular bones during trauma and heat exposure. The pelvis, for example, is a critical point of analysis for forensic anthropologists to gather information on approximate age and sex of an individual. These traits can be easily skewed by trauma and heat, so understanding how trauma and heat impact the pelvic structure is important.

Chapter 3 discusses this concept in more detail, leading into a greater investigation into fracture differentiation of perimortem trauma fractures and heat fractures. Human remains from the Anatomical Gifts Program (AGP) at the University of Alberta were used for this study; this is the same program that the femoral plugs came from. Five calottes and five hemipelves were harvested and transported to the Office of the Chief Medical Examiner in Edmonton, AB for further analysis. X-rays documenting the remains prior to any trauma or heat exposure were taken in case they were needed for further analysis post cremation. The remains were divided; one of each bone type was left as a control, two of each were bludgeoned with a tire iron to reflect blunt force trauma (BFT), and two of each were stabbed and 'slashed' with a 10 inch chef's knife to represent sharp force trauma (SFT). The remains were then re-x-rayed and taken to a local crematorium for burning. The remains were cremated in a standard cremation oven between the temperatures of 350°C and 550°C for approximately six and a half minutes. They were then removed from the oven and left to mostly cool before being transported back to the University of Alberta. Once cooled completely, the remains were glued with a common white glue to stabilize loose structures.

The remains were then analyzed under a Keyence VHX-2000 microscope. 180 images were taken of trauma and heat fractures. The microscope produced 3D images showing in-depth analysis of the depth of each fracture. These are correlated with color scales to show varying values of different fracture types. The point clouds of each image were exported and turned into .csv files, which were imported into Geomagic Studio. From there, virtual 3D models were created to better understand what differences could be noted between the trauma and heat fractures. The models were then imported into Geomagic Design X, where they underwent an auto-surface program to analyze the curvatures found on each model. This entailed the creation of a color-coordinated map to reflect differences in angulations of fracture walls, as well as the curvature from the outer most layer of bone into the fracture wall. The goal was to determine if different angles or slopes could be noted between the trauma fractures and heat fractures. Qualitatively, the color maps show distinct differences between the two. The brief look into microscopic imaging and high definition curvature analysis is a step towards being able to differentiate trauma fracture from heat fractures on cranial and pelvic bones in cases of cremation. There are definitive patterns that separate trauma points of impact from trauma fractures and heat fractures. Using a predetermined color scale allows for accurate testing and repeatability of this study. Having microscopic qualitative data pushes the study of trauma differentiation in cremated remains in the right direction, though there is still much work to be done.

This research also attempted to extract quantitative data from the models. To do so, curves were placed through the fractures on each model, bisecting them perpendicularly. The curves were then individualized and the slope of each curve was analyzed; however, the curves could not be accurately analyzed, as they were not able to be distinguished from one another when pulled from the original 3D model. This meant it was impossible to differentiate trauma fractures from heat fractures looking at the curves of the fractures alone – this means the color analysis from the qualitative study was a significant contributor to discerning fractures on the presented models. More research in improving this method to produce quantitative data is necessary to make identification of perimortem trauma fractures and heat fractures more accessible to the anthropological and scientific communities.

There are of course limitations to the research. These include, but are not limited to the age of the individuals in this study, as well as the number of samples, and the length of exposure to heat for each sample. Based on the literature review from previous chapters, it is known that as individuals age, their bone structures weaken and the histology changes from primary and secondary osteons, to only secondary osteons. With regards to cranial bones, it is known that the diplöe becomes more haphazard and less dense as individuals age. After reviewing the work done in Chapter 3 comparing the histology of an individuals aged between 50 and 62 and the 86 year old from that study, it can be said that the bone structures were markedly similar. It is important to test how trauma and heat act on younger individuals bone structure – how does the collagen react and what changes are noticed between the younger samples and the older ones of this study?

Although the sample size was limited to only five calottes and five hemipelves, the sample size is valid for this study because 180 fractures were gathered in total for analysis. The division between trauma and heat fractures is skewed because of the control samples. This study leads to a better understanding of how heat fractures work in relation to trauma fractures. It is known that heat fractures form as bone is dehydrated and the histological structure degrades. By having a larger number of heat fractures, more information such as what they look like and how they act on cranial and irregular bones only adds to the literature. With respect to the length of heat exposure, the times selected were based off the work done on the comparative study using non-formalin fixed remains. Though the femoral samples were able to burn for a longer time than the whole calottes and hemipelves, it is critical to note that the femoral samples were merely heated in a furnace, whereas the whole samples were placed under direct fire in a cremation oven. This drastically altered the burn time, however, it was more accurate to heat exposure in house fires.

Knowing bone histology changes under the duress of trauma and heat, it is important to remember how collagen and interstitial fluid act to prevent crack tip propagation. This is evident in the CCM's by the way the color distribution changes in known trauma and heat samples. The CCM's of traumatic fractures reflect the collagen pull-out as the histological microstructure fails under pressure from outside forces. The interstitial fluids force the crack tip along cement lines, leaving a ragged, torn fracture wall. This is noted not only in the slope between the outer bone layer and the fracture walls, but in the uneven surface of the fracture walls. The CCM's of trauma models largely highlight this by showing varied, gradual color changes and waves of color. These "flowing" colors in traumatic CCM's represent the microscopic and histological changes of bone. Heat fractures have drastic color changes because there is no elastic collagen or interstitial fluids to slow the propagation of the crack. There is no stopping or hindering the heat fracture because the bone is turning into a brittle, fragile structure. This allows the slope from the outer layer of bone into the fracture wall to be rigid and smoother in nature, with no waves of color. The one exception is noted by the bridging, or stitched pattern on some of the heat fracture CCM's, theoretically, that were produced as the bone was drying out and stiffening in nature.

This project hypothesized that perimortem trauma could be distinguished from heat fractures in cases of cremation in cranial and irregular bones on a microscopic level. Key components of this included understanding bone elasticity and flexibility prior to cremation, which led to theories about why trauma and heat fractures have distinctive characteristics. This understanding accounted for the previously mentioned research on formalin's impact on bone histology, as well as how cranial and irregular bones differs structurally from human long bones and animal bones. Based on the thinned cortical layer of cranial and irregular bone, a greater rate of bone failure was anticipated. After the above discussion and actualized, noticeable differences on the CCM's and curvature analysis of the 3D models, this research was successful at differentiating perimortem trauma from heat fractures in cases of cremation involving formalin fixed human cranial and irregular bones using this novel method.

The technology that was used during this process, as discussed in Chapter 4, helps to pioneer new methods of investigation for forensic anthropologists. Having the ability to look at fractures on a microscopic level allows for a greater breadth of knowledge to be procured. This study opens new avenues of research by pioneering a new technique for the analysis of fracture differentiation. Though this study focuses on cranial and irregular bones, and a separation of trauma fractures from heat

fractures, it is possible to expand this work. With the technology at hand, a catalogue could be created to describe not only fractures found on cranial bones and the hemipelves, but other irregular bones and long bones. This work can be used as a model to develop definitive differences between various blunt and sharp force implements. It may even be possible to apply this methodology to forms of scavenging, weathering and pathology. The possibilities are endless; this research is just the beginning for in depth fracture analysis.

Having the ability to classify trauma is critical to forensic reports because fractures caused prior to death could give evidence of cause of death or events leading up to death. This is crucial in forensically relevant cases to determine if there was a homicide or if the death was accidental. Being able to create a database filled with curvature analyses of varying fracture types would allow forensic anthropologists to better assess trauma noted on human remains. By being able to follow the technical note (Chapter 5) and recreate this process, forensic anthropologists could potentially speed up the analysis with regards to trauma and produce more accurate assessments. Pioneering a new technique means there is still a lot of work to be done, but understanding the basic concepts that allow the methodology to work will help pave the way for new research to better advance the field.

There is much research that still needs to be done to address the questions that have arisen from this research. It is important to test the technical aspects of this work on long bones to see if similar results are noted, as well as testing other types of trauma. Are the same results being seen? Can the curvature rules and assessments be replicated? It would be interesting to note the variations and implications of using alternative types of bone and trauma in order to enhance and grow this study. Knowing bone structure is different between long bones, cranial, an irregular, can these results be replicated? The future potential for this research, as previously discussed, is vast as there is limited research done in the field of trauma and cremated remains. Providing greater information to forensic anthropologists and the medico-legal community is critical to improve methods of investigation and better answer questions surrounding the implication of heat exposure to human remains. Advancing a new technique takes work, but it is time to further knowledge in this area to create a database that could help forensic anthropologists globally. Problems involving the creation of an osteobiography, specifically with regards to trauma and taphonomy, need to be explored and developed to better provide the anthropological community, as well as the medico-legal community, with tried methods and techniques that are tested and consistent and meet the rigour of the court. Without answers to

questions that arise in these areas, there is no advancement in the field, which only hinders academic and scientific communities.

Bibliography

Anon. Formaldehyde. National Center for Biotechnology Information PubChem Compound Database [Internet]. Available from: https://pubchem.ncbi.nlm.nih.gov/compound/712#section=Flash-Point

Baby, RS. 1954. Hopewell Cremation Practices. Ohio Historical Society Papers in Archaeology, 1, 1-8.

Bajaj, D, Geissler, JR, Allen, MR, Burr, DB, Fritton, J. 2014. The resistance of cortical bone tissue to failure under cyclic loading is reduced with alendronate. Bone, 64, 57- 64.

Beisaw, A.M. 2013. *Identifying and interpreting animal bones: a manual*. College Station: Texas A&M University Press

Berryman, HE, Haun, SJ. 1996. Applying forensic techniques to interpret cranial fracture patterns in an archaeological specimen. International Journal of Osteoarchaeology, 6(1), 2-9.

Binford, LR. 1963. An analysis of cremations from three Michigan sites. Wisconsin Archaeology, 44(2), 98-110.

Bohnert, M, Rost, T, Faller-Marquardt, M, Ropohl, D, Pollak, S. 1997. Fractures of the base of the skull in charred bodies — post-mortem heat injuries or signs of mechanical traumatisation? Forensic Science International, 87(1), 55-62.

Bontrager, AB, Nawrocki SP. 2008. A taphonomic analysis of human cremains from the Fox Hollow Farm serial homicide cite. *In* Schmidt C, Symes S. (eds.), The analysis of burned human remains. Academic Press, London, 229-246.

Boskey, AL, Cohen, ML, Bullough, PG. 1982. Hard tissue biochemistry: A comparison of fresh-frozen and formalin-fixed tissue samples. Calcified Tissue International, 34(1), 328-331.

Cattaneo, C, Dimartino, S, Scali, S, Craig, O, Grandi, M, Sokol, R. 1999. Determining the human origin of fragments of burnt bone: A comparative study of histological, immunological and DNA techniques. Forensic Science International, 102(2-3), 181-191.

Chamay, A, Tschantz, P. 1972. Mechanical influences in bone remodeling. Experimental research on Wolff's law. Journal of Biomechanics, 5(2), 173-180

Chen, J, Liu, C, You, L, Simmons, CA. 2010. Boning up on Wolff's Law: Mechanical regulation of the cells that make and maintain bone. Journal of Biomechanics, 43(1), 108-118.

Corega, C, Vaida L, Ilias T, Bertossi D, Dascălu IT. 2013. Cranial sutures and diploae morphology. Romanian Journal of Morphology and Embryology, 54, 1157-1160.

Crowder, C, Rainwater, CW, Fridie, JS. 2013. Microscopic Analysis of Sharp Force Trauma in Bone and Cartilage: A Validation Study. Journal of Forensic Sciences, 58(5), 1119-1126.

Cunningham, C, Scheuer, L, Black, SM, Christie, A, Liversidge, H. 2016. *Developmental juvenile osteology*. Second Edition. London: Elsevier.

Currey J. 2003. The many adaptations of bone. Journal of Biomechanics, 36, 1487–1495.

De Ricqles, A, Meunier, FJ, Castanet, J, Francillon-Vieillot, H. 1991. Comparative microstructure of bone. Bone, 3, 1-78.

Devlin JB, Herrmann NP. 2013. Taphonomy of Fire. *In* Tersigni-Tarrant MT, Shirley NR (eds). Forensic anthropology: an introduction. Boca Raton: CRC Press/Taylor & Francis Group. 307-323.

Dokládal, M. 1971. A further contribution of the morphology of burned human bones. Anthropologic Congress, Prague and Humpolec, 1969, Prague, Academia, 1971. *In* Novotny, V (ed.) Proceedings of the Anthropological Congress Dedicated to Ales Hrdlicka, 1970, 561-568.

Dupras, TL, Schultz JJ. 2013. Changes in forensic contexts. *In* S.A. Symes and J.T. Pokines (Eds.), Manual of forensic taphonomy. CRC Press: Boca Raton.

Dzierzykray-Rogalski, T. 1967. New methods of investigation of bone remains from cremation graves. Anthropologie, 4, 41-45.

Ellingham, STD, Thompson TJU, Islam, M. 2015. Thermogravimetric analysis of property changes and weight loss in incinerated bone. Palaeogeography, palaeoclimatology, Palaeoecology, 438, 239-244.

Faingold, A, Cohen, SR, Reznikov, N, Wagner, HD. 2013. Osteonal lamellae elementary units: Lamellar microstructure, curvature and mechanical properties. Acta Biomaterialia, 9(4), 5956-5962.

Fairgrieve, SI, Molto, E. 1994. Burning Point Canadian case studies of international cremated human remains. In A. Herring & L. Chan (Eds.), Strength in Diversity: a reader in physical anthropology. Toronto: Canadian Scholars' Press Inc.

Freemont AJ. 1993. Basic bone cell biology. International Journal of Experimental Pathology, 74, 411-416.

French, D, Edsall, JT. 1945. Reactions of Formaldehyde with Proteins VI. Cross-Linking of Amino Groups with Phenol, Imidazole, or Indole Groups. Advances in Protein Chemistry, 277-335.

Forbes, G. 1941. The Effects of Heat on the Histological Structure of Bone. The Police Journal, 14, 50-60.

Geomagic Design X [Internet]. 3D Systems. 2018. http://www.3dsystems.com/software/geomagic-design-x

Gonçalves, D, Cunha, E, Thompson, TJ. 2014. Estimation of the pre-burning condition of human remains in forensic contexts. International Journal of Legal Medicine, 129(5), 1137-1143.

Gorski J. 1998. Is All Bone the Same? Distinctive Distributions and Properties of Non-Collagenous Matrix Proteins in Lamellar Vs. Woven Bone Imply the Existence of Different Underlying Osteogenic Mechanisms. Critical Reviews in Oral Biology & Medicine, 9, 201–223.

Grévin, G, Bailet, P, Quatrehomme, G, Ollier, A. 1998. Anatomical reconstruction of fragments of burned human bones: A necessary means for forensic identification. Forensic Science International, 96(2-3), 129-134.

Guilbeau, MG. 1989. *The analysis of saw marks in bone*. Master's Thesis. Tesi. University of Tennessee.

Gupta, H, Zioupos, P. 2008. Fracture of bone tissue: The 'hows' and the 'whys'. Medical Engineering & Physics,30, 1209-1226.

Gurjian ES, Webster JE, Lissner HR. 1949. The mechanism of skull fracture. Journal of the American Medical Association, 54, 106-114.

Gustavson, KH. 1947. Note on the Reaction of Formaldehyde with Collagen. Journal of Biological Chemistry, 169, 531-537.

Hardy CH, Marcal PV. 1973. Elastic Analysis of a Skull. Journal of Applied Mechanics, 40, 838.

Hart, GO. 2005. Fracture Pattern Interpretation in the Skull: Differentiating Blunt Force from Ballistics Trauma Using Concentric Fractures. Journal of Forensic Sciences, 50(6), 1-6.

Herrmann, B. 1977. On histological investigations of cremated human remains. Journal of Human Evolution, 6(2), 101-103.

Herrmann, NP, Bennett JL. 1999. The differentiation of traumatic and heat-related fractures in burned bones. Journal of Forensic Science, 44(3), 461-469.

Hiller, J, Thompson, T, Evison, M, Chamberlain, A, Wess, T. 2003. Bone mineral change during experimental heating: An X-ray scattering investigation. Biomaterials, 24(28), 5091-5097.

Hillier, ML, Bell, LS. 2007. Differentiating Human Bone from Animal Bone: A Review of Histological Methods. Journal of Forensic Sciences, 52(2), 249-263.

Holland, T. 1989. Use of the cranial base in the identification of fire victims. Journal of Forensic Sciences, 34(2), 458-460.

Hubbard RP. 1971. Flexure of layered cranial bone. Journal of Biomechanics, 4, 251–263.

Jowsey, J. 1966. Studies of Haversian systems in man and some animals. Journal of Anatomy, 100(4), 857-864.

Kawasaki, K, Richtsmeier, JT. 2017. Association of the Chondocranium and Dermatocranium in Early Skull Formation. *In* Percival, CJ, Richtsmeier, JT (eds). Building Bones: Bone Formation and Development in Anthropology. Cambridge: Cambridge University Press. 52-78.

Keaveny, TM, Yeh, OC. 2002. Architecture and trabecular bone – Toward an improved understanding of the biomechanical effects of age, sex, and osteoporosis. Journal of Musculoskeletal Neuron Interaction, 2(3): 205-208.

Kimmerle EH, Baraybar JP. 2008. Skeletal trauma: identification of injuries resulting from human rights abuse and armed conflict. Boca Raton: Taylor & Francis.

Klepinger, LL. 2006. Trauma. *In* M. Cartmill & K. Brown (Eds), Fundamentals of forensic anthropology. Hoboken, NJ: Wiley-Liss.

Kronick PL, Cooke, P. 1996. Thermal stabilization of collagen fibers by calcification. Connective Tissue Research, 33.4, 275-282.

Lisowski, FP. 1968. The investigation of human cremated remains. Anthropologie und Humangenetik, 4, 76-83.

Małgorzata, G, Jarosław, S. 2006. The analysis of changes in bone structure and its chemical contents during storage in different environments. Journal of Vibroengineering, 8(3), 11-14.

Marella GL, Perfetti E, Arcudi G. 2012. Differential diagnosis between cranial fractures of traumatic origin and explosion fractures in burned cadavers. Journal of Forensic and Legal Medicine, 19, 175–178.

Mason, JT, O'Leary, TJ. 1991. Effects of formaldehyde fixation on protein secondary structure: a calorimetric and infrared spectroscopic investigation. Journal of Histochemistry & Cytochemistry, 39(2), 225-229.

Mayne, PM. 1990. The identification of precremation trauma in cremated bone. Unpublished master's thesis. Tesi. University of Alberta.

Mayne Correia, P. 1997. Fire modification of bone: a review of the literature. In W.D. Haglund & M.H. Sorg (Eds.), Forensic taphonomy: The postmortem fate of human remains. Boca Raton: CRC Press.

McElhaney JH, Fogle JL, Melvin JW, Haynes RR, Roberts VL, Alem NM. 1970. Mechanical Properties of cranial bone. Journal of Biomechanics, 3, 495-511.

Motherway JA, Verschueren P, Perre GVD, Sloten JV, Gilchrist MD. 2009. The mechanical properties of cranial bone: The effect of loading rate and cranial sampling position. Journal of Biomechanics, 42, 2129–2135.

Nalla, R, Kruzic, J, Kinney, J, Ritchie, R. 2005. Aspects of in vitro fatigue in human cortical bone: time and cycle dependent crack growth. Biomaterials, 26(14), 2183-2195.

Nalla, R, Kruzic, J, Kinney, J, Balooch, M, Ager, J, Ritchie, R. 2006. Role of microstructure in the aging-related deterioration of the toughness of human cortical bone. Materials Science and Engineering: C, 26(8), 1251-1260.

Peterlik, H, Roschger, P, Klaushofer, K, Fratzl, P. 2005. From brittle to ductile fracture of bone. Nature Materials, 5(1), 52-55.

Pointer, K. 2014. Histological Analysis of Cremated Human Bone [Unpublished honour's thesis]. University of Alberta (AB).

Pope, EJ, and Smith, OC. 2004. Identification of traumatic injury in burned cranial bone: an experimental approach. Journal of Forensic Sciences, 49(3), 1–10.

Pritchard JJ, Scott JH, Girgis FG. 1956. The structure and development of cranial and facial sutures. Journal of anatomy, 90(Pt 1), 73-89.

Reznikov N, Shahar R, Weiner S. 2014. Three-dimensional structure of human lamellar bone: The presence of two different materials and new insights into the hierarchical organization. Bone, 59, 93–104.

Shipman, P, Foster, G, Schoeninger, M. 1984. Burnt bones and teeth: An experimental study of color, morphology, crystal structure and shrinkage. Journal of Archaeological Science, 11(4), 307-325.

Silva, MJ, Touhey, DC. 2007. Bone formation after damaging in vivo fatigue loading results in recovery of whole-bone monotonic strength and increased fatigue life. Journal of Orthopaedic Research, 25(2), 252-26.

Skedros, JG, Knight, AN, Clark, GC, Crowder, CM, Dominguez, VM, Qiu, S, Mulhern, DM, Donahue, SW, Busse, B, Hulsey, BI, Zedda, M, Sorenson, SM. 2013. Scaling of Haversian canal surface area to secondary osteon bone volume in ribs and limb bones. American Journal of Physical Anthropology, 151(2), 230-244.

Skrzat J, Brzegowy P, Walocha J, Wojciechowski W. 2004. Age dependent changes of diploe in the human skull. Folia Morphologica, 63, 67-70.

Symes, S, Dirkmaat, DC, Ousley, S, Chapman, E, Cabo, L. 2012. Recovery and interpretation of burned human remains. BiblioGov.

Symes, S, Rainwater, C, Chapman, E, Gipson, DR, Piper, A. 2008. Patterned thermal destruction of human remains in a forensic setting. *In* Schmidt C, Symes S. (eds.), The analysis of burned human remains. Academic Press, London, 15–54.

Tang C, You F, Cheng G, Gao D, Fu F, Yang G, Dong X. 2008. Correlation Between Structure and Resistivity Variations of the Live Human Skull. IEEE Transactions on Biomedical Engineering, 55, 2286–2292.

Thavarajah, R, Mudimbaimannar, V, Rao, U, Ranganathan, K, Elizabeth, J. 2012. Chemical and physical basics of routine formaldehyde fixation. Journal of Oral and Maxillofacial Pathology,

16(3), 400.

Thompson, TJU. 2004. Recent advances in the study of burned bone and their implications for forensic anthropology. Forensic Science International, 146S, S203-S205.

Tubbs, RS, Bosmia, AN. 2012. The human calvaria: a review of embryology, anatomy, pathology, and molecular development. Childs Nervous System, 28, 23-31.

Turunen, MJ, Prantner, V, Jurvelin, JS, Kröger, H, Isaksson, H. 2013. Composition and microarchitecture of human trabecular bone change with age and differ between anatomical locations. Bone, 54(1), 118-125.

Ubelaker, DH. 2009. The forensic evaluation of burned skeletal remains: A synthesis. Forensic Science International, 183(1-3), 1-5.

van Oers, RF, Ruimerman, R, Hilbers, PA, Huiskes, R. 2008. Relating Osteon Diameter to Strain. Journal of Biomechanics, 41, 476-482.

Vaughan, T, McCarthy, C, Mcnamara, L. 2012. A three-scale finite element investigation into the effects of tissue mineralisation and lamellar organisation in human cortical and trabecular bone. Journal of the Mechanical Behavior of Biomedical Materials, 12, 50-62.

Wang, X, Mabrey JD, Agrawal, CM. 1998. An interspecies comparison of bone fracture properties. Bio-medical Materials and Engineering, 8, 1-9.

Wedel, VL, & Galloway, A. 1999. Broken bones: anthropological analysis of blunt force trauma. Springfield, Ill: Charles C. Thomas.

Weiner, S, Traub, W, Wagner, H. 1999. Lamellar Bone: Structure–Function Relations. Journal of Structural Biology, 126(3), 241-255.

White, TD, Black, MT, Folkens, PA. 2012. *Human osteology*. Amsterdam: Elsevier/Academic Press.

Zimmermann, EA, Ritchie, RO. 2015. Bone as a Structural Material. Advanced Healthcare Materials, 4(9), 1287-1304.

Zioupos P, Currey, D, Hamer, AJ. 1998. The role of collagen in the declining mechanical properties of aging human cortical bone. Journal of Biomedical Materials Research, 45.2, 108-116.